

MODELING BURNED ROCK FEATURES AS UNITS
OF SUBSISTENCE INTENSIFICATION

THESIS

Presented to the Graduate Council of
Texas State University-San Marcos
in Partial Fulfillment
of the Requirements

for the Degree

Master of ARTS

by

John A. Campbell, B.A.

San Marcos, Texas
August 2012

MODELING BURNED ROCK FEATURES AS UNITS
OF SUBSISTENCE INTENSIFICATION

Committee Members Approved:

Stephen L. Black, Chair

C. Britt Bousman

Phil Dering

Approved:

J. Michael Willoughby
Dean of the Graduate College

COPYRIGHT

by

John Andrew Campbell

2012

FAIR USE AND AUTHOR'S PERMISSION STATEMENT

Fair Use

This work is protected by the Copyright Laws of the United States (Public Law 94-553, section 107). Consistent with fair use as defined in the Copyright Laws, brief quotations from this material are allowed with proper acknowledgment. Use of this material for financial gain without the author's express written permission is not allowed.

Duplication Permission

As the copyright holder of this work I, John A. Campbell, authorize duplication of this work, in whole or in part, for educational or scholarly purposes only.

ACKNOWLEDGEMENTS

I would like to thank my committee chair, Dr. Steve Black, for all of his support throughout my field research and the writing of this thesis. Through him, I have become a better archaeologist and learned to appreciate the complexity and importance of the little things he calls FCR. I am also grateful to my committee members, Dr. Britt Bousman and Dr. Phil Dering for their advice and assistance along the way. The faculty and staff in the Department of Anthropology at Texas State University-San Marcos have all been very supportive throughout my graduate studies, specifically Mary Gibson, Dr. Jon Lohse, and Carole Leezer.

Several students assisted with my field and laboratory research. Students in the 2010 Texas State Archaeological Field School were critical to covering the survey areas in search of earth ovens. Some of these students returned to assist me later in the year, namely Jeremy Brooks, Chris Davis, Nick Lindzenmeyer, and Travis Metheny. Graduate students David Yelacic, Charles Koenig, Julian Sitters, Kevin McKinney, and Ashleigh Knapp were very helpful in getting me over the many hurdles of this research.

None of this research would have been possible without the access to the properties in the Lower Pecos. First, I would like to thank Jack Skiles of Langtry for allowing me the use of his guest house and access to areas around Eagle Nest Canyon to run the initial tests of my methodology. Thanks also go to Jack and Missy Harrington for allowing me access to their properties at Shumla Ranch and Painted Flat Canyon. Dr.

Carolyn Boyd and the SHUMLA School staff were most gracious in allowing me the use of the SHUMLA campus facilities and in helping collect data for this research. I thoroughly enjoyed helping out with the ninth graders at the SHUMLA Discovery Camp, teaching them about PAP, and getting them involved in archaeology.

I would also like to thank Mark Willis for his assistance with designing the PAP equipment and helping me streamline my methodology. I owe a huge debt of gratitude to Dr. Dinesh Nair, who designed the photogrammetry software for my thesis. Without Dr. Nair's help this whole endeavor would have been for nought.

Finally, I would like to thank my family, especially my parents for their support and words of encouragement. Most importantly, I owe everything to my loving wife Adrienne who has supported me throughout, sacrificed her time, and endured many nights alone with two young kids while I complete this research.

This manuscript was submitted on July 9, 2012.

TABLE OF CONTENTS

	Page
ACKNOWLEDGEMENTS	v
LIST OF TABLES	ix
LIST OF FIGURES	x
ABSTRACT	xii
 CHAPTER	
I. INTRODUCTION	1
II. ENVIRONMENTAL AND CULTURAL SETTING	6
Environmental Setting	6
<i>Geology</i>	7
<i>Soils</i>	8
<i>Regional Climate</i>	10
<i>Comments on Environment</i>	11
Cultural History	12
Previous Investigations	17
III. EARTH OVENS AND SUBSISTENCE INTENSIFICATION.....	20
Burned Rock Features in the Lower Pecos	20
Subsistence Intensification and Burned Rock Features	25
IV. PHOTOGRAMMETRY AND POLE AERIAL PHOTOGRAPHY	37
Photogrammetry	37
Methods	41
<i>Equipment</i>	42
<i>Aligning the Cameras</i>	46
<i>PAP Field Methods</i>	49
<i>Post Processing of the Images</i>	54
V. RESULTS OF INVESTIGATIONS	61
Intensive Survey	61
<i>Previously Recorded Archaeological Sites</i>	67
<i>Sites Recorded During Survey</i>	68

	Painted Canyon Flat (41VV448)	75
	Burned Rock Feature Analysis	77
	<i>Feature C006</i>	79
	<i>Feature A257</i>	83
	<i>Feature C001</i>	87
	<i>Feature C003</i>	91
	<i>Feature C004</i>	95
	<i>Feature C007</i>	99
	<i>Feature C005</i>	101
	<i>Calculating Rock Density</i>	105
	<i>Applying the PAP</i>	111
VI.	CONCLUSIONS.....	116
	Constructing the Equipment	116
	Field Methods	118
	Post Processing	119
	Applying the Results.....	122
	Concluding Comments.....	127
	APPENDIX.....	130
	REFERENCES CITED.....	157

LIST OF TABLES

Table	Page
1. Internal camera geometry	44
2. Pole length based on base-height ratio.....	48
3. Previously recorded archaeological sites on the Shumla Ranch.....	68
4. Sites recorded during the survey of Shumla Ranch	69
5. Summary of feature data.....	78
6. Distribution of rocks by weight class for the western half of C006	81
7. Distribution of rocks by weight class for A257	85
8. Distribution of rocks by weight class for C001	89
9. Distribution of rocks by weight class for C003	93
10. Distribution of rocks by weight class for C004	97
11. Distribution of rocks by weight class for C007	101
12. Distribution of rocks by weight class for C005	103
13. Density of rock control samples	110
14. Feature C005 collected data.....	113
A-1. Feature A257 burned rock data.....	132
A-2. Feature C001 burned rock data.....	135
A-3. Feature C003 burned rock data.....	141
A-4. Feature C004 burned rock data.....	146
A-5. Feature C005 burned rock data.....	149
A-6. Feature C006 burned rock data.....	152
A-7. Feature C007 burned rock data.....	155

LIST OF FIGURES

Figure	Page
1. Outline of the Lower Pecos Archaeological Region adapted from Turpin (2004:267)	13
2. Examples of hot rock cooking facilities, courtesy of A. Thoms (Thoms 2008:Fig. 3)	30
3. PAP equipment without pole.	42
4. Geometry of the PAP	48
5. PAP assembly in use.	52
6. First screen of Stereo3D program where left and right images are loaded.	57
7. Second screen showing the depth image and disparity value.	58
8. Third screen where the volume is measured from the original image.	59
9. The camera geometry and ground disparity entry field from the third screen.	60
10. Locations of the canyons on the Shumla Ranch.	63
11. Survey Areas at Shumla Ranch.	66
12. Painted Canyon Flat survey area.	76
13. Aerial view of C006.	80
14. Distribution of burned rocks by weight in the western half of C006.	82
15. Histogram showing total weight by class for C006.	83
16. Aerial view of A257.	84
17. Distribution of burned rocks by weight in A257	86
18. Histogram showing total weight by class for A257.	87
19. Aerial view of C001	88
20. Distribution of burned rocks by weight in C001	90
21. Histogram showing total weight by class for C001	91
22. Aerial view of feature C003.	92
23. Distribution of burned rocks by weight in feature C003	94
24. Histogram showing total weight by class for C003	95
25. Aerial view of feature C004.	96
26. Distribution of burned rocks by weight in feature C004	98
27. Histogram showing total weight by class for C004	99
28. Aerial view of feature C007.	100
29. Distribution of burned rocks by weight in feature C007	102
30. Histogram showing total weight by class for C007	103
31. Aerial view of feature C005.	104
32. Distribution of burned rocks by weight in feature C005	106
33. Histogram showing total weight by class for C005	107
34. Equipment used to measure the volume and density of sample rocks.	109

35. An example of a stereo pair of images from Feature C005	111
36. Aerial composite of C005 with measured rocks labeled	112
37. Distributions of weight of burned rock by class for all features.....	126
A-1. Feature A257 plan map with measured burned rocks labeled	131
A-2. Feature C001 plan map with measured burned rocks labeled	134
A-3. Feature C003 plan map with measured burned rocks labeled	140
A-4. Feature C004 plan map with measured burned rocks labeled	145
A-5. Feature C005 plan map with measured burned rocks labeled	148
A-6. Feature C006 plan map with measured burned rocks labeled	151
A-7. Feature C007 plan map with measured burned rocks labeled	154

ABSTRACT

MODELING BURNED ROCK FEATURES AS UNITS OF SUBSISTENCE INTENSIFICATION

by

John Andrew Campbell, B.A.

Texas State University-San Marcos

August 2012

SUPERVISING PROFESSOR: STEPHEN L. BLACK

Subsistence intensification is the process by which humans expand their diet breadth to exploit lower ranked and more costly food resources to mitigate the effects of environmental or population stress. Earth ovens represent a critical technological adaptation by which humans can process toxic or otherwise inedible plant foods as a way of augmenting their diet. The Lower Pecos Canyonlands in southwest Texas is an arid landscape prone to seasonal drought and temperature extremes. As a response to long term and periodic shifts in the climate, the prehistoric inhabitants of the region adopted earth ovens as a way to render the locally available desert rosettes, such as lechuguilla and sotol, edible. As a response to environmental stress, earth ovens and their surviving

elements serve as a proxy by which subsistence intensification within a region can be measured. The current research examines the structural elements of earth ovens as a way of understanding the degree to which earth ovens and the plants processed in them contributed to the prehistoric economy. A methodology utilizing Pole Aerial Photogrammetry (PAP) is applied to the documentation of seven earth ovens in Val Verde County, Texas to record the feature parameters, the spatial distribution of burned rock, and individual weights of burned rocks. The collected data was analyzed to interpret the role of feature weight and the degree of burned rock fragmentation in measuring the frequency of use of earth ovens as well as the extent of intensification of the plants cooked in these features.

CHAPTER I

INTRODUCTION

The study of earth ovens and their associated burned rock middens has long been an interest of archaeologists in Texas. These features are ubiquitous cultural manifestations that occupy the uplands and valleys from central Texas into the Big Bend region and westward across the Desert Southwest. Earth ovens represent an adaptive technology that utilizes the stored energy in heated rocks for the prolonged cooking of food. With this technology, groups are able to expand their diet breadth to process and eat plants that would otherwise be inedible. The expansion of a group's diet breadth would be necessary in environments with limited resources, during times of environmental stress, and in times of increased population density. In the Lower Pecos Canyonlands of Texas, prehistoric inhabitants would have faced both an arid environment with limited resources and times of environmental stress from prolonged drought, and perhaps times of excessive population density as well. As a result, the earth oven is a common feature at archaeological sites in the region.

The primary goal of this research is to develop a methodology for applying pole aerial photography (PAP) to quantify the dimensions and weight of earth oven features and establish parameters for studying variation in feature morphology as it relates to subsistence intensification within a regional and local context. The PAP method I use incorporates digital photogrammetry as a way to record features and obtain metric data

that can be compiled to present a detailed three-dimensional map of the features and their associated rocks. The three-dimensional map can in turn be used to measure volumetric data of the burned rocks which can then be used to determine rock weight, and thus potential food yield.

The digital photogrammetry of earth oven features is accomplished through the use of a stereo pair of vertically aligned digital cameras mounted at the end of a telescoping pole. The photographs were processed with photogrammetry software to provide spatial and metric data. Controlled measurements of volume/density by rock type were recorded in the lab from samples collected from rock outcrops and from an experimental earth oven in the region. The PAP method provides a relatively quick process for recording features and generating a more robust set of data than can be collected by more conventional methods. The methodology incorporates items that are relatively low in cost or items that most archaeologists already possess or can easily obtain.

As part of testing this methodology, survey was carried out in southwestern Val Verde County, Texas to identify features that were suitable for this study. Two areas were selected for survey, the Shumla Ranch and the flats above Painted Canyon. The survey at Shumla Ranch was conducted as part of a Texas State University archaeological field school in the summer of 2010 and consisted of an intensive survey of the ranch property by undergraduate students supervised by the author. The primary goals of the Shumla Ranch survey were to train students in the methods and practice of archaeological survey and produce an inventory of the archaeological resources on the ranch. An additional goal was to identify burned rock features suitable for

photogrammetry. The survey of the flats above Painted Canyon was focused on the area within and adjacent to site 41VV448 and was conducted primarily to identify and document earth oven features on the site, as well as to reevaluate the site's components, extent, and integrity. This survey was conducted by volunteer students from Texas State University supervised by the author and Dr. Steve Black. Additionally, one of the features at site 41VV448 was excavated to determine its vertical extent and degree of reuse, as well as to recover organic remains for identification and dating.

In recent years, archaeologists have suggested that earth ovens and their accumulated middens are evidence of subsistence intensification among prehistoric people faced with environmental or population stress (Black et al. 1997; Freeman 2007; Johnson and Hard 2008; Thoms 2008; Yu 2006). Subsistence intensification is an adaptive response to population growth and/or environmental conditions by which groups broaden their diet selections to incorporate lower ranked resources to increase the productivity of their particular geographical niche (Binford 2001). Binford suggested that intensification by hunter gatherers will proceed from hunting terrestrial animals, to exploiting aquatic resources, to collecting wild plants, and finally, the adoption of horticulture. Intensification generally requires new technologies and increased investment of labor to acquire new resources. Earth ovens, which allow for the prolonged cooking, represent a technological adaption to include plant foods that would otherwise be inedible and to cook greater amounts of food in one event. Therefore, earth oven features can serve as a proxy for measuring rates of intensification among hunter gatherers.

Examining burned rock features as part of a population's subsistence intensification can be done at several levels. At the regional level, shifts in technology that support an expanded diet breadth among a population reflect broad cultural adaptations to changing conditions of the environment and people. These regional patterns are derived from the data collected at the local level where information from specific archaeological sites can be used to reveal patterns of inter- and intra-site behavior. An examination of individual features can provide a more detailed picture of the role of technology within a population. It is at this feature level that the proposed methodology is applied to understand the use life of an individual feature as it relates to the level of subsistence intensification within a local population.

The main functional components of an earth oven feature are the fuel, packing material, rocks for heat storage, the oven pit, and the sediment used to cap and insulate the layered oven (Thoms 1989). The quantities of these components are related to the amount of food that is to be cooked, however, burned rocks may be the only component consistently preserved in the archaeological record. For example, it can be assumed that as the amount of food to be cooked increases, the amount of fuel, rocks, and pit size would also need to increase. Dering (1999) constructed a series of experimental earth ovens in the Lower Pecos to test the caloric yield of an earth oven based on the amount of fuel, rock, and preparation time. These experiments quantify components of the earth oven process from which general assumptions can be constructed regarding the use life of a feature, as estimated from the total weight of the rock within a feature. The assumptions form the primary basis for applying the proposed methodology to extract rock weight from burned rock features. The collected data can then be analyzed to

estimate the number of times an individual feature was used and the amount of food that was processed. These estimates, when taken with other archaeological data from the region, will be used to measure the relative use intensity of individual features as a proxy for determining the degree to which prehistoric people were intensifying their subsistence.

In the subsequent chapters, a regional background and research design is presented to outline the details of this proposed methodology and its use within the Lower Pecos Canyonlands. Chapter II provides a brief overview of the environmental and cultural setting that includes a discussion of the geology, soils, and relevant climatic history. This chapter also summarizes the culture history of the Lower Pecos and previous investigations in the region related to archaeological excavation and survey. A discussion of earth ovens and a theoretical framework related to subsistence intensification is presented in Chapter III. Chapter IV includes a discussion of the use of photogrammetry and outlines the methods and software used in the pole aerial photogrammetry. The results of this research are presented in Chapter V and Chapter VI offers conclusions regarding the current research and applications of the methodology for future research.

CHAPTER II

ENVIRONMENTAL AND CULTURAL SETTING

The Lower Pecos Archaeological Region (also known as the Lower Pecos Canyonlands) of Texas is located in the southwestern portion of Texas and adjacent northern Mexico where the Pecos and Devils Rivers enter the Rio Grande. While the region encompasses portions of several counties in Texas and the northern portion of the Mexican state of Coahuila, the focus of the present research is on Val Verde County, Texas in the heart of the region. Throughout the Holocene, the region has supported a diverse array of animal and plant life as well as numerous human groups. The region's arid climate has resulted in a sparsely populated landscape throughout its human history, that necessitated adaptations to the demanding environment. The region contains over 2000 recorded archaeological sites dating from the Paleoindian period to the recent historic period. Rockshelters and caves in the region, coupled with the arid climate, have preserved some of the most remarkable archaeological remains of hunting and gathering in the country, including perishable items such as textiles and food remains, wooden tools, human remains, and elaborate rock art.

Environmental Setting

The Lower Pecos Canyonlands is an arid landscape just beyond the northeastern reaches of the Chihuahuan Desert. The area is dominated by level to rolling uplands

dissected by deep canyons formed by its three most dominant water courses, the Pecos River, the Devils River, and the Rio Grande, and their tributaries. Val Verde County overlaps three natural regions of Texas, the Trans Pecos region in the west, the Edwards Plateau in the east, and a small portion of the South Texas Brush Country in the southeast (Landers 1987; McNab and Avers 1994). This portion of the Trans Pecos is part of the Stockton Plateau at the southern portion of the Great Plains geomorphic region (McNab and Avers 1994). The majority of the Stockton Plateau is characterized by short to middle height grasses and desert shrubs with scattered drought deciduous and juniper woodlands. To the east, the western portion of the Edwards Plateau consists of mesquite-juniper shrubland and savanna with short to middle height grasses (Hall and Valastro 1995). The South Texas Brush Country, which extends to the Gulf Coast and includes the Rio Grande Plain, consists of grassland savannah and dense brushlands of mesquite and other woody plants (Landers 1987).

Geology

The surface geology within Val Verde County is characterized by Cretaceous age limestone, dolomite, and clays in the uplands and Quaternary aged fluvial deposits in the river and stream valleys (GAT 1977, 1981). Within the study area at Shumla Ranch the dominant geologic formation is the Devils River Limestone, consisting of limestone and dolomite that formed during the Lower Cretaceous. Overlying this formation is the Buda Limestone consisting of Upper Cretaceous fine grained limestone and the Buda Limestone and Del Rio Clay undivided, which contains the Buda limestones and Upper Cretaceous, calcareous and gypsiferous siltstones.

Uvalde gravels, which are Tertiary or Quaternary aged fluvial deposits, occur more commonly in the southeast portion of the county and beyond, but a small outcrop of these deposits is also present within the northeast portion of the study area at Shumla Ranch at the highest elevation (GAT 1977). While these Uvalde gravels are commonly associated with fluvial deposits eroded from the plains to the north, deposits on the Shumla Ranch also contain igneous and siliceous gravels from the Big Bend region to the west (Charles Frederick, personal communication 2010). At the southern end of the study area at Shumla Ranch the uppermost formation is the Boquillas Flags which consist of Upper Cretaceous laminated shale and siltstone interbedded with limestone.

At site 41VV448 above Painted Canyon, the area is mapped within the Buda Limestone and Del Rio Clay undivided. However, visual inspection of the area reveals the laminated Boquillas Flags formation overlying the Lower Cretaceous Salmon Peak Limestone. The Salmon Peak Limestone consists of granular limestone with numerous shell fossils (GAT 1977). As expected, the burned rocks identified in the features within the study areas coincide with their adjacent geologic formations.

Soils

The soils within Val Verde County are predominantly mollisols, with some aridisols, that formed in the uplands from the underlying Cretaceous age limestone (Cooke et al. 2007:276; Golden et al. 1982). Mollisols are characterized by the accumulation of calcium rich organic matter that manifests as a soft, thick mollic epipedon (Brady and Weil 2002:103). This mollic epipedon is the upper horizon of the soil and typically forms from the dense roots of grasslands. Aridisols occur in arid

environments that lack sufficient soil moisture to sustain plant growth for more than 90 consecutive days (Brady and Weil 2002:98; USDA 1999:329). Due to the low moisture content of these soils, they are underdeveloped pedogenically, often characterized by a cambic horizon, and normally soluble minerals within the soil tend to redistribute into petrocalcic layers that can prevent root growth. Deep alluvial sediments occur along the Pecos River, Devils River, the Rio Grande, and their tributaries, however, on the lower reaches of the watercourses they are often inundated as a result of the damming of the Rio Grande to create Amistad Reservoir (Golden et al. 1982).

Soils in the county formed under very hot conditions which have had an adverse effect on the moisture content in the soil and therefore, the vegetation these soils can sustain. Taxonomically, these soils are described as thermic (forming under mean annual temperatures between 15° and 22° C) and hyperthermic (forming under mean annual temperatures above 22° C) (Brady and Weil 2002:103). High temperatures also contribute to low soil moisture and therefore low organic activity, which creates an environment conducive to the preservation of organic archaeological remains. Although areas in the county exist with good soil depth and development, the majority of the upland areas, including the study areas around Shumla and Painted Canyon, have very thin, deflated soils with bedrock and numerous cobbles and gravels, mostly clasts of non-stream transported rock, exposed on the surface. Vegetation is also sparse, which exacerbates erosion and exposes the underlying bedrock.

Regional Climate

The regional climate has varied over the course of human occupation within the region. During the Wisconsin Glacial Period at the end of the Pleistocene, much of the region was dominated by woodlands, pinyon parklands, and scrub grasslands between 22,500 and 14,000 RCYBP (Bryant and Holloway 1985:47). This time period was cool and humid and predates human occupation in the region (Bryant and Shafer 1977). Over the next 4,000 years the region shifted to a warmer, drier climate with decreasing oak-juniper woodlands giving way to increasing scrub grasslands (Bryant and Holloway 1985:52; Dering 1979:53). As the Pleistocene gave way to the Holocene around 11,000 RCYBP, several species of fauna, such as mammoth, mastodon, Pleistocene bison, horses, and camels, begin to disappear from the fossil record as well during this time (Dering 2005). From 11,000 to 7,000 RCYBP, during the post-glacial period, the region has a significant decrease in tree pollen in the fossil record coupled with a significant increase in herb and grass pollen (Bryant and Holloway 1985:56). During this post-glacial period, plant remains from Hinds Cave and Baker Cave show evidence of xeric plants within the region such as lechuguilla, sotol, yucca, and prickly pear (Dering 1979).

Between 7,000 and 4,000 RCYBP is a period that Antevs (1955) defined as the Altithermal which represents a drier, less mesic period across much of the Great Plains and Texas. Evidence of this is found in both the fossil pollen record as well as the archeological record which exhibits signs of adaptive tool variability, expansion of diet breadth, and regional abandonment in settlement patterns (Bryant and Holloway 1985:57; McKinney 1981; Meltzer 1999). Although, there are few pollen records from the region during the Altithermal, Dering (1979:63) suggests that much of the regions vegetation

likely resembled the present vegetation. Near the end of this period Bryant and Holloway (1985:59) note several significant flood events that exacerbated erosion of the uplands and bottomlands. The current mesquite-juniper and scrub grassland savannah was established by 4,000 RCYBP and conditions in the region trended towards drier and warmer climate.

Today, the climate in the region is semiarid with dry winters and hot summers. Winds in the region generally blow from the southeast during the summer and fall and from the northeast in the winter and spring (Carr 1967:16; Golden et al. 1982:2). Temperatures in the region are generally very hot in the summer with many days above 38°C (100°F) and moderate to cold in the winter with short isolated periods of freezing weather (Carr 1967; NCDC 2010). Mean annual high temperatures reach 27.2°C (80.9°F) and mean annual low temperatures are 13.7°C (56.7°F). The highest recorded temperature in the region was 45.6°C (114°F) in 1995 at Amistad Dam and the lowest recorded temperature was -16.7°C (2° F) in 1985 at Pandale. Precipitation in the county increases from southwest to northeast and mostly falls during the late summer and early fall (Carr 1967:16). Mean annual precipitation in the west ranges from 35.6 cm (14 in) at Langtry, in the southwest, to 45.5 cm (17.9 in) at Pandale, in the northwest. In the eastern part of the county the mean annual precipitation ranges from 47.2 cm (18.6 in) in Del Rio, in the southeast, to 59.4 cm (23.4 in) at the Fawcett Ranch in the northeast (NCDC 2010).

Comments on Environment

The local environment is critical to the emergence of earth ovens in the subsistence economy of prehistoric hunter gatherers in the region. The emergence of

these features in the archaeological record coincides with shifts in the climate towards more aridity and thus an increase in desert plants such as lechuguilla, sotol, yucca, and cacti. These plants are drought tolerant and suited to the thin rocky soils in the region, which would have increased their importance as a food source as other edible, less tolerant plants became scarce. Unfortunately, historic overgrazing and poor land management in the region has led to the deflation of many archaeological sites, leaving earth ovens exposed on the surface. While rockshelters afford some of the best preserved sites in the region, most have been vandalized.

Cultural History

The Lower Pecos Archaeological Region includes the confluences of the Pecos and Devils Rivers with the Rio Grande (Figure 1) and also the many side canyons and tributaries of these watercourses such as Mile Canyon and Seminole Canyon. Parts of Northern Mexico are also included in this region; however the area south of the Rio Grande is poorly known. Turpin (2004:266) defines this cultural area primarily by the distribution of the Pecos River rock art style. The prehistoric inhabitants of this region consisted of hunter-gatherer groups operating within an arid to semi-arid environment with a diverse subsistence base.

Within the Lower Pecos, two broad categories of sites exist, open air sites and sheltered sites, such rockshelters (Dering 2002:4.4). Site elements vary across these two categories and include lithic scatters, burned rock features, rock alignments, cairns, burials, pictographs, petroglyphs, bedrock mortars, and quarry sites, among others (Dering 2002:4.4-4.5; Shafer 1988). Although some of these site elements are unique to



Figure 1. Outline of the Lower Pecos Archaeological Region adapted from Turpin (2004:267).

one site category, most can occur across both categories. Chronologies for the region have been constructed based on a combination of radiocarbon dates, primarily from rockshelters in the region, feature and artifact types, and artistic styles (Turpin 1991). Turpin (2004) outlines the most recent chronology, consisting of four major cultural periods and twelve subperiods: Paleoindian (Aurora, Bonfire, Oriente), Archaic (Viejo, Eagle Nest, San Felipe, Cibola, Flanders, Blue Hills), Late Prehistoric (Flecha, Infierno), and Historic.

The first inhabitants of the region were hunter gatherers near the end of the Pleistocene, after 14,500 RCYBP. These Paleoindian groups came when the climate was cooler and moister focusing on an economy of big game hunting and nomadic settlement patterns as well as the utilization of large fluted (Clovis and Folsom) and later unfluted lanceolate projectile points (Golondrina and Angostura) (Bement 1989). Paleoindian sites in the Southern High Plains, just north of the Lower Pecos, are generally characterized as kill and butchering sites or camp sites (Holliday 1997). In the Lower Pecos, the remains of this period of settlement are represented at only a handful of sites and these examples are not wholly typical of the period across the rest of the continent. In the Lower Pecos, deposits from this period have been dated based on projectile point types and charcoal found at such sites as Cueva Quebrada, Bonfire Shelter, Arenosa Shelter, Coontail Spin, Mosquito Cave, Damp Cave, and Devils Mouth (Dering 2002:3.5; Dibble and Lorrain 1968; Epstein 1962; Johnson 1964; Nunley et al. 1965; Turpin 1991:22). Among these sites, Bonfire Shelter is unique as the oldest and southernmost bison jump site in North America.

By 9,000 RCYBP, the climate in the region became warmer and drier conditions with larger fauna becoming extinct and the human inhabitants shifted towards new and much more diverse food sources. This is demonstrated by the “Golondrina Hearth,” the oldest cooking feature in the region, discovered at Baker Cave, which dates to this period around 9,000 RCYBP (Hester 1983). As the climate became drier during the Altithermal (7,500 to 5,000 RCYBP) and bison populations were absent, subsistence appears to diversify to lower ranked resources defining the Archaic period (Dering 2002; Meltzer 1999). Adaptations to the changing environment suggest a less mobile hunting and gathering population “tethered” to limited water sources (Taylor 1964), regional abandonment of drier areas, utilization of locally available lithic resources, and wider use of new technologies (Meltzer 1999). However, Dering (1999, 2002) suggests that residential mobility in the Lower Pecos was tied more to, though not exclusive to, plant food and wood fuel availability than permanent water sources. The most significant aspects of the Archaic period in the Lower Pecos are the widespread use of rockshelters, such as Hinds Cave (Dering 2002), earth ovens for baking desert succulents, the emergence of a textile and fiber industry, and the emergence of regionally distinct art. Art in the region consists of portable art (painted pebbles and figurines), monochromatic and polychromatic pictographs, and petroglyphs (Boyd 2003; Dering 2002; Shafer 1975; Turpin 1997, 2004).

Excavations at sites within the region have recovered a total of several hundred prehistoric burials dating primarily to the Archaic and Late Prehistoric periods (Steele and Olive 1989). These interments essentially evolve from shaft burials in the Early Archaic (Seminole Sink) (Turpin 1985) to bundle and shaft burials in rockshelters and

caves during the Middle and Late Archaic (Turpin 2004). Analysis of human remains recovered during the Archaic and Late Prehistoric exhibit both porotic hyperostosis and dental caries usually associated with higher carbohydrate intake (Reinhard 1992). Desert plants such as lechuguilla, sotol, and prickly pear are high carbohydrate foods and calorically sufficient, but contain low levels of iron and B-complex vitamins, which is linked to porotic hyperostosis (Reinhard 1992; Walker et al. 2009). These plants are considered staples of the prehistoric diet in the Lower Pecos and this reliance on high carbohydrate foods has been linked to a higher occurrence of dental caries as compared with other hunter-gatherer populations in Texas (Steele et al. 1999).

The Late Prehistoric period begins around 1,300 RCYBP and is characterized by the presence of the bow and arrow in the region. The earliest evidence of bow and arrow use in the Lower Pecos is based on the presence of arrow points dated to around 1,380 RCYBP at Arenosa Shelter (Dering 2002). Aside from this major technological shift in hunting, subsistence practices remain relatively similar to those during the Archaic. However, the period does see an increase in open sites and annular burned rock middens on uplands, which suggests increasing intensification of desert succulents (Dering 2002; Turpin 1994). Cairn burials, located on upland ridges and promontories, also appear during this period, as well as cremation burials (Dering 2002; Turpin 2004). Rock art during this period changes, with the emergence of the Red Monochrome style and the Bold Line Geometric style. Both of these styles of art are thought by Turpin (2004) to be intrusive styles, partly because of their similarities to southern Plains and southwest styles of art and partly due to the consistency of the Bold Line Geometric, suggesting a fully mature form.

Late Prehistoric occupations are often associated with either Toyah or Infierno phases within the region. Both of these phases overlap geographically and exhibit, steeply beveled end scrapers, four-beveled knives, stemmed arrow points, and bone tempered pottery (Dering 2002; Mehalchick and Boyd 1999). The stone tools are commonly associated with bison hunting and processing at Plains and Texas sites in the Late Prehistoric (Creel 1991). Although rare in the Lower Pecos, pottery attributed to Infierno and Toyah sites in the region are generally identical to Toyah Phase Leon Plain ware in central Texas (Mehalchick and Boyd 1999). The two major differences in these phases are that Perdiz points, diagnostic of Toyah phase, are not generally associated with Infierno phase and rock alignments, that represent possible wikiup or tipi locations, are associated with Infierno phase, but not Toyah (Mehalchick and Boyd 1999). Based on these two differences, both phases overlap geographically and it has been proposed that Infierno phase may represent a Protohistoric intrusion by Plains people or it may be a later iteration of Toyah people (Mehalchick and Boyd 1999). Unfortunately, there are few sites in the region from these phases that have been radiocarbon dated (Dering 2002).

Previous Investigations

Archaeological investigations conducted in the region include surveys, test excavations, and major excavations beginning in the 1930s and continuing into the present (Turpin 2004). Early excavations in the region were conducted by the Smithsonian Institution, the Witte Museum, and the University of Texas (Bement 1989:64) and focused primarily on the excavation of dry caves such as Fate Bell (Pearce and Jackson 1933), the Shumla Caves (Martin 1933), Moorehead Cave (Setzler 1934)

caves on the Horseshoe Ranch (Woolsey 1936), and Eagle Cave (Davenport 1938). The earliest rock art recording was conducted by Jackson (1938) and Kirkland (1938).

Archaeological investigations in the region were limited during World War II, but resumed in the 1950s, when the Diablo Reservoir (now Amistad Reservoir) was proposed (Turpin 1984:7-8), under the auspices of the National Park Service's Texas Archeological Salvage Program at the University of Texas at Austin (Dering 2002:3.15). This program included surveys by Graham and Davis (1958) and by W.W. Taylor and F. Gonzalez-Rul (Gonzalez-Rul 1990; Taylor and Gonzales-Rul 1961) as well as salvage work at the Arenosa shelter (Dibble 1967) and the Devils Mouth Site (Johnson 1959). Excavations were also conducted under this program at Centipede and Damp Caves in 1958 (Epstein 1962), at Coontail Spin, Mosquito, Zopilote, and Doss Caves in 1962, and at Eagle Cave, Fate Bell Shelter, and Bonfire Shelter in 1963 and 1964 (Black and Dering 2008).

Additional investigations included surveys of the lower Devils River (Dibble and Prewitt 1967), Seminole Canyon State Park (Turpin 1982), Hinds Ranch and Blue Hills (Saunders 1992), and Devils River State Natural Area (Turpin and Davis 1990). With the exception of a small number of investigations, the primary focus of previous archaeological work in the region was on the river basins and their margins. This is largely due to the fact that many of the survey investigations in the region were associated with Amistad Reservoir and thus restricted to areas of impact from the reservoir.

Several sites have been excavated in the region, providing a wealth of data with regard to the prehistory of the Lower Pecos. While the sites excavated in the 1930s focused primarily of recovery of material culture, investigations in the 1960s and 1970s

as part of the Amistad Reservoir construction and university field schools were much broader in scope, focusing on both the environmental and cultural history of the region by taking advantage of the excellent preservation of plant food and textile remains, human coprolites, palynology, and radiocarbon dating. Deeply stratified alluvial sites such as Arenosa Shelter (Bryant 1967; Dibble 1967; Patton and Dibble 1982) and Devils Mouth (Johnson 1959, 1964; Sorrow 1968) have contributed to the chronology of the natural and cultural evolution of the region. Bonfire Shelter (Bement 1986; Dibble and Lorrain 1968) remains the oldest (Paleoindian and Late Archaic) and most southerly bison jump site in North America and deposits from this shelter have contributed to understanding early hunting strategies and regional environmental history. However, the degree to which Bonfire Shelter was used, during the Paleoindian period, as a bison jump, or if it was even used as a bison jump has been the subject of debate in recent years (Bement 2007; Byerly et al. 2005; Byerly et al. 2007; Meltzer et al. 2007; Prewitt 2007).

Arenosa, Bonfire, Devils Mouth, and several other sites were all excavated as part of the Texas Archaeological Salvage Project in the 1960s. Investigations at Baker Cave by the University of Texas at San Antonio (Hester 1983) and Hinds Cave by Texas A&M University (Shafer and Bryant 1977) in the 1970s produced considerable data with regard to subsistence, prehistoric ecology, and bioarchaeology through the recovery and analysis of coprolites (Reinhard 1988; Williams-Dean 1978) and plant macro- and micro-fossils (Dering 1979; Reinhard 1988).

CHAPTER III

EARTH OVENS AND SUBSISTENCE INTENSIFICATION

Earth ovens figure prominently in the archaeological landscape of Texas as a technological adaptation reflecting the subsistence economy of prehistoric hunters and gatherers. The features represent prehistoric innovation in converting otherwise inedible plants into nutritional foods to supplement a broad subsistence base and increase the amount of food that could be cooked at one time. Within the Lower Pecos, this technology provided prehistoric people with the ability to extend cooking times utilizing the stored energy in heated stones. Without earth ovens, prehistoric people would have been unable to utilize many of the desert plants during times of environmental stress or increased population. This method of intensification manifests not only in the plant remains associated with earth ovens, but as arrangements of burned rocks ranging from discrete concentrations representing only a few episodes of cooking to extensive accumulations reflecting repeated cooking episodes over thousands of years. As such, the content (rocks) and mass of these features can be used as a proxy for measuring subsistence intensification over time.

Burned Rock Features in the Lower Pecos

Burned rock features are common at most sites in the Lower Pecos. The features consist of once-heated, and often thermally fractured rocks (known as burned or fire-

cracked rocks) that occur as individual clusters (often termed hearths), mounded or annular debris accumulations (burned rock middens), or as more dispersed debris fields in both open and sheltered sites. They occur widely in both the canyons and in the uplands. The distribution of burned rock features has primarily been documented within the context of individual sites or smaller project areas; however, a few investigations have examined this phenomenon as part of large scale surveys.

As part of their survey for Amistad Reservoir, Dibble and Prewitt (1967:118-119) documented burned rock middens primarily within areas of benched alluvium in the bottoms of ephemeral drainages and at the upper reaches of small side canyons. They noted that the locations of features were generally far from active water sources, but their investigations were limited to the canyons and small portions of the adjacent uplands within the lower reaches of the Devils River and a six mile length of the Rio Grande above Amistad Dam. Turpin (1982:159) found similar distributions of the eight burned rock middens recorded during her survey of Seminole Canyon State Park. These middens were found in the upper reaches of Presa and Seminole Canyons on gentle slopes (Turpin 1982:159). Saunders' (1992:342) survey of the Hinds Ranch (uplands above Hinds Cave) and the Blue Hills (uplands about 20 miles north of Hinds Cave) established a high resolution for site recording, documenting a total of 80 possible plant processing features including middens, hearths, and burned rock scatters. However, Saunders did not address the spatial distribution of these features in his study, but looked more at the variation between site type and tool assemblage between his two survey areas. Turpin and Davis (1990:18) conducted a survey of Devils River State Natural Area as part of the Texas Archeological Society's 1989 field school. Burned rock

middens were identified on the banks of intermittent streams, in canyon bottoms, and on upland divides, suggesting a preference for flat, open areas. They concluded that midden locations are tied to resource zones with no preference for upland or canyon localities; however, they noted canyon localities near water showed signs of more intensive use (Turpin and Davis 1990:20).

Excavations have occurred at several sites in the region, however research at Hinds Cave (Shafer and Bryant 1977) and, to a lesser extent, Baker Cave (Hester 1983) have provided the most significant data related to prehistoric diet in the region, specifically the consumption of plants processed in earth ovens. Investigations at the two caves were conducted in the 1970s and 1980s and a variety of plant remains were recovered and analyzed to create a subsistence model for the region. Several theses and dissertations came out of the research at Hinds Cave and Baker Cave addressing the macro and micro botanical remains, coprolites, organic residues, and faunal remains which were very well preserved in the dry protected shelters (Dering 1979; Edwards 1990; Reinhard 1988; Sobolik 1991; Stock 1983; Williams-Dean 1978; Woltz 1998).

The results of these analyses indicate that prehistoric inhabitants in the Lower Pecos had a broad subsistence base including a variety of animals and plants, including xeriphitic plants such as sotol, lechuguilla, prickly pear, etc. Plant and animal remains associated with cooking features, and obviously coprolites (the byproduct of food consumption), are the principal markers for shifts in diet and suppositions about the environment especially with regard to intensification. As a result of the studies at Hinds Cave and Baker Cave, the diet of the Archaic inhabitants of the Lower Pecos is well established, as is the necessity of using earth ovens for processing plants such as desert

xeriphytes. Thus, the food remains serve as one variable for determining periods of subsistence intensification.

One of the first descriptions of the structure of earth ovens comes from Wilson (1930). Wilson described the size, orientation, and composition of burned rock middens in southwest Texas and also related the story of F.M. Buckelew, a captive of the Lipan Apache in 1866. Buckelew described the whole process of roasting sotol in earth ovens, including the size of the pit (several feet in diameter and three to four feet deep), the arrangement of rock, the packing material used, and the dirt capping the pit. Pearce and Jackson (1933), during their excavations at the Fate Bell Shelter, mapped the locations and sizes of seven pits. Attention was given primarily to the function of the pits rather than their formation, with the exception that the apparent intentional placement of ashes and sotol remains on opposite sides of the pits was noted. Ross (1965) identified pits lined with limestone slabs in Eagle Cave, but did not describe these as earth ovens, and given the dimensions he provided (1 to 2 feet in diameter), they may not be ovens. He does map the arrangement of the rocks and the size of the feature (1.5 to 2 feet in diameter) without suggesting their function.

Brown (1991) and Dering (1999) used an ecological approach to study the role of earth ovens from different perspectives. Brown (1991) presented a set of research topics that apply global climatic phenomenon and optimal foraging theory to better understand the subsistence economy of the Lower Pecos. Essentially, Brown proposed that as local climate conditions worsened, certain resources became scarce, necessitating an increased diet breadth and incurring an increased cost of acquiring lower ranked resources. Brown (1991:125) used coprolite studies produced by Alexander (1974) and Stock (1983) to

argue that evidence of dietary shifts found in the coprolites correlates with the onset of the Altithermal (ca. 7,000 RCYBP) and maximums (periods of increased drought) within that period. Based on Brown's proposal we should expect the frequency of earth ovens will correlate with local changes in climate, such as increased or decreased aridity. For example, increased aridity could reduce the amount of forage for animals and thus, the amount of meat available to a community. This shift in resource availability would force the community to seek additional food resources even at the expense of additional labor. Therefore, earth ovens, as specialized plant processing facilities, may increase in frequency during times of environmental stress. Brown (1991:100) also argued that, regardless of climate, as a community depletes the resources within their logistical radius, diet breadth should expand. This suggests that higher ranked resources should dominate the initial occupation of an area with lower ranked resources, such as those processed in earth ovens, more common later in the occupation leading up to abandonment of the area.

Dering's (1999) approach involved using five experimental earth ovens to determine to what extent, calorically, this technology could contribute to the subsistence economy of the region. Dering related the amount of food produced to the size of the central pit in the earth oven, which he based on earth oven features found in the region. He recorded the amount of rock and fuel he used to prepare the food, as well as accounting for the amount of waste rock. Dering estimated that an average of 30 lechuguilla and 25 sotol plants processed in an earth oven would yield 7,656 Kcal and 5,395 Kcal respectively, enough food for one person for three to five days. Using this approach, he concluded that the fuel and food of the resources required for earth ovens would be rapidly depleted within a given area, forcing groups to relocate to new foraging

areas. Dering's research suggests that the structure of earth ovens reflects not only that subsistence intensification was occurring, but also the number of times a feature may have been used within a particular area and how much food it could produce. Combined with Brown's research, analyzing the physical components or mass of an earth oven and its associated midden should yield information relating to the length of occupation, resource availability, and seasonal climate changes.

Subsistence Intensification and Burned Rock Features

Beginning in the Late Paleoindian period and continuing through the Archaic, decreases in large game and the increasingly arid climate in the Lower Pecos see the emergence and increased frequency of earth ovens as a shift towards subsistence intensification. Subsistence intensification is often viewed as a cultural response to increasing population or environmental pressure within a group's occupational range. These pressures require groups to adopt new strategies, primarily increased labor, to increase the food production of a given area, usually resulting in the exploitation of lower ranked or more highly concentrated resources (Binford 2001:188). In general, this means that groups which rely on hunting as a primary subsistence strategy will invest more labor into acquiring aquatic resources and plant foods if intensification becomes necessary (Johnson and Hard 2008:138). This process was suggested by Binford (2001:222):

It is reasonable to suggest that if selective forces (such as a reduction in the area needed to sustain a group) are favoring intensification of production, there may be a progression in resource exploitation down the trophic scale in the direction of lower level resources. In such a successional sequence, other things being equal, hunter-gatherers would shift from terrestrial animals to aquatic resources to, finally, terrestrial

plants in settings in which each of these options is feasible. In settings in which some constraint renders impossible one or more options, other trajectories may be expected.

While plant cultivation and animal domestication are often discussed as forms of intensification, the Lower Pecos lacks archaeological or ethnographic evidence of these practices.

The intensification of resources, specifically wild plants, by hunter-gatherers can be seen in the archaeological record by the presence of plant processing tools and facilities, such as grinding or pounding stones, mortars, and earth oven features. These types of tools and facilities, specifically earth ovens, are used to render plants more digestible and to increase their nutritional value (Wandsnider 1997). The process of cooking food results in increased nutrient density, removal of pathogens and detoxification, and increased storage life (Wandsnider 1997:3). As intensification would require the utilization of a broader range of plant species, the ability to render otherwise inedible plants edible through cooking, as well as transform them into storable units, would have been a key aspect of intensification. Additionally, groups that were able to expand their diet breadth, even at the cost of increased processing, may have had a competitive advantage over other groups as big game became more scarce (Yesner 2004:262).

Earth ovens are the most dominant features on archaeological sites in the Lower Pecos. In her review of the North American ethnographic literature describing earth oven technology, Yu (2006:78) defined some generalized tactics that surround this technology that include the procurement of highly seasonal foods, use of otherwise inedible foods, aggregation of population and labor, specialized processing technology, and the repeated

use of earth oven locations. The most common plants associated with earth oven use in Texas are geophytes, prickly pear, and plants of the Agavaceae family (lechuguilla, sotol, and yucca) (Acuña 2006; Dering 2008). Geophytes, such as wild hyacinth (*Camassia* sp.) and wild onion/garlic (*Allium* sp.) would have been seasonally harvested in the spring and early summer (Boyd et al. 2004), whereas prickly pear and Agavaceae plants would have been available year round. All of these plants generally require prolonged cooking for 36-48 hours to eliminate toxins in the plants and to convert complex chains of carbohydrates into more simple sugars that are easier to digest (Dering 1999:661; Wandsnider 1997). While the degree to which these plants contributed to the prehistoric diet is still unknown, ovens are an efficient way to cook these plants in that heat can be stored in rocks and once buried, will continue to release heat for more than 24 hours (Dering 1999:661; Thoms 2009:576).

The use of earth ovens requires a significant investment of labor to collect the necessary resources, including food, fuel, and rock, for processing plant foods in this way. An increase in the investment of labor most likely required more social organization of foraging and processing activities. Yu (2006) notes that ethnographically, groups in the Pacific Northwest tend to aggregate seasonally in organized foraging groups to collect and process wild hyacinth in earth ovens. This process is normally carried out by the women in the group. However, in the southwest United States, plant processing in earth ovens is more often associated with small, multi-family groups and less gender division of labor (Yu 2006). Additionally, earth ovens may have been employed to cook mass quantities of food to take advantage of seasonally available plants and to prevent spoilage after harvest (Wandsnider 1997:23). Periods of

limited resource abundance, such as seasonally available plants, may have necessitated the aggregation of labor and subsequent organization. As the availability of resources becomes critical, their acquisition and distribution may encourage the group to adopt a more “centralized hierarchy associated with making decisions about group movement, trade, and both intragroup conflict and intergroup warfare” (Yesner 2004:273).

Although several methods can be utilized to create an earth oven, the general process involves a layered arrangement of heated rocks, packing material (such as prickly pear, grasses, or other green plant material), food, and a cap of sediment to retain heat (Ellis 1997:66-76). The packing material acts as both insulation and a source of moisture for steaming, and in some cases additional water may be added to intensify steaming (Ellis 1997:66-76). Once the food has been cooked, overlying sediments are removed and the food is removed for consumption or additional processing, leaving behind the rocks making up the “oven bed” (Black 1997a:259). Use of earth ovens appears to have been the most common means for cooking otherwise inedible plants throughout the Archaic and Late Prehistoric periods in the Lower Pecos.

Although in some areas of North America earth ovens were also used to process meat, their primary utility is mostly attributed to the processing plants that require extended cooking times to render them edible. Meat, in general, requires substantially less or no cooking time. Ethnographic accounts reported by Wandsnider (1997:22, Fig. 6) indicate some commonly pit roasted meats (bear, pork, fowl, reptile) require an average of less than 10 hours of roasting time and larger portions of meats (bison, deer) require between 10 and 20 hours on average. However, Wandsnider (1997:21) suggest that the pit roasting of meats was most advantageous when large portions were required

to be cooked or when a large group of people needed to be fed at one time, such as a feast. In 110 ethnographic cases reported by Wandsnider (1997:19), 77.3 percent of earth ovens were used to process plants, 17.3 percent to process animals, and 5.4 percent to process a combination of both. This distribution indicates that earth ovens are a specialized technology primarily adapted for plant processing.

Burned rock middens represent the accumulation of waste rock material from earth oven cooking episodes. Black and Creel (1997:295) argue that burned rock middens result from repeated use of “center-focused” cooking facilities. The defining characteristic of burned rock midden features is the presence of a primary structural element, such as a centrally located rock-lined pit, which marks the locus of activity (Black and Creel 1997:295). The morphology of the typical burned rock midden is the result of the repeated discard of the waste material around the center; often times manifesting archaeologically as a mounded ring or debris cone (Black 1997b:84-85). Thus, the amount of burned rock waste material should reflect the number of times a particular facility was used, either during a specific episode of use or repeated uses over time.

Earth ovens are obviously not the only source of burned rock. Other sources include open air hearths for warmth, grilling, drying meat, and heating rocks to use as boiling stones (Figure 2) (Thoms 2008; Thoms 2009:577). Boiling stones placed in above ground containers or in water filled pits were used to cook a variety of foods, both plants and animals. Cabeza de Vaca observed the use of boiling stones to cook beans and squash in gourds by indigenous groups living along the Rio Grande (Krieger 2002).

Additionally, boiling water is necessary for extracting the grease from animal bones as evidenced at the Sanders site (Quigg 1997) and the Rush site (Quigg and Peck 1995).

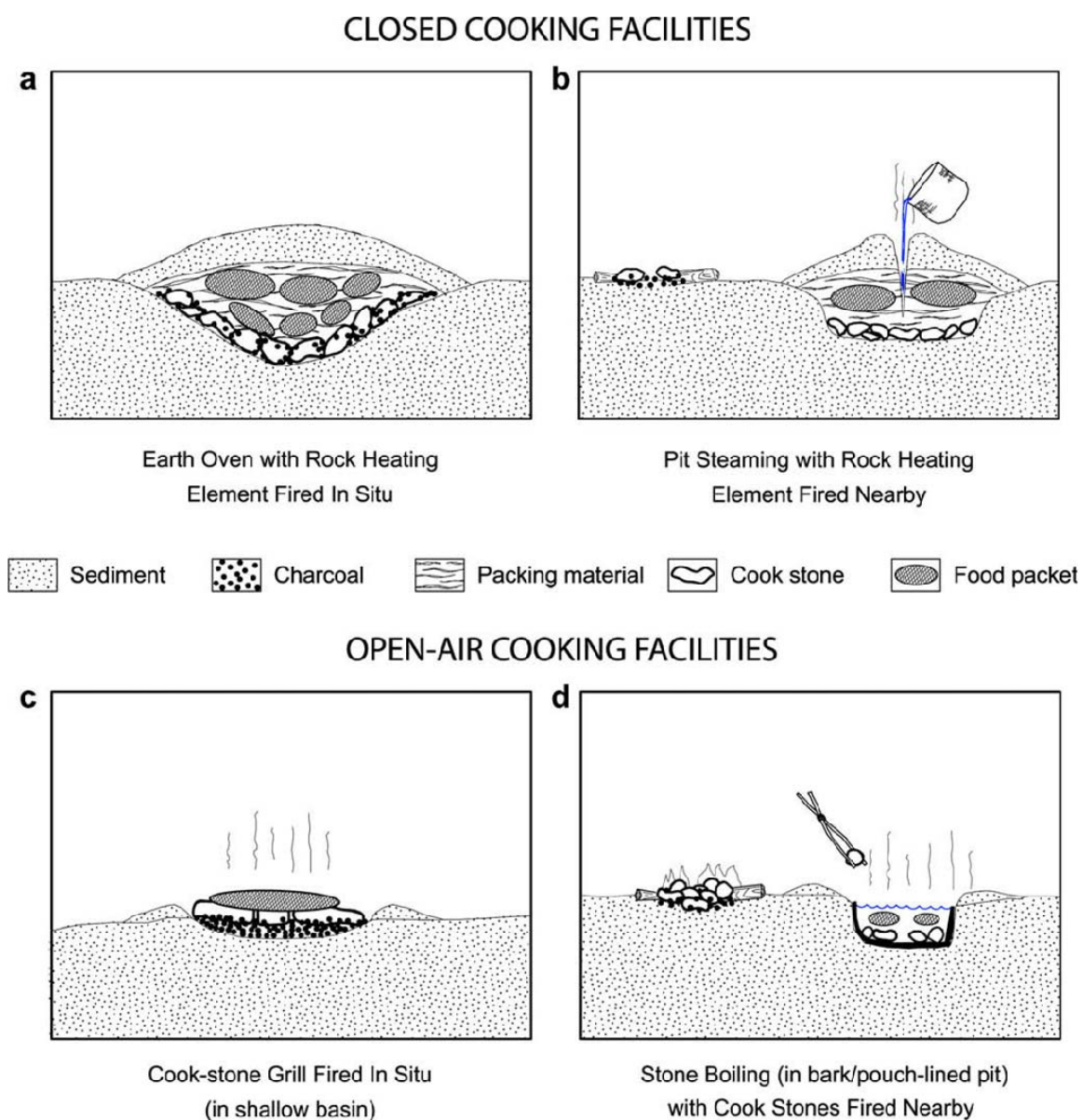


Figure 2. Examples of hot rock cooking facilities, courtesy of A. Thoms (Thoms 2008:Fig. 3).

The use of open air cooking facilities requires no investment in hot rock technology and thus reduced labor costs, however, the loss of heat in open air facilities is considerable when compared to storing heat in rocks and then insulating these from exposure. Open air facilities would likely result in more fuel consumption focused on shorter term cooking episodes (Thoms 2009:576). In this sense, feature type most likely reflects the processing of specific food types rather than a technological evolution in cooking facilities. As such, the increasing presence of earth oven features within a specific area may indicate a shift towards subsistence intensification, specifically plant processing, among a regional population and therefore, these archaeological remains may serve as a proxy for measuring intensification at both the local and regional level (Thoms 2008).

While the presence of earth ovens alone may indicate intensification of plant resources, the number of earth ovens, and the number of times they are reused, or “fired,” will provide a clearer indication to what degree the technology was utilized. Earth ovens in the Lower Pecos range from discrete, low volume features that may have been fired only one or a few times to larger, expansive middens that may represent several hundred firing episodes. The number of times an earth oven has been fired has been estimated through experimental archaeology and ethnographic accounts. The estimates often rely on the quantification of the burned rock mass and/or count towards determining how many times a specific cooking facility may have been used. Although, these estimates are imprecise and not universally applicable, they provide a reference for estimating the degree of use of features.

Estimating the number of firings is difficult because each feature may vary as to the amount of fuel, food, packing material, the size of the central pit, the amount of rock,

and the amount of waste rock generated in each firing. Within the archaeological record it is likely that only the rocks and possibly the central pit (either defined by charcoal remains or rock lining) will be the most commonly surviving elements of the feature. Complicating matters, the use and reuse of earth ovens may displace artifacts from previous occupations, which may occur in the surrounding matrix, as soil is borrowed from one location to cap the oven and then removed and redeposited in another location (Leach et al. 2005). The rearrangement of the feature location could result in diagnostic artifacts, such as projectile points or datable organics, occurring in secondary deposits, the disturbance of previous central heating elements, or the rearrangement of waste rock. Other formation processes subsequent to the use of the feature may include erosion of the feature sediments, displacement of surface rocks by erosion, animals, or people, and subsurface bioturbation by plants and burrowing animals. Earth ovens within the Lower Pecos are most susceptible to erosion due to the sparse vegetation.

The analysis of a burned rock midden at the Panther Springs Creek site (41BX228) was one of the first attempts to quantify feature size as it relates to the behavior surrounding earth oven use (Black 1985). As part of the analysis, Black (1985:299) used rock weights from an excavated sample area to estimate the overall density of burned rock within the feature (per cubic meter), which he then multiplied by the estimated volume to estimate the total rock weight of the feature. His results produced a range of values for the feature, ultimately concluding the estimated total weight of rock within the midden was 104,084 kg, which he states is a conservative estimate. Black proposed that estimates of volume and rock weight from earth ovens and burned rock middens, when compared across multiple sites, would be useful in

formulating hypotheses regarding the behavior associated with these features. He also proposed that experimental processing is necessary to identify the variables related to earth oven activities.

Black (1997a:265-266), in his later analysis of the Honey Creek site in central Texas, estimated the number of times a burned rock midden was used based on ethnographic accounts of sotol processing in northern Mexico and Texas (Tunnell and Madrid 1988). He assumed that an earth oven would require approximately 150 to 200 kg of rock per firing and that these rocks could be reused an average of three or four times. Applying these numbers, Black (1997a:266) estimated that a midden from the site had a total rock weight of 12,054 kg, which was divided by the 150 kg value. This resulting value was then multiplied by the number of times a rock could be reused for firing, which was four and thus he estimated the midden represented about 180 to 320 firing episodes.

Dering's (1999) experimental studies on earth oven cooking in the Lower Pecos used lechuguilla and sotol plants in five experimental earth ovens comparable to Archaic-age features. These experiments found that a single oven firing using 224 kg of wood fuel and 250 kg of rock would yield 5.1 person-days of calories and .13 m³ of rock waste (Dering 1999:665). Dering assumed that rocks in the feature may be used twice. Dering's focus was primarily on the extent earth ovens and their resulting products contributed to the prehistoric economy, as well as the costs of using this technology. He also demonstrated how rapidly plant and rock refuse can accumulate in a short period of time and how quickly food and fuel resources may be depleted across the landscape. Leach et al. (1998) also conducted investigations on an experimental earth oven using

thermocouples to monitor temperature changes in the oven and the rate of rock reuse and discard. Their experiment utilized only 63 kg of wood fuel and 91 kg of limestone rock, estimating that rocks could be used only once or twice before being discarded. The focus of their work was primarily on the temperatures sustained in earth ovens and the degree of fragmentation of the burned rocks through repeated use.

While Black, Dering, and Leach et al. provided important data on the structure of earth ovens, their data only addressed the number of firings within the contexts of their research and cannot be universally applied. A different approach for examining the frequency of earth oven use can be applied based on Black and Lucas' (1998) work at the Higgins site in Bexar County, Texas. Their analysis used various attributes of burned, such as size, weight, and number of facets, to identify strata and central heating elements within a burned rock midden. An important aspect of their research was the degree of fragmentation of the burned rocks. Their basic assumption was that as burned rocks are reused, there is an exponential increase in the number of rock fragments (Black and Lucas 1998:197).

Burned rocks at the Higgins site were identified on a continuum ranging from pristine (unfragmented rocks) to discarded rocks. All of the burned rocks greater than 7 cm in size (length) were classified in one centimeter increments. To account for variations in mass, the distribution was modified using a length-weighted histogram in which the count of each size class was multiplied by the size of that class. The distribution was used to identify and/or verify discrete strata of single use ovens or center focused oven facilities within four major populations of burned rock (Black and Lucas 1998:198). Pristine rocks and discard rocks were categorized by evaluating the

populations of general burned rock population (scattered rocks not found with discrete features) and pristine burned rock population (discrete, mostly unfragmented, arranged concentrations of burned rock) (Black and Lucas 1998:203). The distribution of the two populations were plotted as line graphs and the intersect point of the two lines was estimated to be the size threshold at which a burned would be discarded; estimated at approximately 11.5 cm (Black and Lucas 1998:206).

The primary goal of the current research is to apply the PAP method to collect data that can address questions regarding subsistence intensification. Other methods have been used in the past to collect the same data, but the hope is that the PAP method can expedite, and provide a different perspective on, feature analysis. PAP provides two main sets of data for analysis: aerial images and photogrammetric data. Aerial images provide a different perspective (overhead) of earth ovens than oblique images and can be used to analyze burned rock patterning, quantify feature parameters in two-dimensional space, and manage data within a GIS (when used in congress with a GPS the data can be managed in a real-world coordinate system). The photogrammetric data provides a three-dimensional environment in which rock size and volume can be measured. This research uses the PAP method to record earth oven features and their constituent rocks to make assumptions about the relative frequency of use of earth ovens by using the overall size of the features, the size and patterning of the individual burned rocks, and the degree of fragmentation the rocks have sustained through repeated use.

The approach used by Black and Lucas, primarily the size distribution of burned rocks, is applied to the current research to address basic questions with regard to earth ovens in the Lower Pecos. First, how does the patterning of rocks relate to either the

cultural or environmental formation processes of the feature during and subsequent to its use? Second, can the total weight of the burned rock within the feature be used to address the frequency of use of the feature? Finally, how does the distribution of the burned rocks by weight reflect the degree of fragmentation with regard to the frequency of use of the feature?

CHAPTER IV

PHOTOGRAMMETRY AND POLE AERIAL PHOTOGRAPHY

The primary goal of this research is to use photogrammetry to record burned rock features to obtain metric data, which can then be used to analyze the spatial attributes of individual rocks within the feature and the feature as a whole. To accomplish this, a method called Pole Aerial Photography (PAP) was adapted to incorporate the use of a stereo pair of digital cameras to collect photogrammetric data of features. PAP is nothing more than a camera mounted at the end of a long pole with a remotely operated shutter. The use of PAP is prominent in the real estate industry for obtaining overhead, oblique photos of properties. The method used here follows the same premise of commonly used PAP techniques except photographs are taken vertically from directly over the feature with a stereo pair of cameras. This chapter briefly defines photogrammetry, explains how three-dimensional points are obtained from photographs, and describes the PAP equipment and methods used in this research.

Photogrammetry

Photographs provide both qualitative and quantitative data and are important tools in archaeology. Quantitative data can be extracted from photographs using photogrammetry, which is the “science of measuring photos” (Linder 2006:1). Photogrammetry is commonly applied to measurements in two-dimensional space using a

scale or reference points in a photograph. For example, if a metric scale is placed in the photograph of an artifact, the size (length, width, area, etc.) of the visible portions of the artifact can be determined. When a single photograph is used, the quantitative data can only be referenced within two-dimensional space. To obtain data within three-dimensional space, the subject must be photographed two or more times, each from different camera positions. This method is a form of stereoscopic viewing that works on the same premise as human eyes. Just as human eyes are able to render the world we see in three dimensions, photographs of the same subject from different perspectives can be combined to render the subject three-dimensionally. However, unlike the human eyes, photographs provide a permanent and quantifiable model. When used as an analytical tool, the use of photographs and photogrammetry to capture and render subjects three-dimensionally is a form of remote sensing (Linder 2006:1).

Traditionally, stereo models were created using cameras oriented along a single axis, similar to the alignment of the human eyes. A common application of this method is in aerial surveying for producing topographic maps (Arlinghaus et al. 2004). In aerial surveying, photographs are taken from an airplane at a fixed altitude at intervals along a transect so that photographs partially overlap the subject area. For close range photography this same method can be applied with a single camera or a stereo pair of cameras. Creating an accurate three-dimensional model relies on sufficient overlapping of the photos so that matching points on photographs can be matched with their corresponding positions on the camera's exposure medium (film or digital sensor) and a relative position in real space can be determined. While some current computer applications can assemble three-dimensional models from pictures taken from any angle,

using a systematic method of photography, such as photographing on a transect or with stereo pairs of cameras, ensures a sufficient overlap for a higher degree of accuracy.

Two-dimensional coordinates (X, Y) can be established easily in a single, scaled photograph, but generating three-dimensional coordinates (X, Y, Z) relies on multiple, overlapping photos. Coordinates are derived from these overlapping photos using the process of collinearity (Linder 2006:47; Wong 1980:88). Collinearity is the relationship between the ground coordinates of a desired point, the center of the photograph's projection, rotational coefficients, the photograph coordinates of the principal point (x_p, y_p, z_p), and the focal length (f) of the camera. Assuming an image point of j in photograph i , where x_{ij}, y_{ij} are the photo-coordinates, the ground coordinates can be expressed as X_j, Y_j, Z_j and the projection center can be expressed as X_i, Y_i, Z_i . The rotational coefficients are derived from calculations based on the camera's rotation about the X, Y , and Z axes and is expressed as m_n . This relationship is expressed in the following equation (Wong 1980:88):

$$x_{ij} - x_p + \frac{f[m_{11}(X_j - X_i) + m_{12}(Y_j - Y_i) + m_{13}(Z_j - Z_i)]}{m_{31}(X_j - X_i) + m_{32}(Y_j - Y_i) + m_{33}(Z_j - Z_i)} = 0$$

$$y_{ij} - y_p + \frac{f[m_{21}(X_j - X_i) + m_{22}(Y_j - Y_i) + m_{23}(Z_j - Z_i)]}{m_{31}(X_j - X_i) + m_{32}(Y_j - Y_i) + m_{33}(Z_j - Z_i)} = 0$$

This is a complex equation and is presented here only to demonstrate mathematically how points in three-dimensional space are resolved from two photographs. Today, these equations are handled by photogrammetric software that also corrects for lens distortion, calibrates the photographic equipment used, and controls for other inconsistencies that

can arise during field collection, such as variable rotational coefficients, that can affect the accuracy of the results.

The accuracy of stereophotogrammetric data is dependent on several factors, but is primarily related to the base-height ratio relative to the target and the field of view of the cameras (Linder 2006:13). While the field of view of a camera is fixed, depending on the choice of lenses and its internal geometry, the base distance between a pair of cameras can be adjusted for more or less accuracy. In general, by increasing the base distance, accuracy will improve, however this will also decrease the overlap between photos, limiting the areas that can be analyzed (Linder 2006:14). Overlap can be increased by either increasing the height of the cameras, or by using convergent camera positions (i.e., pointing the cameras toward each other). In relation to human eyesight, the closer a person is to an object, the more relief they are able to see in that object. As distance from the object increases, details in the relief become less apparent. The same premise is underlying camera positions in stereophotogrammetry (Linder 2006:8). Therefore, the idea is to find a suitable balance between overlap, base-height ratio, and field of view.

Another element related to the accuracy of the collected data is camera perspective, or which way the camera is pointed. The advantage of using a stereo-pair of cameras is the consistency in perspective between the pairs of images. This reduces errors that can occur along the X , Y , Z rotational axes if a single camera is used. Additionally, vertical orientation of the cameras maintains a consistent perspective when taking multiple pairs of images across a large area.

Methods

Based on the principles of photogrammetry, I constructed a PAP device (Figure 3) and a method for employing PAP to model burned rock features three-dimensionally and obtain individual rock weights and the total rock weight of the feature. From the three-dimensional model, it is possible to extract the volume of individual rocks and convert the rock volumes to rock weights. Thus, the total weight of all of the rock across the whole feature is obtained through the sum of the individual rocks. Since PAP has not been applied to earth ovens before, I had to design a device and develop a method for using that device. The primary objectives in building and implementing the PAP for use with earth ovens were:

1. Design a PAP device that is easy to construct from easily obtained and affordable materials.
2. Design a PAP device that would capture images perpendicular to the ground surface.
3. Establish a base-height ratio sufficient for accurate data collection.
4. Establish a method that greatly reduced the time of recording burned rock features over traditional methods.

Objectives 1 through 3 were accomplished during this research, however objective 4 was only partially accomplished. Objective 4 was to reduce the time in recording, and while the PAP recording of features in the field was much faster than measuring and mapping rocks by hand, the software used in this research was cumbersome, increasing post

processing time of the photos beyond what could be obtained by traditional methods.

The equipment, field methods, and software are discussed in more detail below.



Figure 3. PAP Equipment without pole.

Equipment

The first step in this process was designing and building a suitable device for mounting the cameras. For the pole, there are several commercially available telescoping poles ranging from painter's poles to vehicle mounted poles that crank into position. Some photographers have also used catfish fishing poles from Europe that can reach lengths of 13 meters. After researching the various options, the most convenient and

affordable solution was a standard painter's pole purchased from a hardware store. To obtain images perpendicular to the ground surface it was necessary to mount the cameras to a swivel so that, regardless of the pole's angle with the ground, the cameras would face straight down. This was accomplished using a standard paint roller with a thin cedar board (trimmed fence board) attached by U-bolts around the roller. The board was used to facilitate the attachment of a mount for the cameras. The camera mount was a 48 inch long aluminum L-bar that was attached to the board with lag bolts. Holes were drilled into the L-bar so that the cameras could be placed 50, 75, or 100 cm apart. A thin strip of adhesive crafting foam was affixed to stabilize the mounted cameras. The cedar board and aluminum L-bar were chosen because of the resistance to rot and mildew of the former and the low weight of the latter. Standard wing nuts were used to mount the cameras. Once finished, the pole simply screws into the handle of the paint roller.

The cameras used for this research were two Canon PowerShot A590 IS point and shoot digital cameras with a resolution of eight megapixels and removable SD card storage. These cameras were used because they have a manual use option, are compatible with the Canon Hackers Development Kit (CHDK), and are relatively inexpensive. CHDK is firmware that is open source and developed by various programmers that expands the functionality of some Canon PowerShot cameras. The internal geometry of these cameras is provided below in Table 1. At the time of this research, this Canon model was no longer being produced. However, there are several models of Canon cameras that meet the above criteria.

Table 1. Internal Camera Geometry

Sensor	1/2.5"
Aspect Ratio	4:3
Sensor Width	5.744 mm
Sensor Height	4.308 mm
Sensor Diagonal	7.180 mm
Focal Length	6 mm

The Canon brand was chosen primarily because of the CHDK firmware that allows for expanded functionality of the camera, especially stereophotogrammetry and the use of a USB remote shutter release. The use of a stereo pair of Canon cameras is facilitated by a firmware module for CHDK called SteroData Maker (SDM). The current firmware is the result of collaboration between programmers via a Yahoo group. The cameras were triggered using a gentSTEREO-proSDM remote purchased from Gentles Limited in the United Kingdom through the USB cables provided with the cameras and two 10-foot USB extension cables. This remote can only be used with the CHDK firmware and SDM module. Velcro cable straps were used to hold the cable to the pole and out of the photos. Finally, ground control targets were printed on yellow cardstock and heavy steel washers were taped to them to weigh them down. Pale yellow cardstock was chosen because during the initial testing of the equipment, it was determined that white targets reflected too much light, overexposing and obscuring the photos.

The cost to build this device was just under \$700 and the cameras were the bulk of that cost at \$250 each. The gentSTEREO-proSDM remote was approximately \$70 with shipping. The painter's pole and aluminum L-bar were purchased for about \$40 each from a hardware retailer. All remaining hardware, including the USB cables, was purchased for about \$30. For the purposes of this study, a waterproof case (Pelican) was

purchased to hold both cameras, the remote, and ten SD cards for about \$70. Ten SD cards were purchased so that individual features could be kept on separate cards since there was no viable option for downloading photos from the SD cards in the field. Both the CHDK software and the SDM software module are open source, available free on the internet, and carry no licensing or use restrictions. The materials and equipment used here were chosen primarily because the materials were easy and affordable to obtain and the device was simple to build. Several other options exist for camera brand, self-built remotes, and material selection that may reduce the costs. Since the cameras represent the bulk of the costs, anyone constructing a device should consider cameras that are already available to the researcher.

As mentioned previously, the CHDK and SDM firmware is necessary to use the gentSTEREO-proSDM remote. This firmware is the result of efforts by individual developers to expand the functionality of Canon cameras. The basic CHDK firmware¹ greatly expands the manual functions of the cameras as well as providing several automated functions that are not available through the Canon firmware. Some of the expanded functions include bracketing, RAW image collection, use of USB remotes, and motion detection. Since the firmware is open source, users can also develop their own scripts for personal customization. The SDM firmware² is a developer modification of CHDK intended for three-dimensional photography with kite aerial photography (KAP), PAP, and other methods. The firmware is installed to the camera's removable media (SD or CF cards) and then the card is manually locked. When the removable media is

¹ Information about the CHDK and the software is available at http://chdk.wikia.com/wiki/Main_Page

² The SDM software includes the basic CHDK software and is available, with supporting documentation, at <http://stereo.jpn.org/eng/sdm/index.htm>

installed and the camera is powered on, the CHDK/SDM firmware will override the manufacturer's installed firmware. The user can then navigate through the SDM menus and submenus to adjust settings. It is important to note that the firmware does not alter the manufacturer's firmware and once the media is removed the camera will revert to the normal firmware. The CHDK/SDM firmware is independently developed and Canon does not offer support for any problems that may arise. The firmware is simple to use, however, and the only options within the firmware that were required for this research were designating each camera as left or right and setting the distance (base) between the two cameras. Each camera was also labeled left and right on the exterior of the camera and each SD card was designated as left or right and lettered (i.e. A-Right, A-Left, B-Right, B-Left, etc.). The CHDK/SDM firmware had to be installed on each SD card.

Aligning the Cameras

Once the PAP device was built it was necessary to establish what the proper height of the pole should be relative to the distance between the two cameras (base-height ratio). During the initial testing of the equipment, certain limitations with the equipment and the environment were identified. The primary limitation during the research was the stability of the PAP equipment, which was primarily related to the length of the pole. First, at the maximum pole length of 5.5 meters, the weight of the cameras created an unstable system. Second, the base distance between the cameras affected the stability of the pole and the ability of the photographer to keep the cameras relatively level. It was discovered that reducing the base distance significantly increased the stability of the equipment. High winds in the Lower Pecos region also reduced the stability of the

equipment, which was ameliorated by reducing pole length and camera base distance. Additionally, the pole had to be held at an angle less than 90° from the ground surface to avoid capturing the pole or the photographer in the photos. To calculate the vertical distance from the ground to the cameras, a pole angle of 60° from the ground surface was estimated based on the photographer holding the pole an arm's length from the body (Figure 4).

A review of photogrammetric literature suggested establishing a base-height ratio between 1:5 and 1:15 (Grussenmeyer et al. 2002:303; Karara 1980:815) for architectural and archaeological projects using close range photogrammetry. Furthermore, Light (1980:953) suggests maintaining at least a 60 percent overlap between photos. The percent overlap, O , can be obtained by dividing the product of the base-height ratio, R , and the focal length, F , by the sensor width, S , minus one, or:

$$O = \frac{R(F)}{S - 1}$$

Based on the internal geometry of the Canon PowerShot A590 IS and using this equation, a 1:5 ratio would result in a 79.1 percent overlap in the photos and a 1:15 ratio would result in a 93 percent overlap. A matrix was created to plot pole length, or slope distance (S_D), versus the vertical distance to the target (V_D) to establish a good balance between accuracy of the collected photos and stability of the equipment (Table 2).

Table 2 lists the base distance available for the cameras based on the equipment design at 1m, 0.75m, and 0.5m. For each base distance the vertical distance was listed for 1:5, 1:10, and 1:15 base to height ratios. The pole length, or slope distance, was calculated using simple trigonometry, based on the 60° angle with the ground surface.

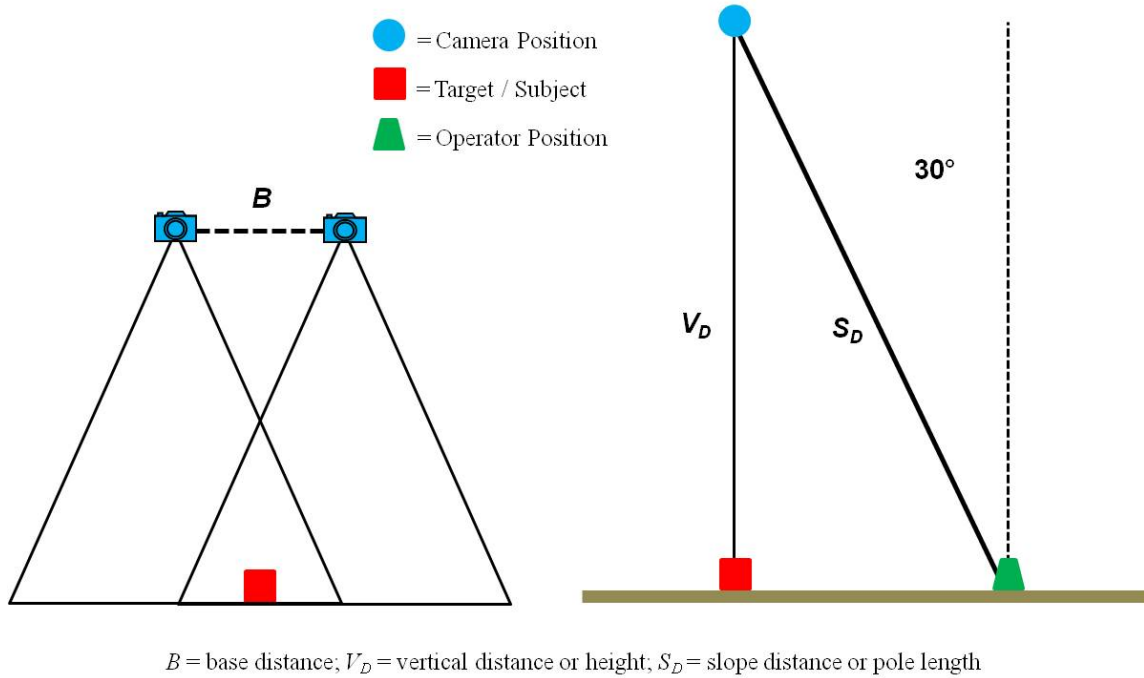


Figure 4. Geometry of the PAP.

Table 2. Pole length based on base-height ratio

	<i>Base = 1m</i>		<i>Base = 0.75m</i>		<i>Base = 0.5m</i>	
<i>Base to Height Ratio</i>	V_D (m)	S_D (m)	V_D (m)	S_D (m)	V_D (m)	S_D (m)
1:5	5	5.77	3.75	4.33	2.5	2.89
1:10	10	11.55	7.5	8.66	5	5.77
1:15	15	17.32	11.25	12.99	7.5	8.66

Any pole lengths over 5.5m had to be excluded leaving only two options, a pole length of 4.33m or 2.89m. The 4.33m pole length was chosen as this had an increased vertical distance, which increased the field of view of the camera. Since the pole length of 4.33m with a base distance of 0.75m results in a 1:5 ratio, a 79.1 percent overlap of the photos is obtained.

PAP Field Methods

Recording features with the PAP required the consideration of the ground cover, lighting, and feature extent. The features selected for PAP had to be cleared of vegetation prior to photographing. This was accomplished with hand clippers and in some cases a weed trimmer. The weed trimmer was useful, but in some cases it was also destructive in that it could move the smaller rocks (<5cm). In general, the focus was on removing the larger shrubby and woody vegetation that could obstruct camera views or hinder photographer mobility, rather than the smaller vegetation such as grasses. Only natural lighting was used and, due to the overhead position of the cameras and pole, it was necessary to avoid shooting at midday when the sun was at its zenith, as this would create shadows of the pole and cameras in the photos. Additionally, it is important to shoot the entire feature at the same time to maintain consistent lighting within all of the photos. The composition and the features within the photos are all used to match these images so a three-dimensional model can be rendered. Excessive shadows, poor lighting, or poor focus can all adversely affect the outcome of the model. The final consideration is the spatial extent of the feature, as this will determine how many ground control points need to be laid out and how much of an area needs to be cleared.

Once the feature had been cleared of vegetation and the subject area defined, a long tape was positioned along one side of the feature, oriented north to south. Ground control targets were then placed at one meter intervals along the tape. The tape was then oriented east to west and additional targets were placed along the tape. Once these two baselines were established, the remaining ground control targets were positioned to create a one meter grid across the feature. These non-baseline targets were simply eyeballed in,

creating an approximate, but sufficient, grid. The overall size of grid was based on the desire to have at least one line of ground control targets just beyond the perimeter of the feature/subject.

After the grid was established, a quick sketch map was drawn showing the relative position of each target by its number. It is important to note here that the ground control targets used in this research come from the PhotoModeler Scanner software and were coded for use with that software. Each target has a unique geometric code that the software recognizes and a number. Although this software was not ultimately used, these targets provide solid reference points that work with other photogrammetry software and also for manually aligning photos, if necessary. Furthermore, the geometric patterns can be viewed in the photos and matched to their numbers, which were not usually visible in the photos. While the arrangement of the numbered targets was arbitrary, recording the number on each target, and its relative location, on the sketch map made it possible to match the geometric pattern on the target in the overhead photo to the number and thus link it to the individual rocks in the map. In general, ground control targets should have some sort of unique reference that the photographer can use for orienting the photos during post processing.

After the grid was established, one corner was chosen in which to place a carpenter's square and chalkboard with the relevant site and feature information. The carpenter's square was used to provide a definitive 90 degree angle to reference in the photos for establishing the coordinate system in post processing. A two meter pocket stadia rod was positioned along the feature, oriented north to south, to provide both a

scale and north reference. A crew of two people can lay out the grid and scales in about five to ten minutes.

The pole-camera assembly was then put together and, using the remote, photos were taken parallel to the established grid. To take these photos, the pole was held by the photographer at an approximately 60° angle with the ground surface, with the paint roller assembly allowing the cameras to swivel into a downward facing position. The pole was positioned so that the resulting photos would be parallel to the grid. For this research, a pair of photos was taken with the base of the pole at every ground control target, approximately one meter intervals (Figure 5). Along the edges of the grid, it was necessary to estimate, due to the angle of the pole, the one meter intervals beyond the targets so that all of the targets were captured in the photos. Photos were taken moving up one grid line and then back down the next (either north-south or east-west) so the pole and cameras maintained a consistent position. The one meter interval was chosen to ensure at least 60 percent overlap between all of the photos and to maintain a systematic order to the photos.

The field of view for the cameras (61.8°) calculated from the internal geometry, was applied to an average camera height of 3.75 meters above the ground. This resulted in images covering an area approximately 3.6 m wide by 2.7 m high, or a 9.7 m^2 area. This translates to a scale of approximately 1:625 with a pixel size of approximately 1 mm^2 . The coverage area and the size of each pixel were also compared to the stadia rod and carpenter's square within the photos and these values are consistent with those scales. Based on the field of view of the cameras, the one meter interval allowed for sufficient overlap of the features in the images. Using the equation for percent overlap described



Figure 5. PAP assembly in use.

above and assuming a one meter base distance between exposure pairs, an overlap of 63.9 percent is obtained, which is still above the 60 percent threshold. Additionally, following a grid in a systematic fashion is important for manually checking the coverage of the photos and noting their relative position, as well as processing the photos in the modeling software, either manually or automatically.

The majority of the PAP work was conducted on bright, clear days in the summer and winter months. The camera exposure was set to an F-stop of 4.5 and a shutter speed of either 1/800 or 1/1000 depending on light conditions. The camera shutters were triggered with the remote, which was pressed once to autofocus the cameras and then pressed a second time to snap the shutters. While the camera shutters always snapped simultaneously, it was discovered that the cameras did not always autofocus at the same time with a difference of as much as three seconds. If the remote was triggered before one of the cameras auto focused, the shutters would get out of sync. The particular cameras used in this fieldwork would beep once they auto focused, a sound which was sometimes hard to hear, but helpful; although maintaining a little patience and allowing about 5 seconds between remote triggering proved to be most prudent.

Once the PAP was completed of a given earth oven, a Magellan Professional MMCX GPS receiver mounted on a tripod was used to record the geographic locations of the four corners of the grid at ground control targets. The GPS was set to collect locational data for no less than three minutes to achieve reasonable accuracy (ca. 30 cm). A sketch map was then drawn of the grid showing the locations and numbers of the ground control targets. The length, width, and weight of select rocks were recorded using a folding ruler, bucket, and hanging scale. Rocks were selected for measuring if they were estimated to be greater than 10 cm in length and were completely exposed on the surface. The length of each rock was measured along its longest axis and the width was measured at the widest point perpendicular to the long axis. These values were recorded in a table and each rock was assigned a letter ID to avoid confusion with the numbered ground control targets. The location of each rock was also drawn on the sketch map so

that it could be correlated with the final model. However, for three of the features the rocks were labeled on an aerial photo made from a composite of the PAP images. This could be done because the measuring of the rocks was conducted at a later time than the PAP, and this proved to be a much easier and more accurate process than drawing a detailed sketch map of the feature.

Post Processing of the Images

Once the PAP images were collected, the photos were downloaded from the SD card to a personal computer and stored on an external hard drive, organized by feature and left/right origin. Once downloaded, the images were examined to ensure the exposure and coverage was complete. The metadata for each image was also checked for any inconsistencies. For this research the CHDK software in the cameras was set to capture JPEG (~4 MB) and RAW (~10 MB) images, although the RAW images were not ultimately used. Since the CHDK software did not label image files as left or right, these files were renamed to identify them as such. It was important to erase the images from the SD card after downloading them and to make sure the exposure counter in the camera was set to start at one when an empty card was inserted. This would ensure that the image pairs had the same file name, albeit stored on separate SD cards.

Four computer applications were used to process the collected data and these were selected based on availability, cost, and preference; other applications may prove to be more appropriate. The first application was Microsoft ICE (Image Composite Editor), which is free to download. This software is designed to stitch photos for panoramas, but was used to create composite, overhead aerials of the features. This software worked

very well for that purpose and only a few minor errors were observed, mainly minor distortion in some parts of the composite image. Microsoft ICE allows some editing of the composite image such as cropping and adjusting resolution and composite images can be exported from this software in various file formats. The composite images were used to identify and map rocks within the features, and were also imported into ArcMAP and georeferenced using the collected GPS data. ArcMAP was used to map the features within a geographic information system (GIS) relative to site boundaries and physiography. The individual rocks in each feature were also traced in ArcMAP so that they would be referenced in a GIS and so scaled plan maps of the features could be produced.

Three-dimensional models of the features were created using 123D Catch from Autodesk, which is also free to download. This software combines uploaded photos on its server and creates a three-dimensional model resolving spatial coordinates and calibrating the cameras based on camera position and the image metadata. This software also worked very well, although in some cases it could not match some images to the model. In these cases, it was necessary to manually match points or features between the images. Essentially, this software creates a point cloud from the combined images and then a polygonal mesh. Once the model has been created, it can be oriented to an arbitrary grid and scale. The software has a measurement tool, but this simply measures distances based on a designated scale. Models in this application can be exported in various file formats that are compatible with AutoCAD and other 3D modeling programs. Ultimately, this software was used merely to create models for visual purposes since quantifications in this program are limited to linear distance measurements.

The final application used was created specifically for this research by Dr. Dinesh Nair, Chief Architect in the Vision Research and Development division of National Instruments Corporation (NI). NI is a global corporation, headquartered in Austin, Texas, that specializes in a graphic based software tools for engineers and scientists. Dr. Nair's work is primarily related to three-dimensional vision and analysis and his contribution to this research was pro bono as it paralleled his current research. This Stereo3D software was created using LabView (NI's graphical programming platform) and was based on photograph recognition software used by NI. This software was designed to measure the volume of the individual rocks in each feature and was used because a commercially available application was not found with the same functionality. In fact, exhaustive research into measuring volume in abstract three-dimensional models yielded very few indications that other researchers are involved in this type of analysis. Overall, this software was cumbersome and time consuming, which is primarily a result of limited time for developing the software. However, it was an accurate tool for obtaining volumes for rocks and that was the primary goal.

The NI software basically measured the volume of a designated area by calculating the volume of pixels within that area. A depth image model was created in the program from an image pair using the process of collinearity. The software had three screens for processing the photos. On the first screen (Source Images) the left and right images of a stereo pair were loaded into the program (Figure 6). Once the images are loaded, the user executes the program's matching function. No other actions are necessary on this first screen.

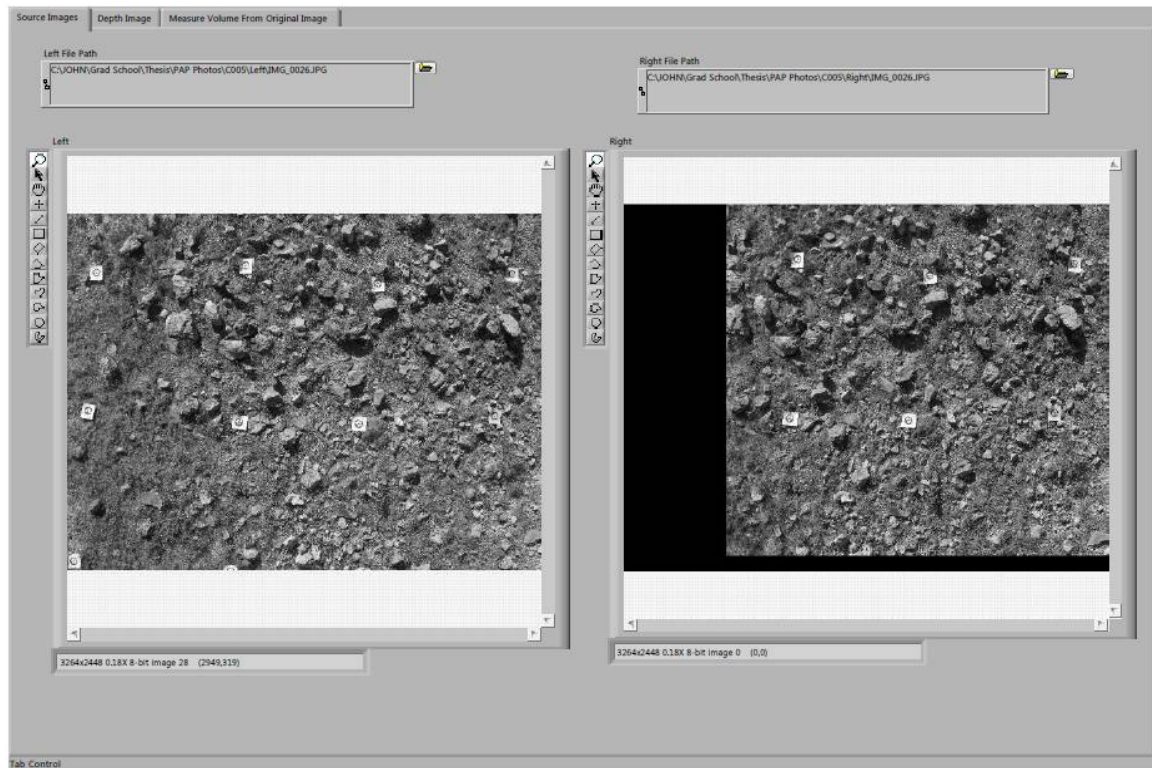


Figure 6. First screen of Stereo3D program where left and right images are loaded.

As the software did not automatically calibrate the images to the camera, the images had to be manipulated manually to get an accurate match. Calibration was accomplished by adjusting the X-axis and Y-axis locations of the photos on the second screen (Depth Image) of the program (Figure 7). The X and Y offsets could not be predicted, but were adjusted up or down by an interval of one unit until a clear model of the target rock or rocks was obtained. The resulting model was a grayscale image with variations in contrast representing variations in disparity between the rocks (brighter) and the ground surface (darker). This depth image generally resembled an hourglass shape with areas outside the hourglass being too distorted to render based on the X and Y offsets of the photos. The X and Y offsets of the photos could be further adjusted to move the correctly calibrated area of the model to capture different portions of the image



Figure 7. Second screen showing the depth image and disparity value.

pair. The volumes for one to five rocks, depending on their position relative to the image, could be processed from a single pair.

Once the depth image was created, an individual rock volume would be measured using the third screen (Measure Volume from Original Image). To do this, an outline of the selected rock was traced over either the left or right image (not the contrasting depth image) using a drawing tool in the program; either image was suitable to use (Figure 8). Rock Z in feature C005 is used as an example in these screenshots of the program. The internal geometry and camera positions were already programmed into the software, but it was necessary to provide the program with the disparity value of the ground surface adjacent to the selected rock (Figures 7 and 8). The ground disparity value was obtained by switching back to the depth image and hovering the mouse cursor over the ground

surface adjacent to the rock. The ground disparity value would be displayed at the bottom of the image (Figure 9). Once this value was entered on the third screen, the “Calculate” button was clicked to generate the volume of the outlined area in both cubic millimeters and cubic centimeters. The volume was recorded in an Excel spreadsheet so that it could be converted to a weight and compared to the weights measured in the field.



Figure 8. Third screen where volume is measured from the original image.

The major limitation of the Stereo3D program consisted of significant distortion of the images around the edges of the model. This limited the amount of space that was accurately displayed and thus increased the time to process all of the feature photos. Additionally, the software only processed one image pair at a time, also increasing the processing time. Due to these limitations it took between 30 and 40 hours to process the

Sensor Width (mm)	Sensor Height (mm)	
<input type="text" value="5.744"/>	<input type="text" value="4.308"/>	
Focal Length (mm)		
<input type="text" value="6"/>		
Pixel Width (mm)		
<input type="text" value="1"/>		
Baseline Distance (mm)	Ground Disparity (pixels)	Ground Distance (cm)
<input type="text" value="750"/>	<input type="text" value="1371"/>	<input type="text" value="330.509"/>

Figure 9. The camera geometry and ground disparity entry field from the third screen.

photos for a single feature. As a result, only one feature, C005, was selected for use with this program. However, 60 rocks were measured within feature C005 in the field and all of those rocks were measured using the Stereo3D program. This is a sufficient sample size since the use of this program is directed towards measuring the volume of individual rocks not the overall volume of individual features. Overall, the software calculated the volumes of the modeled rocks well, as discussed in the following chapter. The primary affect on accuracy in this method is that the software can only model what it can see in the images. Therefore, it does not capture the recesses between the underside of a rock and the ground surface. The program simply assumes vertical sides to the rocks and also a horizontal bottom surface of the rocks.

CHAPTER V

RESULTS OF INVESTIGATIONS

The investigations consisted of four phases. The first phase involved an intensive survey of the Shumla Ranch and a revisit to Painted Canyon Flat (41VV448) to identify deflated earth oven features suitable for recording. The second phase was applying the PAP method to each of the targeted features. During the third phase, a sample of burned and unburned rocks were collected from the survey area and analyzed in the laboratory to determine the average density of rock used in the features. Finally, the PAP photos were processed in the laboratory. The field investigations were conducted during the summer and fall of 2010 and associated laboratory work was conducted in the subsequent fall and spring at Texas State University-San Marcos.

Intensive Survey

The initial fieldwork consisted of an intensive archaeological survey of a portion of the Shumla Ranch property. The focus of the survey was primarily on the identification of archaeological deposits related to prehistoric and historic settlement in the region. The Shumla Ranch property was chosen since this area was the location of the Texas State 2010 field school and represented a broad area encompassing both upland and canyon settings. The SHUMLA School campus occupies a small area at the western edge of the ranch and consists of four buildings and a camping area. The

SHUMLA School campus is active at various times during the year for schools and workshops. Although several archeologists have walked the Shumla Ranch and identified archaeological deposits, few sites had been officially documented. There are five previously recorded archaeological sites within the survey area and 25 new archaeological sites were recorded during the survey.

The survey was limited to the northwestern pasture of the ranch, an area that is not actively used for livestock agriculture. This area covers 1,140 acres and extends southwest to northeast along the Pecos River, which flows along the northwest edge of the property. Of these 1,140 acres, only 850 acres were surveyed due to time constraints. At the northern tip of the survey area, the Pecos River turns more than 90 degrees to the southeast, bordering the northeast edge of the property. This bend in the river is known as the Shumla Bend. The survey area on the ranch consists of high, rolling uplands dissected by deep canyons that drain to the northwest and northeast into the Pecos River. The canyons that dissect the uplands are known only by local names and the four largest are called Javelina Canyon, Mountain Laurel Canyon, Sheep Canyon, and Tunnel Canyon (Figure 10).

Physiographically, the Shumla ranch is similar to the surrounding region west of the lower Pecos River with high, deflated uplands, sparse vegetation, and deeply incised, narrow canyons. Due to the deflated nature of the survey area, the ground surface visibility is very high, between 80 and 100 percent, with small patches of shallow sediments intermixed with exposed bedrock. Most of the ground surface is littered with limestone boulders, cobbles, and channery stones that often exhibit highly pitted surfaces

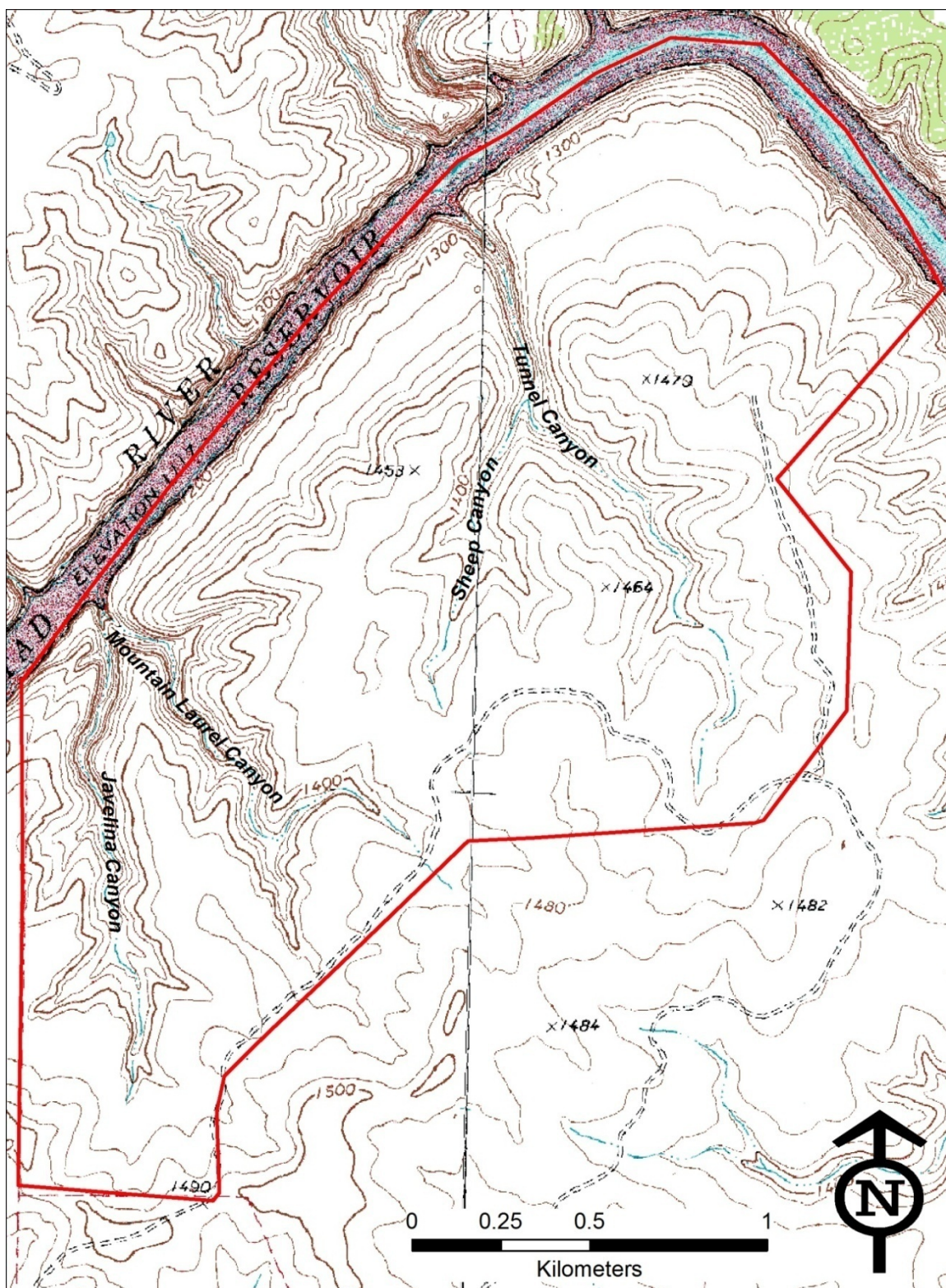


Figure 10. Locations of the canyons on the Shumla Ranch (Shumla and Pecos High Bridge 7.5' USGS quadrangle maps).

due to long-term corrosion from rainwater. The top slopes of the canyons are generally exposed bedrock faces that descend in a stepped fashion until plunging steeply into the canyon bottoms. The canyon bottoms do not have perennial water flow, however, washed out surfaces with large boulders, cobble and gravel deposits, and carved recesses indicate that flash floods are severe and not uncommon. The canyons also may have small, seep springs that flow during wet seasons. A slowly seeping spring was noted in Javelina Canyon during the survey. Caves, rockshelters, and smaller recesses are common in all of the canyons in the region and are the result of karst features exposed during canyon down cutting, faults, or water erosion on the outer bends of the stream flow. Due to the depth of the canyons, these karst features can occur at any elevation.

Vegetation over the survey area is sparse, but varied. The portion of the ranch that was surveyed has been unused by grazing livestock for several years and therefore, has more vegetation than more heavily grazed ranches in the area. The most dominant upland plant that was observed is cenizo, a leafy, pale green shrub that occurs over the entire survey area. Other dominant plants include guajillo, blackbrush, catclaw acacia, lechuguilla, sotol, short grasses, and several cacti including prickly pear, dog pear, horse creeper, and other varieties. Although some trees do occur sporadically in the uplands, these are most common in the canyon bottoms and include mesquite, persimmon, walnut, and oak. Animal wildlife in the survey area was seen rarely and the most common occurrence was a small flock of feral sheep primarily around Tunnel Canyon. Other wildlife was observed in the area and included whitetail deer, quail, indigo snakes, rattlesnakes, scorpions, lizards, jackrabbits, cottontail rabbits, and javelinas.

The survey was conducted by the author and a crew of five students that alternated every week. In general, the first four days of the week were devoted to surveying the uplands and the final day we would survey the canyons. The Shumla Ranch was organized into ten different survey areas based on topography (Figure 11). The investigations were limited to an inspection of the ground surface only, no subsurface tests were excavated. The crew walked transects spaced at approximately 15 m intervals, using a compass to maintain heading (as necessary) and spacing. The survey transects generally followed the contours of the survey area to avoid crossing steep terrain. When artifacts or features were encountered, the crew would gather and conduct a more thorough inspection of the ground surface.

Artifacts and features identified in the field were plotted on a sketch map and samples of artifacts (all tools, diagnostic artifacts, and the approximate limits of debitage concentrations) and all features were plotted using a GPS. Diagnostic artifacts, such as projectile points, and certain tools were photographed in the field and collected. The tasks of note taking, photography, and using the GPS were rotated among the students each day. Two GPS units were carried on the survey and designated as Unit A and Unit B. GPS-plotted artifacts and features were assigned the corresponding letter and a sequential three digit number to provide unique identification (i.e. A005, B057, etc.). Collected artifacts were bagged in paper bags and returned to the field laboratory at the end of each day. Students would spend the evening hours before dinner washing and cataloging artifacts from the survey. Photographs were downloaded every evening, organized by date, and stored on a personal computer.

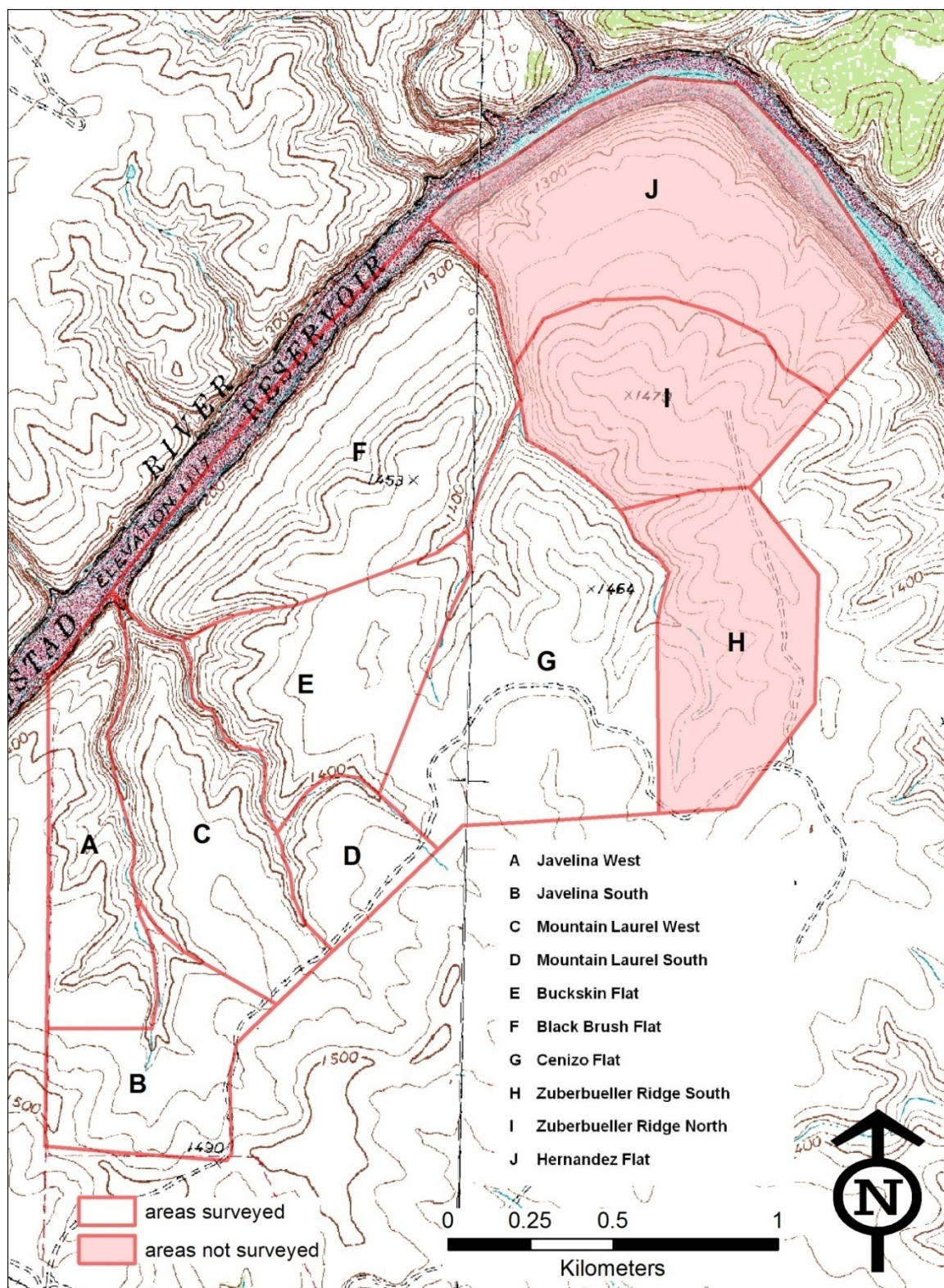


Figure 11. Survey Areas at Shumla Ranch (Shumla and Pecos High Bridge USGS 7.5 minute quadrangles).

A State of Texas Archeological Site Form was completed for each site recorded during the survey and this information was entered into the Texas Historical Commission's TexSite software. Maps of each site were generated in ArcMap and site boundaries were drawn based on the limits of archaeological deposits and the topography. All information was submitted to the Texas Archeological Research Laboratory to obtain state trinomials for each site. A total of 25 new sites were recorded including seven rockshelters. Burned rock concentrations were identified in both the uplands and in all of the rockshelters. Excluding the shelters, there were total of 39 burned rock features documented at the Shumla Ranch.

Previously Recorded Archaeological Sites

There were five previously recorded sites within the survey area at Shumla Ranch (Shumla Cave, Nine Mile Bend, 41VV419, 41VV1526, and Javelina Heights) (Table 3). All of the sites, with the exception of Javelina Heights, are rockshelters located in the canyon walls of the Pecos River and were recorded in the 1970s and 1980s by the National Park Service. Shumla Cave, Nine Mile Bend, and 41VV1526 are not easily accessed from the uplands and were not revisited during the survey. Site 41VV419 is located at the terminus of the Hernandez Trail and was revisited during a tour of the ranch, but was not reevaluated. The Hernandez Trail is a historic trail and crossing of the Pecos of River. The trail crosses the broad upland above the Pecos River in the northeastern portion of the survey area and continues down the canyon wall to 41VV419. There is no obvious evidence of the crossing and the only remnants of the trail that have good integrity are along the wall of the canyon. The trail was not documented as part of

this survey. Finally, Javelina Heights was the focus of excavations during the field school and was therefore not investigated as part of the survey. The site was recorded by archaeologists with the SHUMLA School the previous winter.

Table 3. Previously recorded archaeological sites on the Shumla Ranch.

<i>Trinomial</i>	<i>Site Name</i>	<i>Description</i>	<i>Period</i>	<i>Size (m²)</i>
41VV240	Shumla Cave	Large cave on Pecos River with a low density of artifacts including burned rock, lithics, and four bedrock mortars; no rock art.	Unknown Prehistoric	477
41VV419		Shallow overhang and cave on Pecos River with a deep ashy midden containing burned rock, lithics, and bedrock mortars; pictographs present.	Unknown Prehistoric	150
41VV1221	Nine Mile Bend	Extensive burned rock midden and associated overhang on the Pecos River with lithics and tools; no rock art.	Unknown Prehistoric	3,900
41VV1526		Small overhang on the Pecos River with only a single large mussel shell; no rock art.	Unknown Prehistoric	35
41VV2005	Javelina Heights	Open campsite on an upland above Javelina Canyon with stone alignments, lithics, Late Prehistoric projectile points, and burned rock; site is shallowly buried.	Late Prehistoric	38,400

Sites Recorded During the Survey

Twenty five sites were recorded during the course of the survey that included prehistoric and historic archaeological deposits (Table 4). Seven of the sites are rockshelters (width > depth) or caves (depth > width) located in the canyons leading to the Pecos River. All of the sheltered sites had extensive burned rock middens, with the

exception of Mesquite Shelter. Burned rock was typically concentrated near the outer edge of the shelter opening, with a talus of burned rock extending from the opening and down slope. The lack of a burned rock midden at Mesquite Shelter is most likely a result of the steep canyon wall below the shelter not being conducive to talus slope formation rather than a lack of hot rock use at the shelter. Lithic artifacts were common in the shelters including debitage, unifacial and bifacial tools, projectile points, and ground stone tools. Bedrock mortars were also common as well as animal bone, and mussel shell.

Table 4. Sites recorded during the survey of Shumla Ranch.

<i>Trinomial</i>	<i>Site Name</i>	<i>Description</i>	<i>Period</i>	<i>Size (m²)</i>
41VV2007	Blue Moon Shelter	Rockshelter in Javelina Canyon with a burned rock midden, lithic scatter, biface, manos, metates, bedrock mortars, and mussel shells; pictographs present.	Late Archaic	100
41VV2008	Half Moon Shelter	Narrow shelter in Javelina Canyon with few artifacts in shelter. Artifacts are mostly scattered in broad talus of burned rock, lithics, and mussel shell; no rock art.	Unknown Prehistoric	34
41VV2009	Javelina Grid Shelter	Small shelter below Javelina Heights in Javelina Canyon with a burned rock midden, manos, lithics, tools, dart points, and bedrock mortars; grid pattern etched in ceiling.	Early and Late Archaic	63
41VV2010	Mountain Laurel Shelter	Large shelter in Mountain Laurel Canyon with an eroding earth oven and associated midden, lithics, tools, bedrock mortars, and animal bones; pictographs present.	Middle and Late Archaic	280

Table 4 continued.

<i>Trinomial</i>	<i>Site Name</i>	<i>Description</i>	<i>Period</i>	<i>Size (m²)</i>
41VV2011	Mesquite Shelter	Shelter located in Mountain Laurel Canyon with a low density of burned rock and lithics. One possible bedrock mortar; possible petroglyph.	Unknown Prehistoric	150
41VV2015		Open campsite on a deflated upland terrace with stone alignments, tools, projectile point, lithics, a burned rock feature, and historic age glass and metal; large rock cairn or alignment.	Late Archaic and Historic	10,000
41VV2016		Open campsite on a deflated upland terrace with tools, lithics, mussel shells, burned rock features, and historic age glass.	Unknown Prehistoric and Historic	12,500
41VV2017		Open campsite on a broad upland terrace above the Pecos River with projectile points, tools, ground stone, burned rock features, and stone alignments.	Early and Middle Archaic	12,850
41VV2018		Lithic scatter on upland ridge above the Pecos River with a projectile point, lithics, and tools. Possible crevice burial.	Unknown Prehistoric	9,400
41VV2019		Open campsite on a promontory overlooking the mouth of Mountain Laurel Canyon with a low density scatter of lithics and historic age cans and metal.	Unknown Prehistoric and Historic	605
41VV2020		Open campsite and burned rock midden with scattered lithics, drill, and core. Burned rock is concentrated in three locations.	Unknown Prehistoric	5,935
41VV2021		Open campsite on an upland terrace with stone alignments, low density scatter of lithics, tools, and burned rock.	Unknown Prehistoric	19,188

Table 4 continued.

<i>Trinomial</i>	<i>Site Name</i>	<i>Description</i>	<i>Period</i>	<i>Size (m²)</i>
41VV2022	Bear Scat	Open campsite on an upland terrace with stone alignments, lithics, projectile point, ground stone, and one burned rock feature.	Middle Archaic	8,555
41VV2023	Cenizo	Open campsite on an upland terrace with stone alignments, tools, lithics, projectile points, mano, and a core.	Middle and Transitional Archaic	9,690
41VV2024		Low density lithic scatter on a deflated upland terrace overlooking Javelina Canyon.	Unknown Prehistoric	346
41VV2025		Open campsite on an upland terrace with a low density scatter of lithics, projectile points, possible stone alignments, and burned rock.	Transitional Archaic	7,834
41VV2026		Low density lithic scatter on a deflated upland terrace overlooking Javelina Canyon. Non diagnostic dart point found.	Unknown Prehistoric	487
41VV2027		Open campsite on an upland terrace with scattered lithics, tools, and a projectile point.	Middle Archaic	3,097
41VV2028		Open campsite on a deflated upland terrace with a stone alignment and low density scatter of lithics.	Unknown Prehistoric	3,862
41VV2029		Open campsite on an upland terrace with numerous tools, lithics, and a burned rock feature.	Unknown Prehistoric	21,053
41VV2030		Mutliple clusters of lithics and tools on an upland terrace.	Unknown Prehistoric	1,332
41VV2031	Flea Cave	Small cave with a scatter of lithics, tools, and burned rock; faded pictograph.	Unknown Prehistoric	75

Table 4 continued.

<i>Trinomial</i>	<i>Site Name</i>	<i>Description</i>	<i>Period</i>	<i>Size (m²)</i>
41VV2032	Ram Skull Cave	Small cave with projectile points, tools, manos, bedrock mortars, and burned rock; artifacts extend onto talus in front of cave. No rock art.	Early Archaic	200
41VV2096	Javelina South	Open campsite on an upland terrace at the headwaters of Javelina Canyon with lithics, 12 burned rock features, and historic aged timbers, glass and metal.	Unknown Prehistoric and Historic	78,000
41VV2097	Hernandez Flat	Open campsite and hearth field on a broad upland terrace above the Pecos River with lithics, tools, projectile points, two burned rock middens, several burned rock features, and stone alignments; historic trail crosses site.	Middle Archaic	74,141

Rock art was present in four of the shelters. Blue Moon Shelter and Flea Cave each have a single pictograph, but they are faded and indiscernible as to their style. Mountain Laurel Shelter has the most pictographs of all the shelters recorded during the survey and includes both Pecos River and Red Linear styles of art, which have been attributed to the Middle and Late Archaic respectively (Turpin 2004). The pictographs in Mountain Laurel Shelter are mostly anthropomorphic figures with exaggerated hair. Javelina Grid contains the only petroglyphs in the survey area. The petroglyphs consist of a broad grid pattern that is etched into the ceiling and back wall of the shelter. Half Moon Shelter, Ram Skull Cave, and Mesquite Shelter do not have any rock art.

The remaining 18 sites are open campsites and artifact scatters located in upland settings. All of the upland sites are severely deflated with little or no sediment and

artifacts and features exposed on the surface or just resting on the bedrock. Artifacts found at the sites included lithic debitage, formal and informal stone tools, ground stone, mussel shells, and burned rock. Projectile points were found at several of the sites and included Almagre, Arenosa, Langtry, Pandale, Paisano, Val Verde, Ensor-Frio, Bell, and Perdiz styles, which range in date from the Early Archaic into the Late Prehistoric. The tool assemblage was dominated primarily by informal and unifacial tools such as modified flakes. Other tools included unifacial, crescent-shaped “sotol” knives, bifaces, manos, and drills. The majority of the tools were made from locally available chert and igneous rocks found in gravel deposits along Zuberbueller Ridge. The gravels on Zuberbueller Ridge are Pleistocene age stream deposits from the Pecos River and Rio Grande and reflect material types from the Big Bend region and the southern Plains (Charles Frederick, personal communication).

Burned rock features were found on several of the upland sites as well as low density scatters of burned rock. A total of 39 burned rock features were recorded in the uplands and these ranged from small isolated concentrations of burned rock to burned rock middens. The large number of natural limestone clasts on the ground surface over much of the survey area often made it difficult to identify burned rocks because the natural clasts were of a similar size and color, and often times naturally fractured. Javelina South and Hernandez Flat had the most documented features, consisting of scattered hearths and earth ovens with some potential for buried deposits. Only two burned rock middens were found in open campsites sites, both at Hernandez Flat. In general, the burned rock features on the uplands sites were very deflated and the rocks were often displaced by sheet erosion or livestock. As a result, only four of the 39

features identified on the Shumla Ranch were selected for PAP. The four features were all completely exposed on the surface and were least disturbed of all the features.

Another common feature identified at several of the upland sites were stone alignments. The alignments are thought to be the remains of wikiups or ramadas that are suspected to date to the Late Prehistoric and possibly earlier. Due to the lack of sufficiently deep sediment, the arrangements of small boulders were apparently used as anchors for the wooden posts that supported a small structure or were used to weigh down the hides that covered such structures. The alignments were the subject of many a debate during the field school. During a lecture at the field school, Charles Frederick related that the surface of the rocks in the region become pitted as a result of rain water dissolving the rock. As such, rocks that are moved from one location to another should exhibit a different degree of pitting than the surrounding bedrock. This approach was applied during the survey, which made it easier to distinguish the apparent cultural alignments from natural arrangements of rock. Using this approach, several features were identified as purposeful circular arrangements of rock that are clearly the result of human manufacture. Therefore, it is reasonable to infer that some of the stone alignments may be the remains of wikiups or ramadas.

Historic artifacts found at the sites were generally low in number and consisted of metal, glass, and wood. The only historic feature identified was a large ring-shaped cairn at site 41VV2015, which is thought to be most likely the remains of a shepherd's camp structure as it occurred amid a light scatter of glass, tin cans, and other metal. However, it is possible that this cairn is actually a prehistoric burial cairn that has been looted, leaving the central portion empty. Another scatter of tin cans and other metal was

found at 41VV2019, which may be the remains of historic camp. At Javelina South, wooden railroad timbers, glass, and metal suggest an association with the railroad just east of the site. Finally, a gravel bed and materials used for oil drilling are located on top of Zuberbueller Ridge, activities which occurred in the 1960s. Overall, the historic assemblage at the ranch consists mainly of metal and broken bottle glass that is primarily associated with the hunting and ranching activities that have occurred over the last century.

Painted Canyon Flat (41VV448)

Painted Canyon is located southeast of Seminole Canyon on the Zuberbueller Ranch (Figure 12). The canyon gets its name from Painted Shelter, a long narrow shelter with extensive Red Monochrome paintings of large anthropomorphic and animal figures. Painted Canyon is spring fed and the water flows year round. Painted Canyon Flat is a broad upland terrace just above, and east of Painted Shelter. A historic stacked stone ranch house is on a slope of the canyon between the shelter and the upland flat. The upland site at Painted Canyon Flat (41VV448) is an extensive scatter of lithics and burned rock, including 26 burned rock features, which is bounded by the canyon to the west and north and a high crescent shaped ridge to the east. There are also two possible prehistoric stone alignments at the northern end of the site. Two possible historic age sheepherder camps occupy the crescent shape ridge at the east end of the site and consist of a small stone wall at the south end of the ridge and a hearth at the north end.

Painted Canyon Flat was not surveyed as part of the field school but was reevaluated in the summer and winter of 2010 by Junior High School students from the SHUMLA Discovery Camp and volunteers from Texas State. The site was chosen for

PAP due to the presence of three well defined, deflated earth oven features. The deflated nature of the features allowed for the removal of burned rocks for measurement without significantly disturbing any underlying matrix. The investigations at the site included PAP documentation of three features, mapping the site with a total station, and excavation of Feature C006.

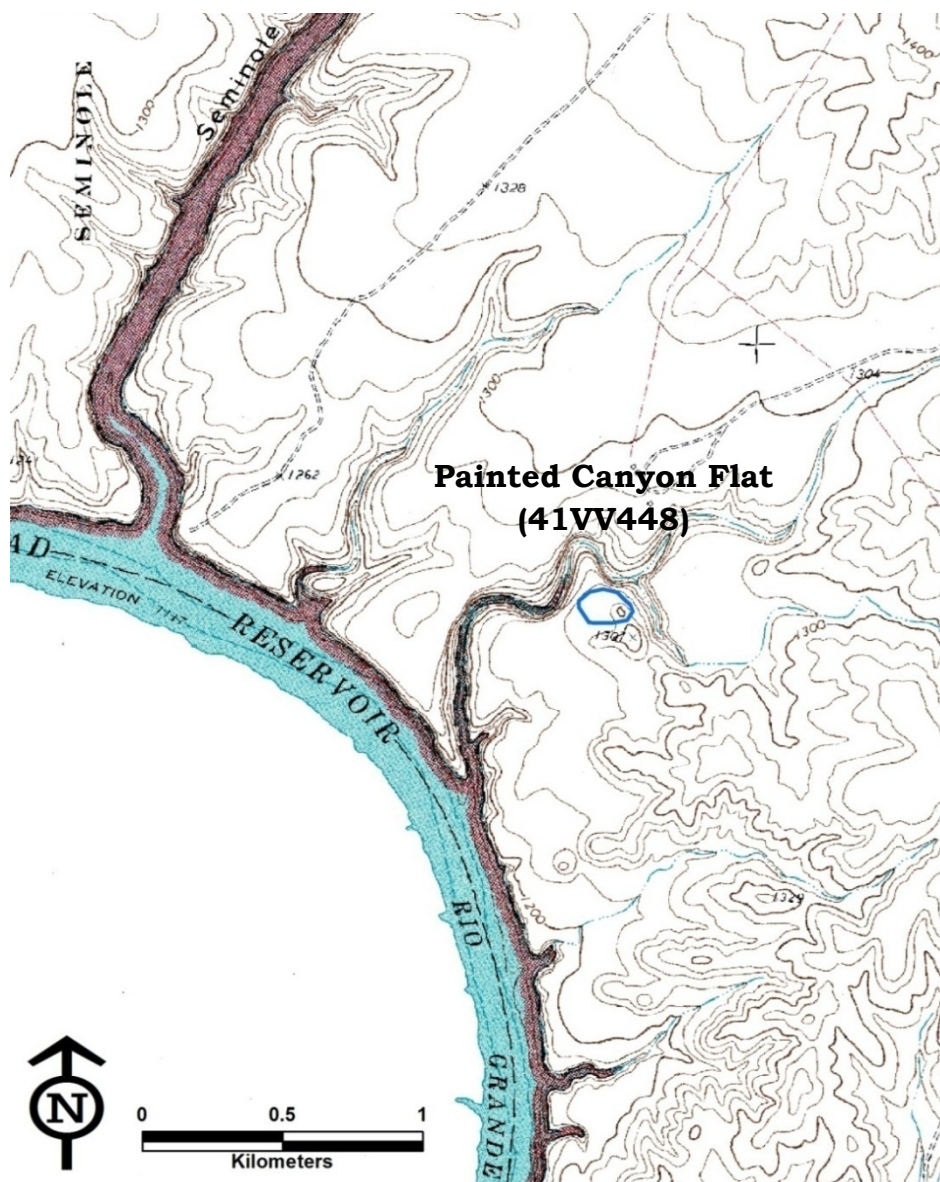


Figure 12. Painted Canyon Flat survey area (Seminole Canyon USGS 7.5 minute quadrangle).

Burned Rock Feature Analysis

A total of 65 burned rock features were documented during the survey of the Shumla Ranch and Painted Canyon Flat. Many of the features consisted of small burned rock clusters. Eleven of the features were recorded using the PAP method because they were the most substantial in size, discrete, and they were sufficiently deflated to expose the majority of the feature's rocks. Four of the eleven features were not analyzed because they were early experiments with PAP and did not produce usable photos due to poor lighting and inconsistent methods. The remaining seven features (C001, C003, C004, C005, C006, C007, and A257) were all recorded with PAP using the methods outlined in the previous chapter.

A total of 660 photos were taken of these features, or 330 stereo pairs. The images for each feature were stitched into a single composite aerial image of the feature. The composite image was then imported into ArcMap and georeferenced according to the GPS data. Weighed rocks in the feature were digitized by tracing to create individual polygons for each rock and unweighed rocks were digitized with a single point. The unweighed rocks were all of the rocks in a feature that appeared to be less than 10 cm in size and culturally deposited. Each of the unweighed rocks was assigned an arbitrary weight of 0.1 kg. To estimate the degree of fragmentation for each feature, the weight values for the all of the burned rocks were arbitrarily divided into five classes (Class I, the lowest weight, through Class V, the heaviest weight) at an interval of one kilogram. All of the unweighed rocks for each feature were included within Class I along with weighed rocks that were one kilogram or less in weight. The data was then organized in a spreadsheet to determine the total weight of each class of rocks and plotted on a

histogram by class. The distances between rocks within each feature were estimated using the measuring tool in ArcMap.

Table 5 summarizes the basic data collected from the seven features and the complete data set for each feature is in Appendix A. The diameter is based on the inferred limits of the central heating element of each feature. Estimated rock counts reflect the sum of the measured rock and the unweighed rocks. The count and weight of the measured rocks, as well as the volume is also provided in the table. The volume given for each feature is the volume of the measured rock, derived by dividing the weight (g) of the burned rocks by an average rock density of 2.72 g/cm³.

Table 5. Summary of feature data.

<i>Feature</i>	<i>Site</i>	<i>Diameter (m)</i>	<i>Measured Sample</i>			<i>Estimated Feature Totals</i>		
			<i>Count</i>	<i>Weight (kg)</i>	<i>Volume (cm³)</i>	<i>Count</i>	<i>Weight (kg)</i>	<i>Volume (cm³)</i>
A257	41VV2016	2.0 - 2.4	52	85.63	31481.6	213	101.73	37400.74
C001	Painted Canyon Flat	2.7 - 3.4	155	304.77	112047.8	366	325.87	119805.15
C003	Painted Canyon Flat	2.8	129	188.97	69474.3	275	203.57	74841.91
C004	Javelina South	2.5	58	68.31	25114.0	425	83.7	30772.06
C005	Javelina South	1.8 - 2.1	61	94.88	34882.4	430	131.78	48448.53
C006*	Painted Canyon Flat	2.2	55	174.27	64069.9	111	179.97	66165.44
C007	Hernandez Flat	2.3	68	97.34	35786.8	183	108.84	40014.71

*The Measured Sample and Estimated Feature Totals for feature C006 are for western half of the feature only.

All of the features appear to be the deflated, discrete remains of earth ovens. The lack of extensive burned rock accumulations around the features suggests they were used only a few times, possibly within a single occupational episode. Feature C006 is the first feature discussed below since it exhibited the least amount of rock fragmentation and most likely represents a single use earth oven. Feature C005 is presented last because it was the only feature processed using the Stereo3D program. The decision to use only one feature in the Stereo3D program was made because of time constraints. Feature C005 was arbitrarily chosen and it is assumed that the program would have performed similarly for all of the features.

Feature C006

Feature C006 is located on the Painted Canyon Flat site (41VV448) near features C001 and C003. The feature is circular in shape with a diameter of 2.2 m. A total of 111 burned rocks occur within western half of the feature (Figure 13). Only 55 of the burned rocks from the western half of the feature were measured and weighed, resulting in a total weight of 174.27 kg and a volume of 64,069.9 cm³ (Table 6). When combined with the estimated weight of the 56 unweighed rocks, the total weight of the western half of the feature is 179.97 kg and doubling this number would give a total estimated weight for the entire feature of around 360 kg. The feature appeared to be well exposed on the surface, but excavations of the southwestern half of the feature indicated that sediments extend to between 10 and 15 cm below the ground surface. The burned rocks within the feature are densely packed with less than five centimeters between rocks and few, if any, are buried. The feature is on a gradual slope that descends to the west and a narrow, ephemeral drainage, which runs northeast to southwest, is forming to the south.



Figure 13. Aerial view of C006.

Table 6. Distribution of rocks by weight class for the western half of C006.

<i>Size Class</i>	<i>Weight Range (kg)</i>	<i>n</i>	<i>Total Weight (kg)</i>	<i>% total</i>
I	0.01-1.00	79 (56*)	18.71	10.4
II	1.01-2.00	8	12.47	6.9
III	2.01-3.00	7	17.28	9.6
IV	3.01-4.00	2	7.45	4.1
V	>4.00	15	124.06	68.9
	<i>Totals</i>	<i>111</i>	<i>179.97</i>	<i>100.0</i>

* unweighed rocks at 0.10 kg each.

The southwestern half of the feature was excavated to determine the depth of deposits and recover charcoal plant remains for identification and dating. Since the burned rocks in the western half C006 were weighed for use with PAP, the southwest quarter of the feature was excavated initially. Excavation in this area indicated a slight basin shape in profile and that bisecting the feature along the northwest-southeast axis would provide the best profile of the feature. Organic preservation in the feature was good, with numerous charred wood fragments and some seeds. The profile of the feature exhibited a shallow, basin shape with a single, thin lens of charcoal directly beneath the rocks, along the bottom of the basin. This single, thin lens of charcoal may signify the oven was only used once, as multiple uses would likely have result in a layered and jumbled arrangement of rock and charcoal from repeated firings. Radiocarbon dates were obtained from three wood samples (mesquite, buckthorn, and acacia) dating to 335 ± 15 , 345 ± 15 , and 315 ± 15 RCYBP within the latter part of the Late Prehistoric period. The dates are consistent with a Perdiz arrow point found just down slope from the feature.

The distribution by weight of the burned rocks shows that with the exception of a few large rocks the majority of burned rocks are concentrated in the center of the feature (Figure 14). Most of the larger rocks are intact or slightly fragmented in place. Burned rocks from the eastern half of the feature are included on Figure 15 for perspective and were not used in analysis. There is also a relatively low quantity of small fragmented rocks and the lack of any discernible discard area. The weight distribution of burned rocks within the feature suggests it may have only been used once (Figure 15). Burned

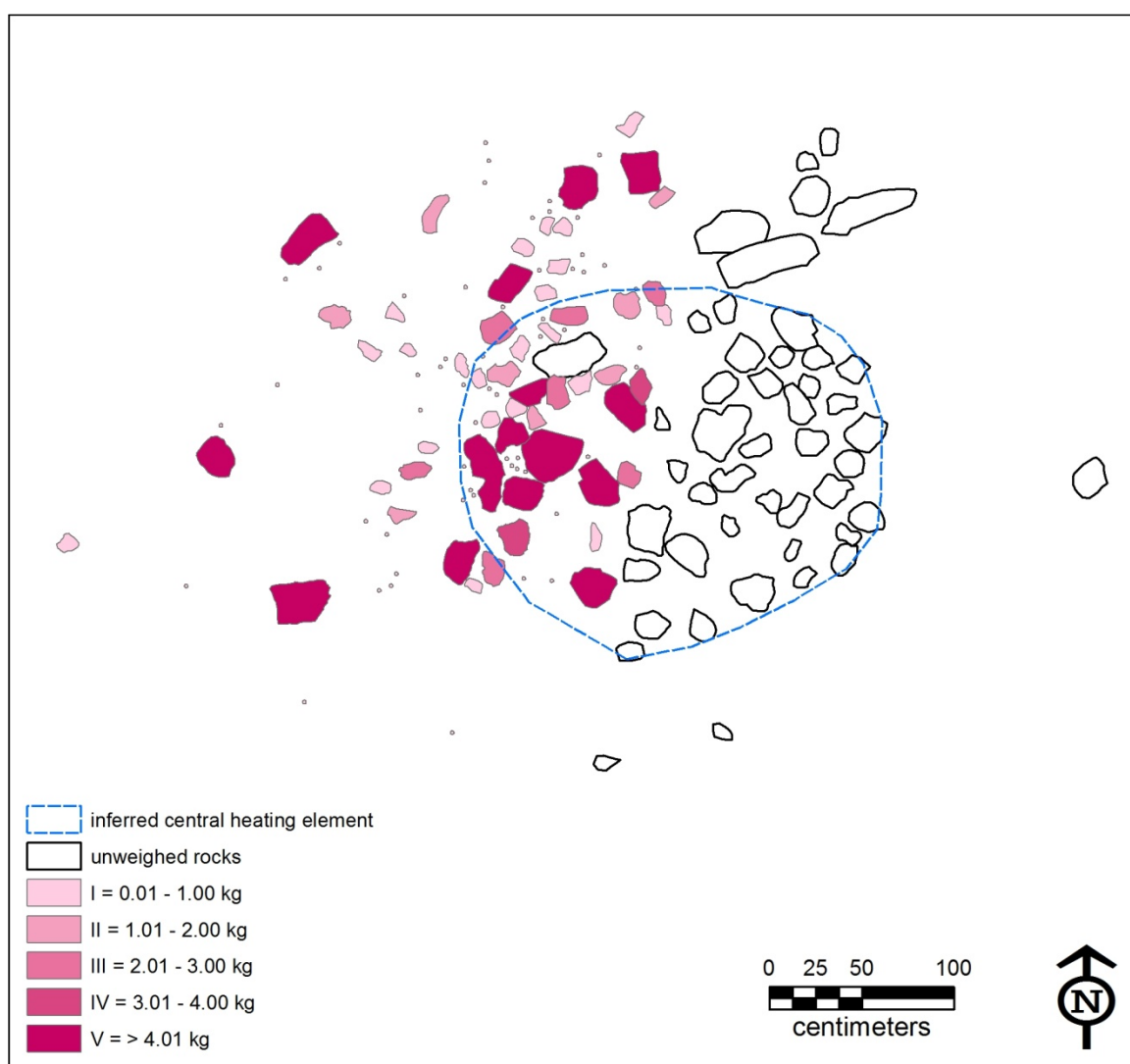


Figure 14. Distribution of burned rocks by weight in the western half of C006.

rocks located outside of the central heating element are generally distributed to the west and north, which may be the result of erosional forces, rather than discard, since the areas west and north are slightly down slope from the feature's center. The low weight of the more fragmented burned rocks, as well as a tightly concentrated central heating element of larger burned rocks suggests that this feature was probably used only once. Feature C006 appears to have the shortest use-life of the seven features examined during this research.

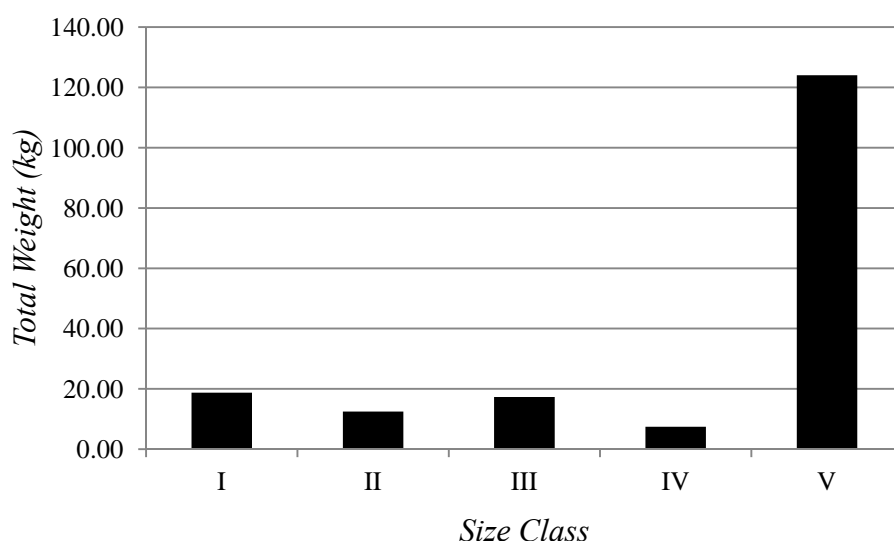


Figure 15. Histogram showing total weight by class for C006.

Feature A257

Feature A257 was recorded during the Shumla Ranch survey on an upland terrace overlooking the Pecos River (Black Brush Flat) within the boundaries of site 41VV2016. The feature is ovate in shape with a width of 2.0 m (northwest to southeast) and a length of 2.4 m (northeast to southwest) (Figure 16). The ground slopes downward slightly from northwest to southeast and areas around the feature are subject to severe sheet



Figure 16. Aerial view of A257.

erosion during heavy rains. There are approximately 213 rocks within the feature, of which 52 were measured and weighed in the field. The total weight of the measured rock is 85.63 kg and the volume of this weighed rock is 31,481.6 cm³. The estimated weight of all the burned rock in the feature, including the unweighed rocks, is 101.73 kg (Table 7). The density of the rocks is low with distances between rocks averaging about 20 cm.

Table 7. Distribution of rocks by weight class for A257.

<i>Size Class</i>	<i>Weight Range (kg)</i>	<i>n</i>	<i>Total Weight (kg)</i>	<i>% total</i>
I	0.01-1.00	183 (161*)	32.14	31.6
II	1.01-2.00	17	22.61	22.2
III	2.01-3.00	5	12.75	12.5
IV	3.01-4.00	3	10.85	10.7
V	>4.00	5	23.38	23.0
<i>Totals</i>		<i>213</i>	<i>101.73</i>	<i>100.0</i>

* unweighed rocks at 0.10 kg each.

Probing the feature with a trowel indicated a thin veneer of sediment overlying bedrock approximately 1 to 3 cm in thickness suggesting that buried deposits within the feature are unlikely. No charcoal was observed within the feature. Figure 17 shows the distribution of burned rocks in the feature by weight. The distribution of rocks indicates the heaviest, and least fragmented burned rocks are concentrated in the center with the more fragmented rocks distributed to the east, south, and west. The scatter of more fragmented rocks may be the result of discard or displacement by erosion down the gradual slope. However, there are no discernible rock discard piles. Over 50 percent of



Figure 17. Distribution of burned rocks by weight in A257.

the burned rocks in the feature are the more fragmented Class I and II rocks, suggesting more than one or two episodes of use (Figure 18).

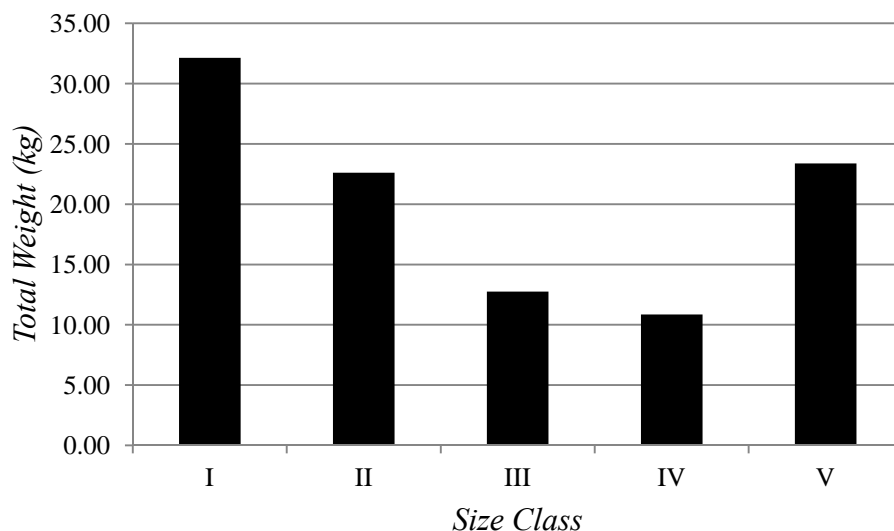


Figure 18. Histogram showing total weight by class for A257.

Feature C001

Feature C001 is located within Painted Canyon Flat (41VV448) on the Zuberbueller Ranch on a broad upland terrace overlooking Painted Canyon to the west and north. Features C003 and C006 are also located on this terrace. The feature is ovate, 2.7 m wide and 3.4 m long, with the heaviest concentration of rocks in the southwestern half (Figure 19). A total of 366 burned rocks are estimated for the feature, of which 155 were measured and weighed in the field. The total weight of the measured rock is 304.77 kg, which was converted to a volume of 112,047.8 cm³. Combined with the 211 unweighed burned rocks in the feature the total estimated weight is 325.87 kg (Table 8). Burned rocks in the feature have a relatively dense arrangement, with several rocks overlapping, and distances between rocks of less than 20 cm. The feature sits on level ground and had very little vegetation cover. Lithic debitage was found within the feature including a single obsidian flake beneath one of the burned rocks.



Figure 19. Aerial view of C001.

Table 8. Distribution of rocks by weight class for C001.

<i>Size Class</i>	<i>Weight Range (kg)</i>	<i>n</i>	<i>Total Weight (kg)</i>	<i>% total</i>
I	0.01-1.00	278 (211*)	62.03	19.0
II	1.01-2.00	42	59.69	18.3
III	2.01-3.00	20	49.06	15.1
IV	3.01-4.00	9	30.25	9.3
V	>4.00	17	124.84	38.3
<i>Totals</i>		<i>366</i>	<i>325.87</i>	<i>100.0</i>

* unweighed rocks at 0.10 kg each.

Probing with a trowel revealed only thin sediments, one to five centimeters thick. However, some of the larger rocks were sufficiently buried that they were not picked up for fear of disturbing the feature. Likewise, smaller burned rock fragments could be buried. The presence of small pieces of charcoal less than one centimeter in size was observed underneath several of the rocks. Figure 20 shows the distribution of burned rocks by weight indicating a circular concentration of the heaviest rocks in the western half of the feature that is most likely the central heating element. The smaller fragmented burned rocks are represented across the feature, but they appear to be concentrated to the north and east of the inferred central heating element. The histogram in Figure 21 shows that the feature has a relatively high percentage of heavier, unfragmented burned rock (Class V) and a relatively equal distribution of rock among weight classes I through IV, which suggests some reuse of C001.

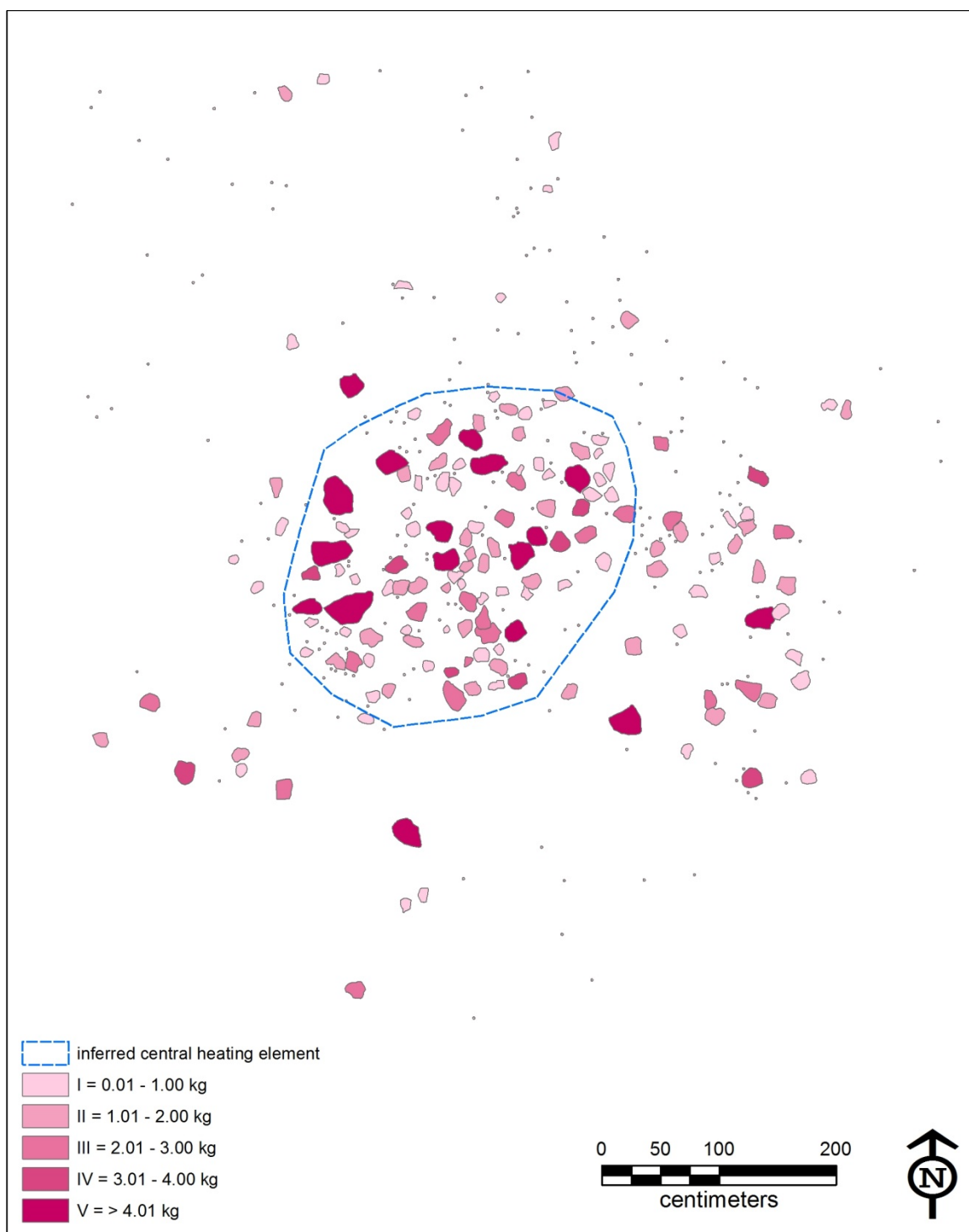


Figure 20. Distribution of burned rocks by weight in C001.

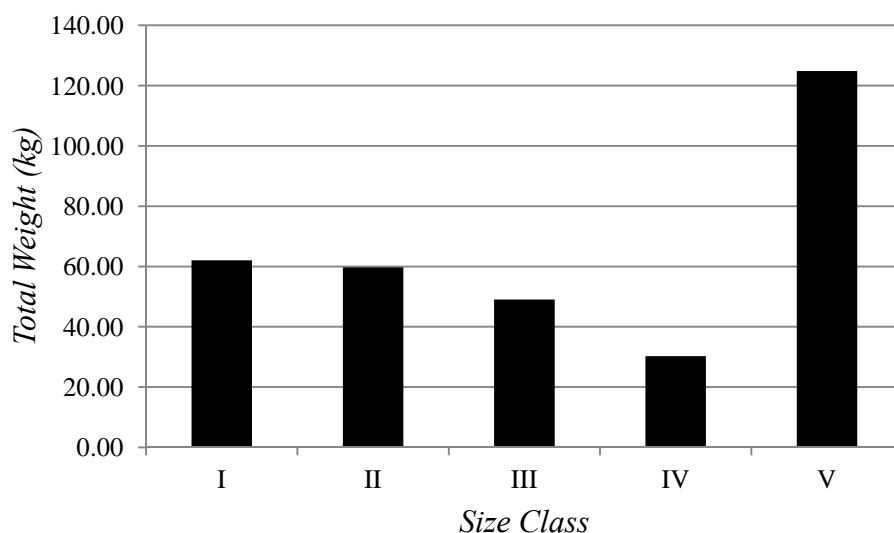


Figure 21. Histogram showing total weight by class for C001.

Feature C003

Feature C003 is also located on Painted Canyon Flat (41VV448) and is the most deflated feature on the site with very little vegetation. C003 is amorphous in shape and approximately 2.8 m in diameter, with the bulk of the larger rocks forming a slightly circular concentration of burned rock in the northwestern portion of the feature (Figure 22). The feature is surrounded by a two-track road that is used for parking during visits to Painted Canyon. The visits to the canyon also bring a lot of pedestrian traffic. A total of 275 burned rocks are estimated to be within the feature, of which 129 were measured and weighed in the field. The total weight of the measured rocks is 188.97 kg, which converts to a volume of 69,474.3 cm³. Combined with the 146 unweighed rocks the total estimated weight of C003 is 203.57 kg (Table 9). A low density of lithic debitage is scattered across the feature and a few small flecks of charcoal were noted beneath some of the rocks.



Figure 22. Aerial view of feature C003.

Table 9. Distribution of rocks by weight class for C003.

<i>Size Class</i>	<i>Weight Range (kg)</i>	<i>n</i>	<i>Total Weight (kg)</i>	<i>% total</i>
I	0.01-1.00	222 (146*)	54.62	26.8
II	1.01-2.00	28	37.80	18.6
III	2.01-3.00	8	19.56	9.6
IV	3.01-4.00	5	16.77	8.2
V	>4.00	12	74.82	36.8
<i>Totals</i>		<i>275</i>	<i>203.57</i>	<i>100.0</i>

* unweighed rocks at 0.10 kg each.

The sediments within the feature are very shallow, only one to two centimeters thick, and bedrock is exposed on the ground surface in some areas. The distribution of the burned rocks by weight is mapped on Figure 23, which indicates a circular arrangement of rocks in the northwestern half of the feature and a possible disarticulated central heating element in the southeastern half. The smaller fragmented burned rocks are concentrated mostly to the southeast and the northeast of the inferred central heating element. The histogram in Figure 24 shows the relatively highest percentage of burned rocks are unfragmented (Class V) followed by a relatively high percentage of fragmented rocks (Class I). Although, there appears to be some form to the feature, it is less dense than C001 and C006 with distances between rocks as large as 25 cm. Some of the burned rocks appear to be arranged randomly suggesting that portions of the feature have been disturbed by erosion, livestock, and pedestrian traffic. The arrangement of rocks may be the result of two partially overlapping central heating elements, such that rocks from one feature may have been robbed from the other and reused.

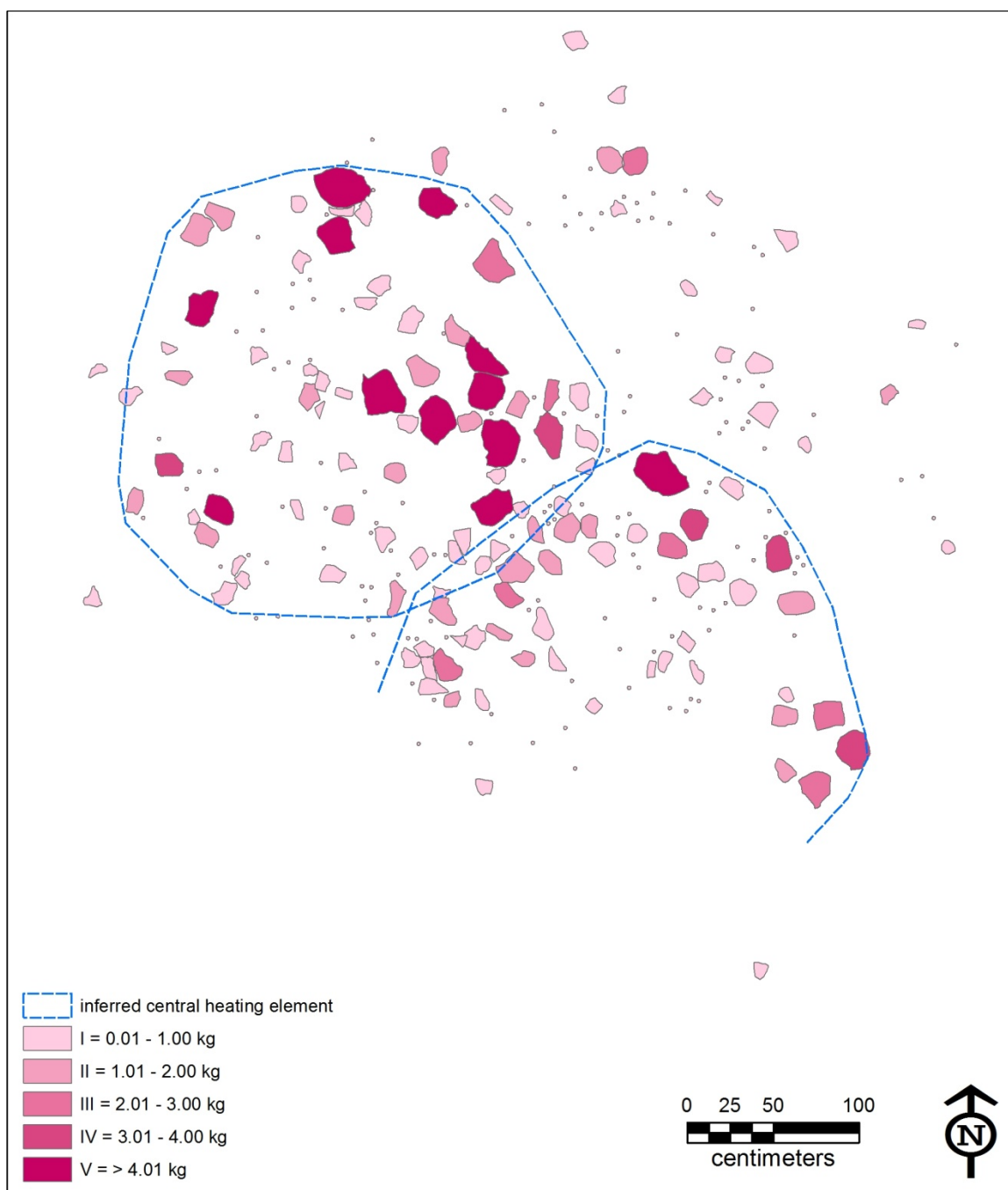


Figure 23. Distribution of burned rocks by weight in feature C003.

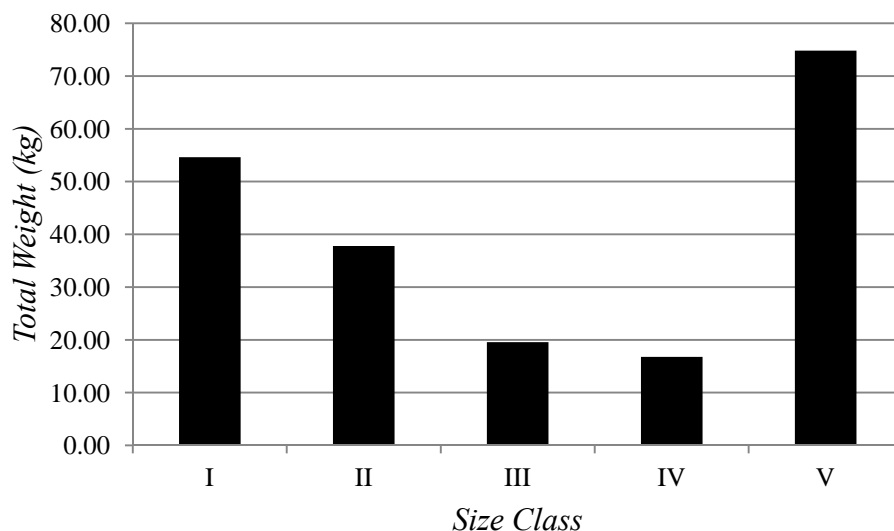


Figure 24. Histogram showing total weight by class for C003.

Feature C004

Feature C004 is located on the Shumla Ranch within the boundaries of the Javelina South site (41VV2069) along with feature C005. C004 is circular in shape with a concentrated ring of burned rock around a slightly mounded center (Figure 25). The diameter of the feature is 2.5 m and contains an estimated 425 rocks, of which only 58 were measured and weighed in the field. Only 58 rocks were weighed because the feature had a high density of fragmented rocks less than 10 cm in size. There were also larger, partially buried rocks that could not be removed without disturbing the feature sediments. The total weight of the measured burned rock was 68.31 kg with a volume of 25,114.0 cm³. Including the 367 unweighed rocks in the total weight produces an estimated weight of 83.70 kg (Table 10). The disparity between weighed and unweighed rocks means the total weight of C004 is underestimated. Most of the burned rocks in the feature appear to be densely concentrated, with several rocks overlapping, and distances



Figure 25. Aerial view of feature C004.

Table 10. Distribution of rocks by weight class for C004.

<i>Size Class</i>	<i>Weight Range (kg)</i>	<i>n</i>	<i>Total Weight (kg)</i>	<i>% total</i>
I	0.01-1.00	400 (367*)	57.55	54.8
II	1.01-2.00	18	26.65	25.4
III	2.01-3.00	3	7.28	6.9
IV	3.01-4.00	3	9.52	9.1
V	>4.00	1	4.01	3.8
<i>Totals</i>		425	105.01	100.0

* unweighed rocks at 0.10 kg each.

between rocks of less than 10 cm. A few flecks of charcoal were observed beneath several of the rocks.

Probing with a trowel indicated that sediments continued to a depth of five to ten centimeters, suggesting that some burned rocks may be buried. The distribution of burned rocks by weight (Figure 26) indicates that a circular, ringed-shaped concentration of burned rock at the center of the feature is likely the central heating element. Figure 26 also shows the large amount of fragmented rocks that are less than 10 cm in size. These highly fragmented rocks are scattered across the whole feature with no clear indication of discard piles. The histogram in Figure 27 shows that largest percentage of the total rock is highly fragmented with low numbers in the other weight classes. The distribution of the burned rocks by weight class suggests that C004 was reused several times. This distribution does not include the larger, partially buried rocks and therefore, skews the histogram in favor of the lighter rocks.

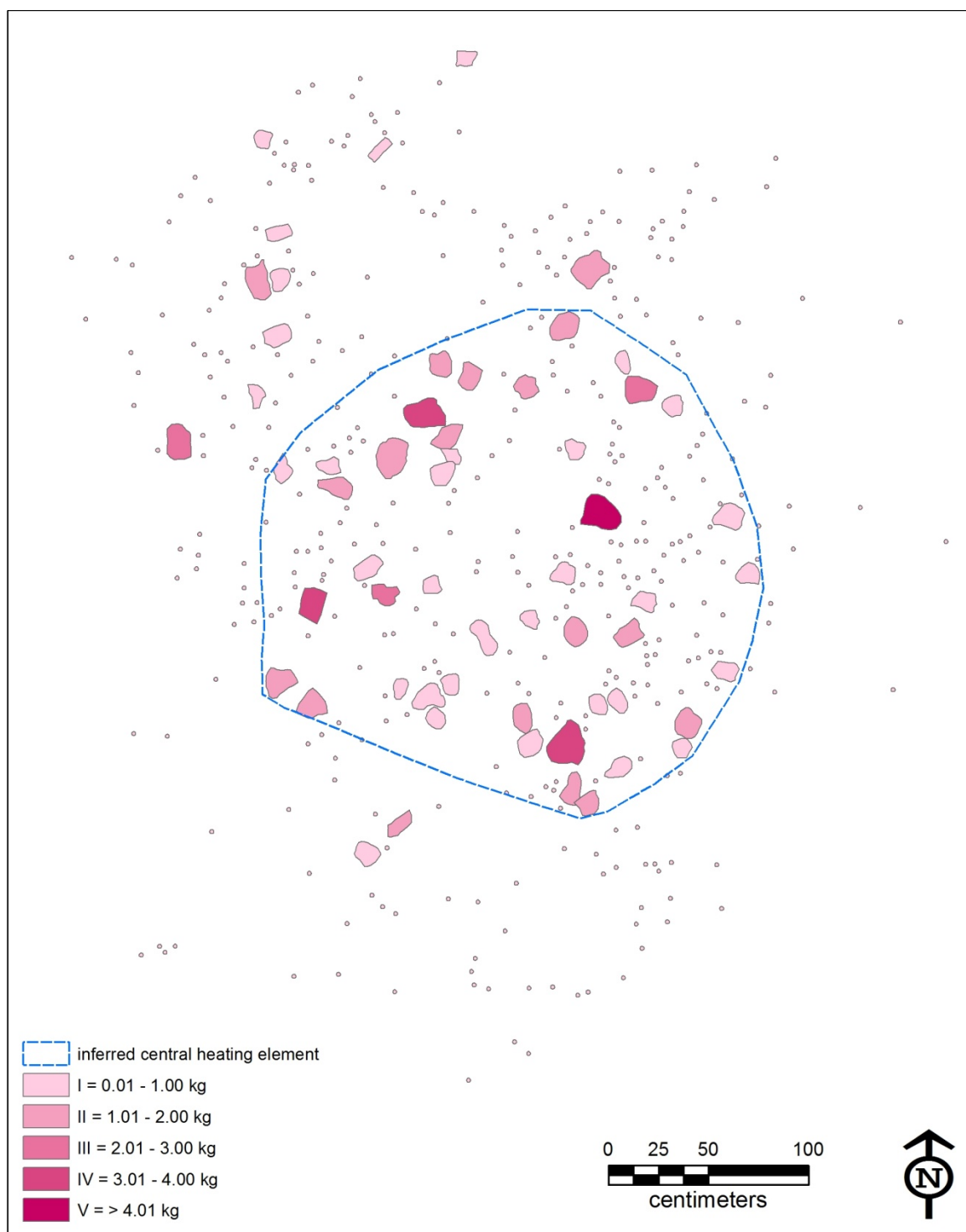


Figure 26. Distribution of burned rocks by weight in feature C004.

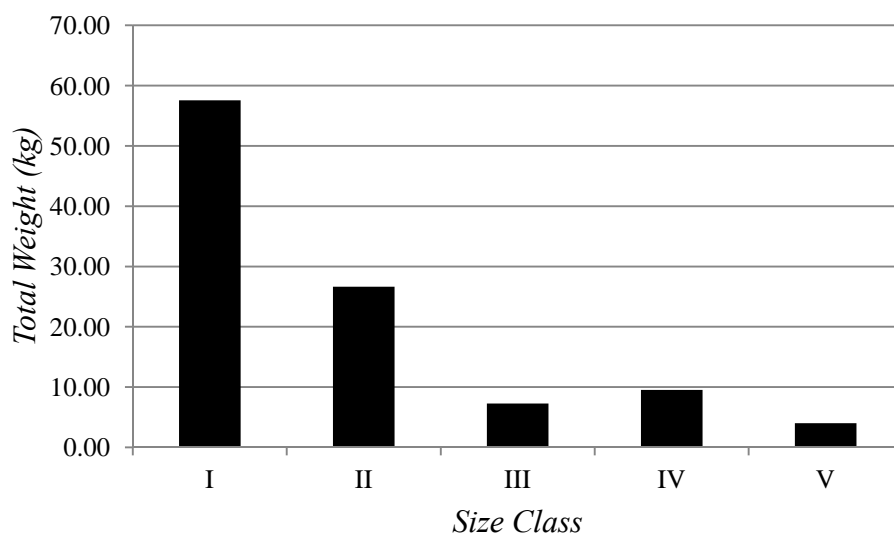


Figure 27. Histogram showing total weight by class for C004.

Feature C007

Feature C007 is located on Henandez Flat (41VV2097), a broad terrace at the northeast corner of the Shumla Ranch overlooking the Pecos River. The feature is circular in shape with a diameter of 2.3 m and rocks arranged approximately 10 to 15 cm apart (Figure 28). There are an estimated 183 burned rocks in the feature, of which 68 were measured and weighed. Most of the rocks are concentrated in the central and southeast portions of the feature indicating the central heating element. There were also larger, partially buried rocks that could not be removed without disturbing the feature sediments. The total weight of the measured rocks was 97.34 kg with a volume of 35,786.8 cm³. Combined with the 115 unweighed rocks from C007, the total estimated weight is 121.49 kg (Table 11). Probing with a trowel indicated sediments extending as deep as 10 cm. Small charcoal flecks were observed on the underside of some of the rocks.



Figure 28. Aerial view of feature C007.

Table 11. Distribution of rocks by weight class for C007.

<i>Size Class</i>	<i>Weight Range (kg)</i>	<i>n</i>	<i>Total Weight (kg)</i>	<i>% total</i>
I	0.01-1.00	147 (115*)	33.93	31.2
II	1.01-2.00	22	31.03	28.5
III	2.01-3.00	8	20.29	18.6
IV	3.01-4.00	4	14.04	12.9
V	>4.00	2	9.55	8.8
<i>Totals</i>		<i>183</i>	<i>108.84</i>	<i>100.0</i>

* unweighed rocks at 0.10 kg each.

Figure 29 indicates the largest rocks are concentrated in the southeast portion of the feature with fragments deposited all around the central heating element except in the southeast. The histogram in Figure 30 shows a relatively higher percentage of fragmented rock (Class I) within the feature relative to the heavier, unfragmented rocks (Class V). The distribution of the burned rocks by weight class suggests that C007 was reused more than once. This distribution does not include the larger, partially buried rocks and therefore, skews the histogram in favor of the lighter rocks.

Feature C005

Feature C005 is located on the Shumla Ranch on the Javelina South site (41VV2096) near feature C004. The feature is circular in shape, measuring 2.9 m in diameter, and was well exposed, although some clearing of the vegetation was necessary (Figure 31). The estimated total count of burned rock in the feature was 430, of which 61



Figure 29. Distribution of burned rocks by weight in feature C007.

were measured and weighed in the field. The total weight of the measured burned rocks was 94.88 kg with a volume of 34,882.4 cm³. Like C004, feature C005 has a high

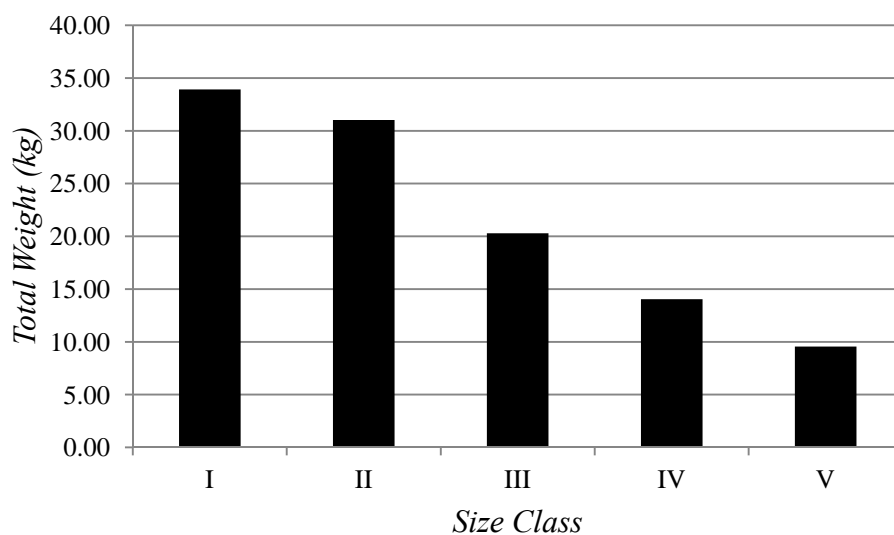


Figure 30. Histogram showing total weight by class for C007.

density of burned rock consisting mostly of smaller fragments less than 10 cm apart.

Adding the estimated weight of the 369 unweighed fragments would give a total weight of approximately 159.46 kg (Table 12). Some charcoal flecks were observed beneath the burned rocks.

Table 12. Distribution of rocks by weight class for C005.

<i>Size Class</i>	<i>Weight Range (kg)</i>	<i>n</i>	<i>Total Weight (kg)</i>	<i>% total</i>
I	0.01-1.00	400 (369*)	59.18	44.9
II	1.01-2.00	18	23.11	17.5
III	2.01-3.00	4	9.14	6.9
IV	3.01-4.00	5	16.81	12.8
V	>4.00	3	23.54	17.9
<i>Totals</i>		<i>430</i>	<i>131.78</i>	<i>100.0</i>

* unweighed rocks at 0.10 kg each.



Figure 31. Aerial view of feature C005.

Probing the feature with a trowel did not indicate much depth to the sediment, less than five centimeters. Like C004 and C007, some of the large rocks were partially buried and not measured. Although the feature is circular in shape, the heaviest rocks appear to be randomly arranged and the lighter, smaller fragments of rock are distributed around the northern and western edges of the central heating element (Figure 32). Similar to C004, the Class I rocks represent the highest percentage of rocks in C005 with lower percentages in the heavier rock weight classes. The histogram in Figure 33 depicts the distribution of weights by class and indicates that the feature was probably reused several times. This distribution does not include the larger, partially buried rocks and therefore, skews the histogram in favor of the lighter rocks.

Calculating Rock Density

The Stereo3D program was used to generate a model from the PAP photos for measuring the volume of individual burned rocks. To convert the volume of a rock to a weight, the density of the rock must be obtained. To accomplish this, a method was established to obtain an average density from a sample of naturally occurring rocks from the Lower Pecos Canyonlands. The average density coefficient could then be applied to measured rocks from the field to obtain a volume from weight and to the rocks measured with the PAP to get a weight from volume. A sample of 30 limestone rocks was collected from the field. These rocks were burned and unburned, collected from an experimental earth oven and the three geologic formations of the surrounding landscape. The sample rocks included limestone from the Buda limestone/Del Rio clay formation, the laminated Boquillas Flags, and the fossiliferous Salmon Peak limestone.



Figure 32. Distribution of burned rocks by weight in feature C005.

The method for obtaining the density of the rocks relied on measuring the amount of water displaced by the individual rocks. A rock placed in a bucket of water will displace an amount of water equal to the volume of the rock. The displaced water is

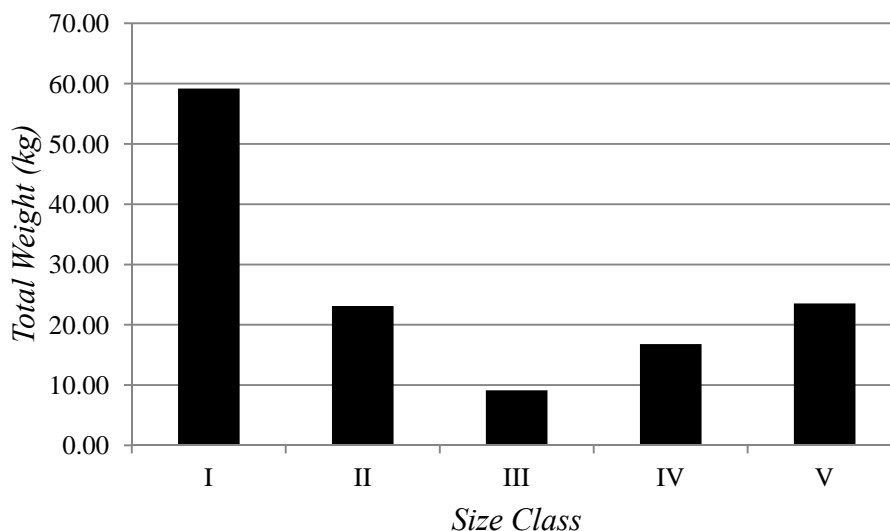


Figure 33. Histogram showing total weight by class for C005.

captured in a graduated cylinder and weighed. Since 1000 cm^3 (or 1000 mL) of pure water equals 1000 g, this was applied to calculate the volume of the water from the weight of the water. Originally, the volume of the water was to be measured in the graduated cylinder instead of weighing the water, but graduated cylinders of an adequate size were not available at an acceptable scale (less than 50 mL) for a reasonable cost.

This method used the weight (W_o) of the displaced water in grams divided by the density of the water (D_w) in g/cm^3 to arrive at the volume of the water. Density is calculated by dividing the weight of the water by the volume, thus the density of pure water would be one g/cm^3 . Pure water was not available, so tap water was used instead. Since the density of tap water can vary from pure water, it was necessary to calculate the density of the water by measuring exactly 1000 mL of water in a graduated cylinder and weighing it on a digital scale. The weight of the water, minus the weight of the cylinder,

is then divided by the volume (1000 mL). As the density of water is affected by changes in temperature, it was necessary to measure the density of the tap water periodically throughout the process. This method can be expressed in the following equation where V_r is the volume of rock/water, W_o is the weight of the rock/water, and D_r is the density of the rock/water:

$$V_r = \frac{W_o(g)}{D_r(g/cm^3)}$$

A hole was cut into the side of a square, plastic, five gallon bucket and a short piece of PVC was connected to the bucket at a downward angle with adhesive (Figure 34). The bucket was then filled with water until water began to overflow through the PVC. Once the PVC overflow stopped, a rock was weighed dry and then placed in the bucket and the resulting overflow was captured in a separate container. The water in this separate container was then poured into a graduated cylinder and weighed on a digital scale. The water weight was divided by the measured water density to arrive at the volume of the water and thus the rock. Subsequent rocks would be placed into the bucket until it was too full and then the rocks would be taken out and the process resumed. Finally, the dry weight of each of the control samples was divided by its measured volume to obtain the density. The density values for all 30 control samples were averaged to obtain a density of 2.72 g/cm^3 for limestone in the Lower Pecos Canyonlands (Table 13). Some variation in the density of the rocks was expected due to unknown moisture content in the rocks, the different types of limestone, and burned and unburned rock samples. However, the data indicate that the average density of the unburned rock

samples (2.82 g/cm^3) is higher than the average density of the samples of burned rock (2.67 g/cm^3). The current sample size is too small to determine if this variation is significant, but future studies that incorporate a larger sample size may be able to use that data to address research questions regarding rock density and heating as it relates to fragmentation. For instance, rocks that become less dense by heating may become more porous and thus, incur higher degrees of water saturation, which may result in a higher likelihood of fragmenting during subsequent heating episodes.



Figure 34. Equipment used to measure the volume and density of sample rocks.

Applying the PAP

The collected images from Feature C005 were processed using the NI Stereo3D modeling software created for this research. This aspect of the whole process proved to be very time consuming as it took around 30 minutes to process a single pair of photos. There were a total of 49 stereo pairs of images for Feature C005 (Figure 35) and each pair needed to be adjusted horizontally to correct for distortion on the outer edges of the images. In some cases, the volume of more than one rock could be calculated from a single stereo pair. The data collected from the field is shown in Table 14 and includes the length, width, and actual weight of each selected rock. The volume of each rock was calculated by dividing the measured weight by the density coefficient of 2.72 g/cm^3 . The Stereo3D volume for each of the 61 rocks was calculated using the Stereo3D program and these numbers were multiplied by the density coefficient to obtain a weight. Figure 36 provides a key to measured rock locations by Rock ID.

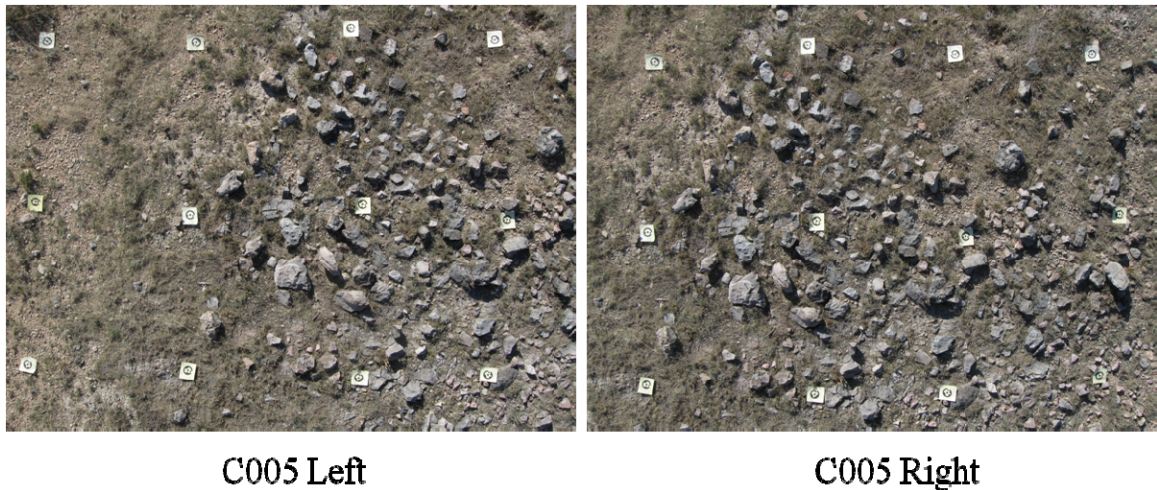


Figure 35. An example of a stereo pair of images from Feature C005.

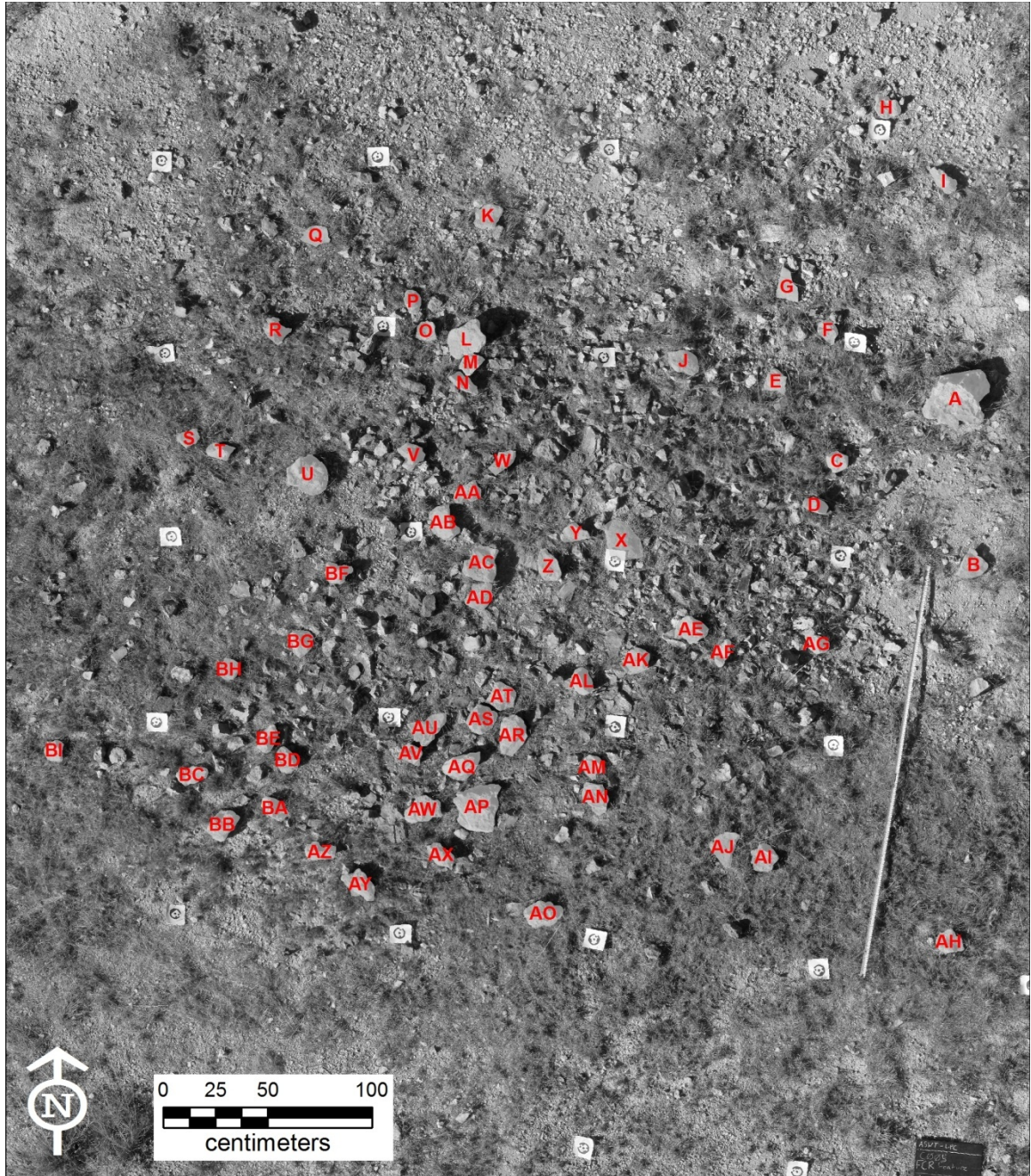


Figure 36. Aerial composite of C005 with measured rocks labeled.

To test the efficacy of using the PAP method to record the weights of burned rock, the mean of the actual weight of the rocks (recorded in the field) was compared to the mean of the weights generated by the Stereo3D program. The mean calculated for the actual weight of the rocks was $m_{aw} = 1555.4$ g and the mean of the weights from

Table 14. Feature C005 collected data.

<i>Rock ID</i>	<i>Length (cm)</i>	<i>Width (cm)</i>	<i>Actual Weight (g)</i>	<i>Volume (cm³)</i>	<i>Stereo3D Volume (cm³)</i>	<i>Stereo3D Weight (g)</i>
A	34.0	31.0	12990	4775.7	4873.4	13255.6
B	15.0	16.0	1080	397.1	389.6	1059.7
C	11.0	10.0	600	220.6	225.3	612.8
D	10.0	8.0	680	250.0	241.2	656.1
E	9.0	9.0	430	158.1	160.3	436.0
F	11.0	8.0	420	154.4	152.6	415.1
G	15.0	10.0	440	161.8	159.7	434.4
H	12.0	13.0	620	227.9	229.1	623.2
I	16.0	6.0	520	191.2	193.7	526.9
J	16.0	13.0	1300	477.9	470.6	1280.0
K	16.0	11.0	1030	378.7	388.9	1057.8
L	18.0	18.0	3470	1275.7	1263.4	3436.4
M	12.0	7.0	880	323.5	330.4	898.7
N	15.0	6.0	800	294.1	292.5	795.6
O	11.0	9.0	570	209.6	205.8	559.8
P	12.0	9.0	490	180.1	178.3	485.0
Q	14.0	10.0	340	125.0	126.2	343.3
R	8.0	10.0	730	268.4	266.7	725.4
S	9.0	8.0	980	360.3	363.4	988.4
T	13.0	8.0	880	323.5	320.9	872.8
U	20.0	17.0	4440	1632.4	1674.5	4554.6
V	12.0	9.0	940	345.6	339.4	923.2
W	15.0	11.0	730	268.4	265.3	721.6
X	21.0	15.0	3430	1261.0	1278.1	3476.4
Y	11.0	9.0	760	279.4	276.5	752.1
Z	15.0	9.0	1010	371.3	363.4	988.4
AA	15.0	9.0	720	264.7	271.6	738.8
AB	24.0	16.0	3140	1154.4	1178	3204.2
AC	20.0	15.0	3290	1209.6	1176.4	3199.8
AD	14.0	14.0	1190	437.5	445.7	1212.3
AE	13.0	11.0	1360	500.0	519.2	1412.2
AF	14.0	6.0	650	239.0	233.6	635.4
AG	15.0	12.0	2170	797.8	822.1	2236.1
AH	11.0	10.0	1200	441.2	432.8	1177.2
AI	13.0	12.0	1080	397.1	388.5	1056.7

Table 14 continued.

<i>Rock ID</i>	<i>Length (cm)</i>	<i>Width (cm)</i>	<i>Actual Weight (g)</i>	<i>Volume (cm³)</i>	<i>Stereo3D Volume (cm³)</i>	<i>Stereo3D Weight (g)</i>
AJ	15.0	13.0	920	338.2	331.6	902.0
AK	12.0	11.0	850	312.5	320.3	871.2
AL	12.0	10.0	1210	444.9	456.7	1242.2
AM	10.0	10.0	860	316.2	324.8	883.5
AN	15.0	10.0	1380	507.4	523.1	1422.8
AO	18.0	13.0	2150	790.4	800.2	2176.5
AP	20.0	20.0	6110	2246.3	2307.4	6276.1
AQ	19.0	14.0	2540	933.8	965.4	2625.9
AR	21.0	14.0	3480	1279.4	1204.2	3275.4
AS	13.0	11.0	1610	591.9	579.5	1576.2
AT	12.0	11.0	1330	489.0	501.8	1364.9
AU	19.0	13.0	2280	838.2	872.9	2374.3
AV	10.0	7.0	1020	375.0	372.4	1012.9
AW	17.0	11.0	1400	514.7	531.7	1446.2
AX	10.0	10.0	660	242.6	240.1	653.1
AY	19.0	11.0	1250	459.6	477.3	1298.3
AZ	14.0	10.0	1240	455.9	429.4	1168.0
BA	13.0	8.0	790	290.4	293.5	798.3
BB	16.0	10.0	1850	680.1	700.2	1904.5
BC	15.0	8.0	880	323.5	326.8	888.9
BD	12.0	8.0	900	330.9	327.4	890.5
BE	14.0	8.0	840	308.8	310.1	843.5
BF	13.0	10.0	1570	577.2	591.6	1609.2
BG	15.0	11.0	820	301.5	299.3	814.1
BH	10.0	8.0	910	334.6	328.9	894.6
BI	10.0	10.0	670	246.3	248.1	674.8
<i>Totals</i>			<i>94880</i>	<i>34882.4</i>	<i>35161.8</i>	<i>95640.1</i>

Stereo3D were $m_{pw} = 1567.9$ g. A two-tailed t-test was used for this comparison and the null hypothesis (H_0) was that there is no significant difference between the two means (H_0 : $m_{aw} = m_{pw}$; H_1 : $m_{aw} \neq m_{pw}$). The t-test resulted in a t-score of 0.9705, $df = 120$, which is less than one and therefore not significant. Based on this result the null hypothesis is

accepted and the application of photogrammetry in calculating the volume and weight of burned rocks is acceptable.

CHAPTER VI

CONCLUSIONS

The purpose of this research was to apply the methods of photogrammetry to the recording of exposed earth oven features on the ground surface. The reason for testing this method was the hope that a quicker method of using digital cameras to record the size and weights of individual rocks in the field could replace the time spent recording rocks manually. Since no one had ever applied this method to earth ovens, it was necessary to construct the equipment, formulate a method for recording the feature, and find a suitable process for extracting metric data from stereo image pairs. This chapter summarizes each of the aspects of this method, proposing alternatives where appropriate, and discusses the pros and cons of applying the PAP method to earth ovens and archaeological fieldwork in general.

Constructing the Equipment

Designing and building the PAP equipment proved to be a pretty simple process and the goal of constructing this equipment at a low cost was accomplished. The use of the paint roller as a pivot point for the mounted cameras was an idea from Mark Willis that simplified the whole process. Using this paint roller, a standard painter's pole would attach at the end and the remaining parts were purchased relatively cheaply at a hardware store. Additionally, a pole of any length can be substituted without having to alter the

design of the camera mount. Purchasing items from a hardware retailer also made the replacement of any parts that much easier, since the only part that had to be special-ordered was the remote trigger for the cameras. The simple construction also means that just about anyone can build and repair it. Obviously, the cameras were the most expensive part of this equipment, but most archaeologists already own cameras and this method can most likely be adapted for several brands of cameras. The digital cameras used in this research were very easy to use and the removable media made it easy to organize data from multiple features on different SD cards for later downloading and processing. The equipment was also very light in weight and was easily transported by hand to and from features across rugged terrain without any problems.

The main limitation with this equipment was the length of the pole and its stability when fully extended. This necessitated shortening the length to a manageable distance, which reduced the amount of ground that could be covered. While this was not problematic for this research since the features recorded were relatively small in size, this could be an adverse factor when recording a larger midden. Another limitation is the length of the USB cable connecting the remote trigger with the cameras. Since USB cables transmit both power and data, a supplemental power source or booster may be needed for cables over ten feet in length. Finally, the use of the pole created shadows in the images which limited the photography to the mornings and afternoons when the sun was not directly overhead. While the shadows could potentially have an adverse effect on the photogrammetry, they were avoided simply to have clean-looking, uniform images. Overall, the equipment performed very well and proved to be very durable, surviving many trips in and out of the bed of a pickup truck.

Field Methods

The initial experiments with recording features were frustrating while trying to determine the correct overlap and sequence for taking the photos, but once this was resolved it was a seamless process. The main aspects of the method that resolved a lot of the initial problems were laying the ground control targets down in a grid rather than randomly, and then using those targets to guide shooting the photos in a systematic fashion. The systematic photography of the features ensured that the images were all generally aligned in the same direction and had relatively equal overlap between them. The photos from the initial experiments were taken at random from the across the feature, often times just pivoting the camera position around the base of the pole to get coverage. This made identifying the location of individual photos very difficult and complicated the stitching the composite image together. Clearing the features was the only labor intensive aspect of the process, although at times prolonged use of the PAP equipment would take a toll on the arms and legs.

Fortunately, the small size of the sampled features meant that the total time to lay out the grid and take all of the photographs was usually only around thirty minutes. Mapping, measuring, and weighing the rocks by hand in the field took two to four hours depending on the number of rocks. The mapping of the rocks was done only as a reference for matching individual rocks to the images and therefore the rocks' outlines were simply sketched using the ground control targets for reference. Mapping these rocks in a more meticulous fashion by hand or even using a total data station would greatly and needlessly increase the time spent on the site. There was also the constant fear of dropping the pole-mounted cameras during PAP recording, which was relieved by

having a second person on hand to help raise and lower the equipment. Having a second person to watch and listen to the cameras also proved useful since the observer could stand back and ensure that the cameras remained parallel to the ground surface, that the photographer did not miss any portions of the feature, and that the camera shutters were in synch.

Given the equipment and circumstances, the method created for this research needs little improvement. The primary limitations of the PAP method are the size and condition of the area to be recorded. First, using this method in an area with a lot of trees or other overhead obstructions could be frustrating and require modifications to this method: lowering the pole would decrease the base distance of the cameras and increase the number of required images. The obstructions could be cleared, but that could result in increased time in the field as well as unnecessary environmental impact. Second, the PAP method is really most suitable for small areas. I would estimate that areas exceeding 100 m² would be hard to manage as far as maintaining a consistent grid and systematic approach. For larger areas, the cameras could be mounted to a balloon or kite to increase the area of coverage, but that requires a different approach. For the purposes of this research, the PAP method met the goal of reducing feature recording time in the field.

Post Processing

The post processing time for the images was unacceptably high. This was mostly due to the Stereo3D software used, where as other aspects, such as stitching the images and mapping the features in ArcMap, was reasonable. The images collected in the field were reviewed for image quality, but none of the images needed editing prior to

processing them in the software. All that was required was organizing the photos by feature and left or right orientation. A free program called File Renamer Basic was used to change the names of all the images to include the feature number, exposure number, and an L or R for orientation. The Microsoft ICE program was very useful for stitching the photos together to use as a reference as well for inputting the stitched image into a GIS. The use of Autodesk's 123D Catch was done simply to visualize the model in 3D space. Finally, the method used for calculating an average density for the limestone in the region was a simple process with good results.

As stated, the Stereo3D software was biggest limitation to this method and did not meet the requirements for reducing time in calculating burned rock weights. However, given that this software was created specifically for this research in a short amount of time, it performed exceptionally well at calculating the volumes of the individual rocks from image pairs. In general, the software is underdeveloped in that a lot of the processing had to be done manually and running the calculations is slow due to the high resolution of the images. It was also designed specifically for use with these particular cameras and these images, meaning the parameters, such as the internal geometry of the cameras and the resolution of the photos, was written into the software code, so it was not possible to alter the original images (i.e., compress files) prior to modeling them. The engineer who designed the software has said that eventually he could automate most of the process and also adapt it for handling more than one pair of images at a time.

The option to design a program specifically for this research was not considered at the outset. It was presumed that commercially available photogrammetry software would be able to easily calculate the volume of individual rocks based on the image pairs.

Three programs were explored in this regard, Leica Photogrammetry Suite, Photomodeler Scanner, and AgiSoft PhotoScan. As best as I could determine, none of these programs can calculate volume to an accurate enough level to satisfy the goals of this research. Additionally, with the exception of PhotoScan, these programs have a steep learning curve related to 3D design software, mapping, and image-related programs.

As a second option, Autodesk's 123D Catch was used to build a model and mesh from the photos and then export this model to a 3D design program such as Blender or MeshLab. Both Blender and MeshLab are free to download and use and are commonly used by designers of 3D objects for video games. However, neither of these programs would calculate volumes within a 3D model. Extensive research on the Internet and various publications found that calculating volumes for 3D objects, especially randomly shaped burned rocks, is not used very much at all and is not part of a currently available program.

The third option then was to have software designed, which came about when I sought the help of a friend who was able to adapt one of National Instrument's existing programs for this research. Although this software was time consuming to use, the resulting volumes are very close to those measured in the field and the subsequent t-test confirms there is no significant difference between the means of the two populations. Thus, the PAP method is effective at accurately rendering exposed earth ovens and their constituent burned rocks whereby these measurements can be applied to other archaeological models.

Applying the Results

Ultimately, the goal of this research was to test the usefulness of the PAP method in recording burned rock features. However, this begs the question, how is this data applicable archaeologically? First, how does the patterning of rocks relate to either the cultural or natural formation processes of the feature during and subsequent to its use? Second, can the total weight of the burned rock within the feature be used to address the frequency of use of the feature? Finally, how does the distribution of the burned rocks by weight reflect the degree of fragmentation with regard to the frequency of use of the feature?

Using the composite images provided a unique perspective of each feature for observing the patterning of burned rocks. By georeferencing the composite image in a GIS, it was also possible to examine the feature within a regional context as well as within the feature itself. Once the rocks measured in the field were digitized in ArcMap, their values (weights) could be classified and color coded for identifying the larger, unfragmented rocks or smaller, fragmented rocks. Then patterns were inferred based on the distribution of the rocks with respect to the central heating element, distance between rocks, possible discard areas, and formation processes. All of the features had recognizable central heating elements that consisted of concentrated areas of the heaviest rocks. Feature C006 had the tightest cluster of rocks at its center, while A257 had the most diffuse cluster with the other features falling somewhere in between.

The average distance between the rocks was measured with the distance tool in ArcMap. Both C003 and A257 had greater distances between the rocks than the other features which is most likely the result of their location. C003 is on more of a slope than

the other two features recorded at Painted Canyon Flat (C001 and C006), which has seriously deflated the surrounding matrix and likely displaced some of the rocks.

Pedestrian traffic at the site may have also have an effect on the feature since it is in close proximity to the road and parking area. A257 is positioned on a deflated terrace overlooking the Pecos River and this area has heavy sheet wash erosion during rainstorms.

The only feature with apparent discard piles was C003, which had a concentration of burned rock along the southeast edge of the central heating element. The concentration is likely not due to erosion since the landform slopes down to the west. However, the inferred central heating element's location may also be incorrect. Although, no other clearly defined discard piles were observed among the other features, lighter fragments of rock tend to accumulate on one side of each of the features. The direction of accumulations is not consistent, but for features A257 and C006 they correlate with the down slope side of the features, which are more prevalent on A257 and C006. Accumulations at C001, C004, C005, and C007 were deposited downwind of the regions prevailing southeasterly winds. C003 was an anomaly in that the accumulations were deposited on the southeast and northeast sides of the central heating element, upwind and upslope from the central heating element.

Ascertaining the frequency of feature use by the total weight of rock in the feature is accomplished primarily through experimental work, where the actual number of firings is known and the rock weight and reuse can be quantified. Unfortunately, the number of experiments that provide these kinds of data are small, resulting in only generalized estimates of feature reuse when applied to the archaeological record. As the number of

experiments increase, as well as the types of data collected, calculating feature reuse will become more accurate.

Looking at the total weight of each of the features for the current research, there appears to be a notable difference in total estimated weight between Shumla Ranch and Painted Canyon Flat. The features at Painted Canyon Flat (C001, C003, and C006) are two to three times heavier than the features at Shumla Ranch (C004, C005, and C007). The difference in weights is most likely due to proximity of the features to limestone sources. While there is no shortage of limestone in either area, the features at Painted Canyon Flat are closer to outcrops with numerous, large limestone slabs. The close proximity to the outcrops may have made it easier to bring in larger rocks and possibly a surplus of rock.

Ultimately, the degree of fragmentation of the burned rocks is the best indication of frequency of use of earth ovens. The burned rocks for each of the features were divided into five weight classes to determine the degree of fragmentation with Class I being the lightest, or smallest, and apparently most heavily fragmented rocks, and Class V being the heaviest, or largest, and least fragmented rocks. The distribution of weights for each feature is presented in Figure 37 with the top four histograms representing the features at Shumla Ranch and the bottom three histograms representing the features at Painted Canyon Flat. In general, a comparison of the weight distribution for each of the features indicates that the Painted Canyon Flat features have a relatively lower percentage of highly fragmented rock than the Shumla Ranch features. Feature C006 exhibits the highest percentage of unfragmented rocks of the entire sample as well as a low amount of highly fragmented rocks.

Based on the skewed weight class distribution of C006 and the presence of only a single lens of charcoal beneath it, it is argued that this feature represents a single-use event. Features C001 and C003, also at Painted Canyon Flat have weight distributions that trend towards a higher amount of heavier, unfragmented rocks and a lower amount of highly fragmented rocks. However, their distributions indicate higher amounts of fragmented rock than C006 and suggest some reuse at these features. Features C007 and A257 have variable percent weights across all classes which may indicate moderate reuse of these features. Finally, C004 and C005 exhibit relatively high percentages of highly fragmented rock and relatively low percentages of unfragmented rock. While this may be indicative of several episodes of reuse, it could also be the result of buried rocks that are not represented in the sample.

The comparison of these features based on the degree of fragmentation is interesting in the differences between the Shumla Ranch and Painted Flat Canyon. Overall, Shumla Ranch features exhibit a much lower total weight with a higher percentage of highly fragmented rock, while the Painted Canyon Flat features exhibit a much higher total weight with lower percentage of highly fragmented rock. While the data used in the distribution of burned rocks may be inaccurate in some of the features because of the unweighed rock (both partially buried, unmeasured rocks and estimated weights for rocks less than 10 cm in size), the total weight estimates and weight distributions are close approximations of relative feature use. Although these comparisons were made with the actual weights measured in the field, using the PAP should obtain similar results, as evidenced by the result of comparing the measured weights in C005 to the Stereo3D generated weights.

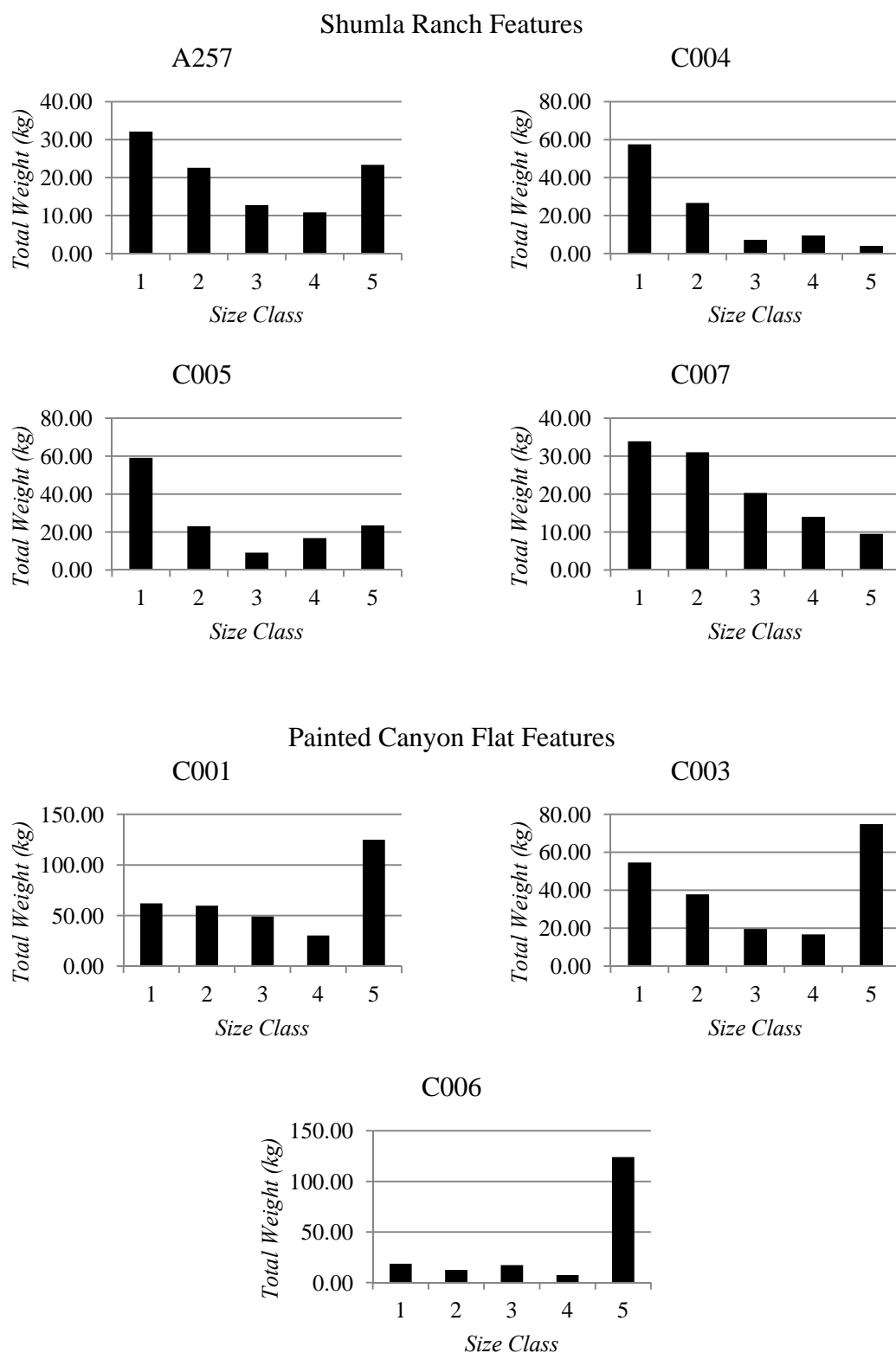


Figure 37. Distributions of weight of burned rock by class for all features.

Concluding Comments

The PAP method provides an alternative approach to the study of earth ovens and archaeology in general. The most important aspect of PAP, and remote sensing in general, is that the process is non destructive thereby leaving archaeological deposits intact for future research. The method is easy to apply and relatively inexpensive. The biggest challenge for the author during the research was the technological learning curve of the software and photogrammetry in general. However, the method developed here worked very well in the field, resulting in reliable, accurate photos. In hindsight, some elements that would improve this method include:

- Generating models based on different image resolutions to ascertain the variation in accuracy. I only used one resolution for my photos, it would be interesting to compare the results of differing resolutions to arrive at a minimum value needed to save processing time.
- Collect more accurate GPS coordinates for the ground control points. Collecting shots on four points was sufficient, but the limited spent at each target did not allow for sub meter accuracy.
- Use different camera filters to evaluate the features from different perspectives. For example, I had postulated using infrared photography to photograph the features in the hope that vegetation would be minimized and rocks would be highlighted.
- Weigh all of the rocks or a representative sample from all size classes. The 10 cm size threshold for rocks during data collection was likely too

large and the results would have benefited considerably by having the weights of all rock within the feature.

- Collect more types of data from the features. Although collecting the length, width, and weight of each rock took a couple of hours for each feature, most of that time was spent drawing and handling the rocks. Adding a few extra data sets, such as number of facets, material type, etc. would have been a great benefit to the study without adding too much time.
- Conduct limited excavations to determine the extent to which feature elements may be buried. The excavation at C006 was critical to verifying that the feature was most likely a single use oven. Shovel tests excavated around the periphery of the features would have provided more insight into the nature of deposits within and around the features.
- Collect measurements on partially buried rocks. Obtaining size estimates (such as length, width, and height) of the partially buried rocks should allow for reasonable estimates of their weight.

Another area where PAP is ideally suited is in spatial application such as GIS. As demonstrated in this research, PAP collected data can be obtained in a short period of time with a high degree of accuracy. Barring the need for calculating volumes, many three-dimensional aspects of the collected photos can be acquired as point clouds that can be imported into a GIS and georeferenced. Two-dimensional composite images can also be imported and georeferenced and various elements within the images can be digitized,

as was done within this research. Once in a GIS this data could be processed using spatial statistics to address archaeological questions. For instance with regard to the PAP images recorded here, statistics could be applied to look for patterns in how burned rocks are distributed around the central core of the feature taking into consideration the size or weight of each rock. Other attributes could be included as well, such as rock type, burned or unburned, the number of facets, and the addition of other artifact types. Remote sensing with cheap digital cameras offers a unique opportunity for collecting high quality geospatial data without the expense in cost or time of LiDAR or even total data stations. The choice of equipment should be determined by the desired scale.

The field of photogrammetry and 3D modeling is developing rapidly due to the convergence of high quality inexpensive cameras and powerful consumer computers. A big part of this is the photogrammetry software which obviates the need for expensive, calibrated cameras. The software has also made the need for stereo pairs of cameras less important as the errors inherent in non-paired images can be corrected. Moreover the availability of this technology to the average consumer is creating a large pool of users that are finding new and creative ways to apply photogrammetry. Regardless of the changing technology and methods within the field of photogrammetry, the images archaeologists collect can provide valuable, and as yet undiscovered, data. If archaeologists include PAP as part of their field research, the data can be used by current or future researchers to address research questions with new technology or better methods.

APPENDIX

BURNED ROCK DATA FOR SELECTED FEATURES

The following appendix provides the data collected for the seven burned rock features that were discussed in the previous chapters. The data is tabulated and accompanied by a map of the features showing the location, by Rock ID of each of the measured rocks. The features are presented numerical order starting with A257 then C001, C003, C004, C005, C006, and C007.

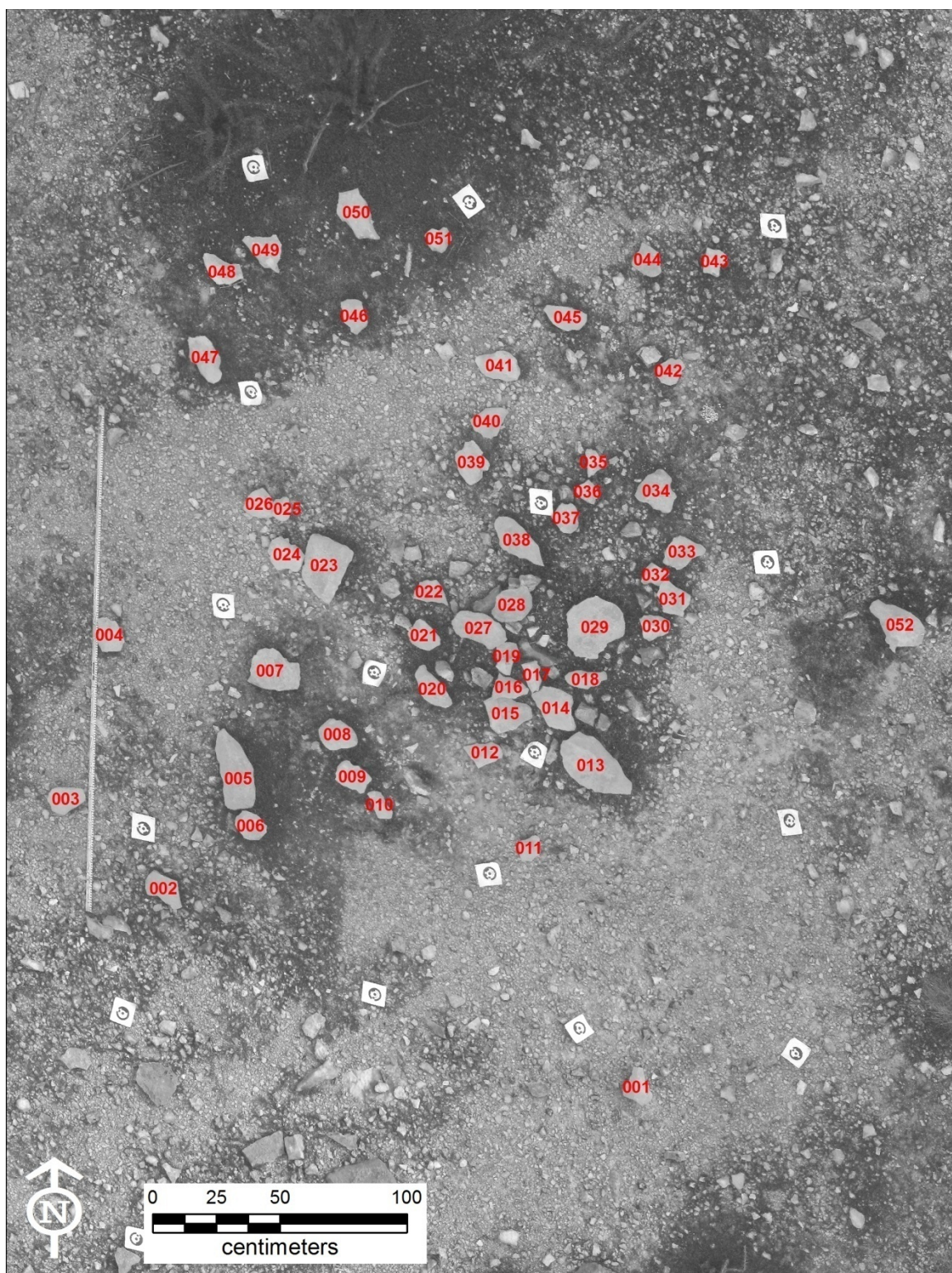


Figure A-1. Feature A257 Plan Map with measured burned rocks labeled.

Table A-1. Feature A257 burned rock data.

<i>Rock ID</i>	<i>Length (cm)</i>	<i>Width (cm)</i>	<i>Weight (kg)</i>	<i>Volume (cm³)</i>
001	15.0	12.0	1.20	441.2
002	14.0	14.0	1.01	371.3
003	16.0	11.0	1.24	455.9
004	14.0	11.0	0.81	297.8
005	33.0	13.0	4.69	1724.3
006	12.0	12.0	1.06	389.7
007	21.0	17.0	3.76	1382.4
008	14.0	12.0	0.88	323.5
009	13.0	12.0	0.94	345.6
010	12.0	7.0	0.28	102.9
011	9.0	12.0	0.61	224.3
012	14.0	10.0	0.91	334.6
013	30.0	20.0	4.77	1753.7
014	21.0	17.0	2.88	1058.8
015	20.0	16.0	2.67	981.6
016	16.0	9.0	0.74	272.1
017	11.0	7.0	0.56	205.9
018	18.0	8.0	1.01	371.3
019	16.0	8.0	0.94	345.6
020	18.0	12.0	1.28	470.6
021	10.0	12.0	0.84	308.8
022	15.0	10.0	0.79	290.4
023	24.0	18.0	5.04	1852.9
024	16.0	15.0	1.01	371.3
025	11.0	8.0	0.35	128.7
026	13.0	13.0	0.99	364.0
027	23.0	13.0	1.97	724.3
028	18.0	15.0	1.58	580.9
029	24.0	24.0	3.19	1172.8
030	13.0	10.0	0.66	242.6
031	14.0	14.0	0.90	330.9
032	10.0	9.0	0.88	323.5
033	15.0	11.0	0.60	220.6
034	18.0	16.0	2.16	794.1
035	11.0	8.0	0.97	356.6
036	10.0	9.0	0.74	272.1
037	12.0	11.0	1.49	547.8
038	25.0	13.0	3.90	1433.8

Table A-1 continued.

<i>Rock ID</i>	<i>Length (cm)</i>	<i>Width (cm)</i>	<i>Weight (kg)</i>	<i>Volume (cm³)</i>
039	18.0	14.0	4.21	1547.8
040	16.0	11.0	2.53	930.1
041	18.0	12.0	1.98	727.9
042	13.0	9.0	1.27	466.9
043	10.0	9.0	0.59	216.9
044	12.0	11.0	0.63	231.6
045	17.0	10.0	1.06	389.7
046	14.0	10.0	1.13	415.4
047	19.0	12.0	1.50	551.5
048	14.0	13.0	1.11	408.1
049	13.0	17.0	1.71	628.7
050	20.0	14.0	2.51	922.8
051	10.0	9.0	0.43	158.1
052	22.0	17.0	4.67	1716.9
<i>Totals</i>			<i>85.63</i>	<i>31481.6</i>

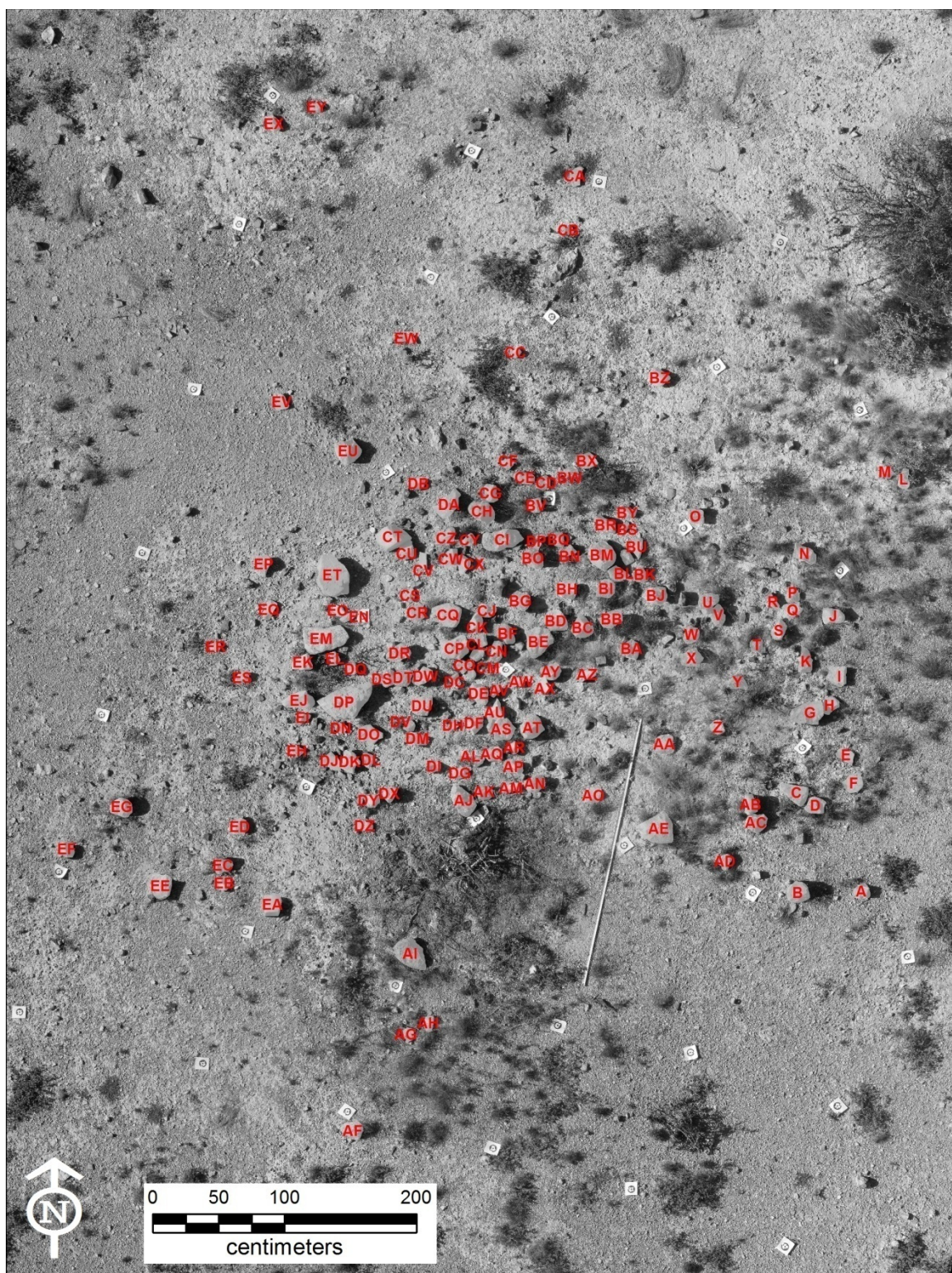


Figure A-2. Feature C001 plan map with measured burned rocks labeled.

Table A-2. Feature C001 burned rock data.

<i>Rock ID</i>	<i>Length (cm)</i>	<i>Width (cm)</i>	<i>Weight (kg)</i>	<i>Volume (cm³)</i>
A	11.0	9.0	0.94	345.6
B	17.0	16.0	3.67	1349.3
C	20.5	14.5	2.57	944.9
D	14.0	12.0	1.96	720.6
E	13.5	10.0	0.47	172.8
F	16.5	16.0	0.97	356.6
G	23.0	15.5	5.63	2069.9
H	15.0	10.0	0.98	360.3
I	14.5	13.5	1.59	584.6
J	16.0	12.0	2.26	830.9
K	19.0	10.0	1.15	422.8
L	14.0	10.0	1.89	694.9
M	13.0	10.0	0.84	308.8
N	19.0	10.5	3.06	1125.0
O	13.5	11.0	2.02	742.6
P	13.0	10.0	0.69	253.7
Q	14.0	12.0	1.29	474.3
R	14.5	4.5	0.73	268.4
S	10.0	9.5	1.13	415.4
T	10.0	10.0	0.36	132.4
U	14.0	15.0	2.31	849.3
V	17.0	11.0	1.96	720.6
W	15.0	10.0	1.14	419.1
X	15.0	11.0	1.96	720.6
Y	10.0	9.0	0.46	169.1
Z	10.0	8.0	0.69	253.7
AA	13.0	13.0	1.38	507.4
AB	15.0	11.0	2.45	900.7
AC	15.0	14.0	1.76	647.1
AD	12.0	8.0	0.48	176.5
AE	24.0	18.0	12.58	4625.0
AF	16.0	12.0	2.14	786.8
AG	11.0	9.0	0.44	161.8
AH	11.0	8.0	0.47	172.8
AI	25.0	18.0	5.25	1930.1
AJ	16.0	10.0	2.38	875.0
AK	11.0	7.5	1.06	389.7
AL	12.0	11.0	2.24	823.5

Table A-2 continued.

<i>Rock ID</i>	<i>Length (cm)</i>	<i>Width (cm)</i>	<i>Weight (kg)</i>	<i>Volume (cm³)</i>
AM	13.0	6.0	0.57	209.6
AN	16.0	11.0	3.79	1393.4
AO	14.0	10.0	1.03	378.7
AP	16.0	11.0	1.73	636.0
AQ	12.0	11.0	0.96	352.9
AR	10.0	9.0	0.45	165.4
AS	14.0	17.0	2.97	1091.9
AT	17.0	15.0	5.95	2187.5
AU	19.0	12.0	2.18	801.5
AV	9.0	7.0	0.54	198.5
AW	11.0	6.0	0.93	341.9
AX	10.0	9.0	0.46	169.1
AY	13.0	13.0	1.37	503.7
AZ	12.0	7.0	0.58	213.2
BA	12.0	13.0	0.90	330.9
BB	19.0	13.0	2.51	922.8
BC	18.0	12.0	3.45	1268.4
BD	14.0	14.0	4.66	1713.2
BE	22.0	23.0	6.27	2305.1
BF	16.0	10.0	1.98	727.9
BG	16.0	12.0	2.68	985.3
BH	17.0	15.0	1.88	691.2
BI	20.0	16.0	3.34	1227.9
BJ	18.0	13.0	2.78	1022.1
BK	11.0	8.0	0.93	341.9
BL	15.0	8.0	0.49	180.1
BM	19.0	16.0	6.00	2205.9
BN	9.0	7.0	0.56	205.9
BO	17.0	9.0	2.41	886.0
BP	9.0	5.0	0.82	301.5
BQ	12.0	10.0	0.68	250.0
BR	19.0	11.0	1.42	522.1
BS	12.0	6.0	0.51	187.5
BT	11.0	10.0	0.71	261.0
BU	15.0	8.0	0.72	264.7
BV	10.0	10.0	1.30	477.9
BW	10.0	12.0	0.69	253.7
BX	18.0	12.0	1.16	426.5

Table A-2 continued.

<i>Rock ID</i>	<i>Length (cm)</i>	<i>Width (cm)</i>	<i>Weight (kg)</i>	<i>Volume (cm³)</i>
BY	12.0	10.0	0.76	279.4
BZ	13.0	12.0	1.93	709.6
CA	16.0	8.0	0.57	209.6
CB	8.0	7.0	0.26	95.6
CC	9.0	7.0	0.25	91.9
CD	11.0	8.0	0.21	77.2
CE	14.0	7.0	1.14	419.1
CF	9.0	8.0	0.39	143.4
CG	14.0	11.0	1.36	500.0
CH	20.0	14.0	5.16	1897.1
CI	26.0	13.0	5.86	2154.4
CJ	11.0	11.0	0.90	330.9
CK	13.0	12.0	1.39	511.0
CL	11.0	10.0	1.12	411.8
CM	12.0	9.0	1.10	404.4
CN	16.0	9.0	1.11	408.1
CO	11.0	8.5	0.74	272.1
CP	21.0	21.0	5.18	1904.4
CQ	19.0	16.0	4.05	1489.0
CR	12.0	11.0	0.90	330.9
CS	8.0	5.0	0.38	139.7
CT	20.0	15.0	7.57	2783.1
CU	12.0	11.0	1.26	463.2
CV	12.0	5.5	0.39	143.4
CW	13.5	6.0	0.79	290.4
CX	12.0	10.0	0.58	213.2
CY	10.0	7.0	0.72	264.7
CZ	14.0	8.0	1.38	507.4
DA	16.0	16.0	2.50	919.1
DB	12.0	8.0	0.79	290.4
DC	14.0	12.0	1.43	525.7
DD	8.0	6.0	0.53	194.9
DE	20.0	13.0	2.69	989.0
DF	13.0	9.0	1.31	481.6
DG	18.0	12.0	3.33	1224.3
DH	11.0	8.0	0.59	216.9
DI	10.0	10.0	0.54	198.5
DJ	16.0	13.0	1.27	466.9

Table A-2 continued.

<i>Rock ID</i>	<i>Length (cm)</i>	<i>Width (cm)</i>	<i>Weight (kg)</i>	<i>Volume (cm³)</i>
DK	16.0	12.0	2.05	753.7
DL	11.0	9.0	0.34	125.0
DM	14.0	10.0	1.08	397.1
DN	11.0	9.0	0.39	143.4
DO	19.0	14.0	1.57	577.2
DP	41.0	24.0	19.00	6985.3
DQ	9.5	7.0	0.72	264.7
DR	19.0	15.0	3.19	1172.8
DS	16.0	11.0	0.60	220.6
DT	14.0	11.0	1.39	511.0
DU	19.0	17.0	2.74	1007.4
DV	10.5	10.0	0.33	121.3
DW	14.0	10.0	1.59	584.6
DX	13.0	9.0	1.53	562.5
DY	12.0	11.0	0.97	356.6
DZ	13.0	9.0	0.65	239.0
EA	16.0	14.0	2.34	860.3
EB	11.0	9.0	0.51	187.5
EC	13.0	11.0	1.53	562.5
ED	12.0	9.0	1.14	419.1
EE	17.0	16.0	3.03	1114.0
EF	13.0	11.0	1.22	448.5
EG	13.0	15.0	2.84	1044.1
EH	9.0	10.0	0.47	172.8
EI	11.0	8.0	0.52	191.2
EJ	24.0	13.0	4.24	1558.8
EK	14.0	12.0	3.39	1246.3
EL	10.0	8.0	0.72	264.7
EM	34.0	21.0	11.12	4088.2
EN	12.0	6.0	0.33	121.3
EO	11.0	7.0	0.59	216.9
EP	16.0	10.0	1.58	580.9
EQ	16.0	8.0	0.75	275.7
ER	10.0	8.0	0.34	125.0
ES	11.0	9.0	0.78	286.8
ET	32.0	23.0	11.05	4062.5
EU	19.0	16.0	5.27	1937.5
EV	12.0	9.0	0.60	220.6

Table A-2 continued.

<i>Rock ID</i>	<i>Length (cm)</i>	<i>Width (cm)</i>	<i>Weight (kg)</i>	<i>Volume (cm³)</i>
EW	15.0	7.0	0.38	139.7
EX	14.0	10.0	1.12	411.8
EY	11.0	9.0	0.63	231.6
<i>Totals</i>			<i>304.77</i>	<i>112047.8</i>

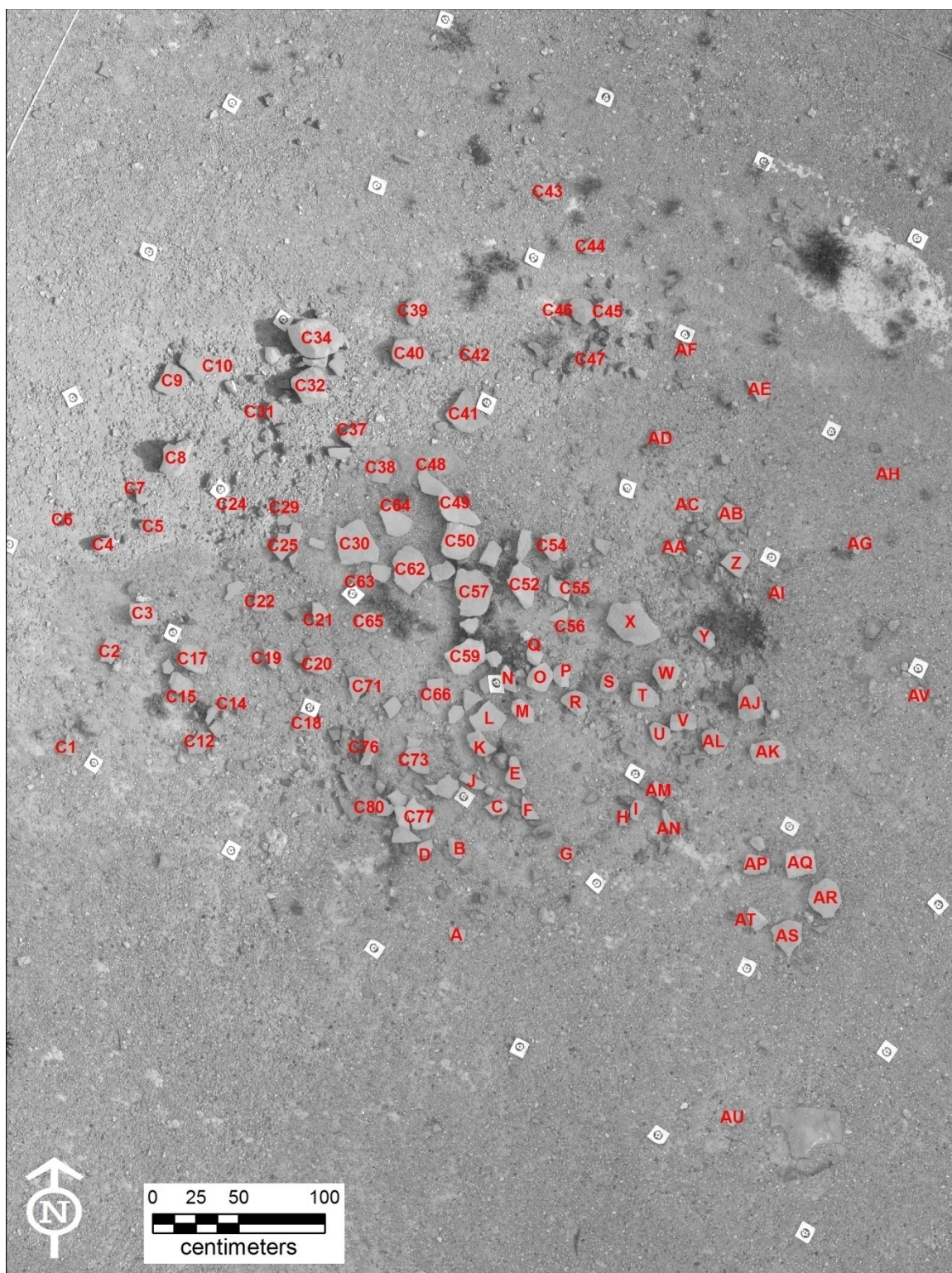


Figure A-3. Feature C003 plan map with measured burned rocks labeled.

Table A-3. Feature C003 burned rock data.

<i>Rock ID</i>	<i>Length (cm)</i>	<i>Width (cm)</i>	<i>Weight (kg)</i>	<i>Volume (cm³)</i>
A	10.0	8.0	0.35	128.7
B	12.0	6.0	0.41	150.7
C	11.0	10.0	1.09	400.7
D	18.0	11.0	1.76	647.1
E	16.0	8.0	0.40	147.1
F	13.0	9.0	0.58	213.2
G	9.0	6.0	0.57	209.6
H	10.0	4.5	0.26	95.6
I	15.0	7.0	0.59	216.9
J	13.0	4.0	1.01	371.3
K	17.0	12.0	2.35	864.0
L	15.0	16.0	1.55	569.9
M	13.0	10.0	1.50	551.5
N	10.0	7.0	1.03	378.7
O	17.0	11.0	1.89	694.9
P	10.0	17.0	1.23	452.2
Q	10.0	8.0	0.95	349.3
R	17.0	14.0	0.90	330.9
S	14.0	11.0	0.74	272.1
T	19.0	13.0	2.29	841.9
U	12.0	11.0	0.41	150.7
V	15.0	8.0	0.58	213.2
W	15.0	10.0	3.01	1106.6
X	34.0	20.0	6.41	2356.6
Y	13.0	9.0	0.41	150.7
Z	13.0	13.0	0.90	330.9
AA	10.0	7.0	0.73	268.4
AB	16.0	13.0	0.31	114.0
AC	11.0	10.0	0.12	44.1
AD	12.0	7.0	0.50	183.8
AE	11.0	12.0	0.69	253.7
AF	9.0	10.0	0.53	194.9
AG	11.0	12.0	1.59	584.6
AH	12.5	8.0	0.32	117.6
AI	11.0	7.0	0.34	125.0
AJ	19.0	10.0	3.72	1367.6
AK	13.0	12.0	1.82	669.1
AL	13.0	14.0	0.94	345.6

Table A-3 continued.

<i>Rock ID</i>	<i>Length (cm)</i>	<i>Width (cm)</i>	<i>Weight (kg)</i>	<i>Volume (cm³)</i>
AM	7.0	10.5	0.48	176.5
AN	14.0	6.0	0.24	88.2
AO	8.0	6.0	0.36	132.4
AP	14.0	11.0	1.49	547.8
AQ	16.0	14.0	2.94	1080.9
AR	20.0	19.0	3.15	1158.1
AS	22.0	16.0	2.26	830.9
AT	11.0	8.0	1.19	437.5
AU	9.0	8.0	0.23	84.6
AV	8.0	8.0	0.37	136.0
C1	11.0	12.0	0.59	216.9
C2	15.0	9.0	1.44	529.4
C3	11.0	18.0	3.26	1198.5
C4	7.0	13.0	0.95	349.3
C5	18.0	4.5	1.02	375.0
C6	13.0	5.0	0.32	117.6
C7	10.0	5.0	0.17	62.5
C8	23.0	15.0	5.64	2073.5
C9	18.0	15.0	1.29	474.3
C10	18.0	19.0	1.06	389.7
C11	10.0	10.0	0.48	176.5
C12	20.0	10.0	0.66	242.6
C13	10.0	9.0	0.28	102.9
C14	13.0	6.0	0.52	191.2
C15	15.0	13.0	1.52	558.8
C16	10.0	9.0	0.33	121.3
C17	19.0	14.0	4.35	1599.3
C18	13.0	14.0	0.52	191.2
C19	13.0	7.0	0.66	242.6
C20	12.0	13.0	1.39	511.0
C21	10.0	10.0	0.76	279.4
C22	12.0	9.0	0.53	194.9
C23	16.0	8.0	0.28	102.9
C24	12.0	11.0	0.20	73.5
C25	18.0	12.0	1.02	375.0
C26	10.0	5.0	0.24	88.2
C27	9.0	5.0	0.30	110.3
C28	11.0	9.0	0.21	77.2

Table A-3 continued.

<i>Rock ID</i>	<i>Length (cm)</i>	<i>Width (cm)</i>	<i>Weight (kg)</i>	<i>Volume (cm³)</i>
C29	14.0	9.0	0.26	95.6
C30	25.0	25.0	4.39	1614.0
C31	12.0	9.0	0.51	187.5
C32	22.0	21.0	5.04	1852.9
C33	13.0	6.0	0.77	283.1
C34	27.0	20.0	14.90	5477.9
C35	15.0	10.0	0.74	272.1
C36	13.0	7.0	0.28	102.9
C37	14.0	9.0	0.82	301.5
C38	16.0	11.0	0.65	239.0
C39	15.0	8.0	1.49	547.8
C40	20.0	17.0	5.59	2055.1
C41	21.0	20.0	2.91	1069.9
C42	13.0	5.0	0.55	202.2
C43	14.0	12.0	0.68	250.0
C44	12.0	9.0	0.53	194.9
C45	17.0	14.0	2.37	871.3
C46	15.0	13.0	1.59	584.6
C47	13.0	6.0	0.41	150.7
C48	19.0	11.0	1.27	466.9
C49	29.0	15.0	5.75	2114.0
C50	24.0	20.0	5.94	2183.8
C51	13.0	9.0	1.10	404.4
C52	25.0	17.0	3.63	1334.6
C53	14.0	7.0	2.37	871.3
C54	18.0	12.0	0.62	227.9
C55	10.0	7.0	0.45	165.4
C56	12.0	7.0	0.32	117.6
C57	27.0	20.0	6.44	2367.6
C58	10.0	7.0	0.81	297.8
C59	24.0	17.0	4.45	1636.0
C60	9.0	7.0	0.69	253.7
C61	14.0	10.0	1.07	393.4
C62	21.0	25.0	5.92	2176.5
C63	13.0	10.0	0.39	143.4
C64	20.0	16.0	1.29	474.3
C65	12.0	11.0	1.75	643.4
C66	15.0	10.0	0.77	283.1

Table A-3 continued.

<i>Rock ID</i>	<i>Length (cm)</i>	<i>Width (cm)</i>	<i>Weight (kg)</i>	<i>Volume (cm³)</i>
C67	13.0	10.0	0.59	216.9
C68	11.0	10.0	0.61	224.3
C69	12.0	9.0	0.31	114.0
C70	13.0	10.0	0.67	246.3
C71	16.0	12.0	0.88	323.5
C72	11.0	8.0	0.21	77.2
C73	21.0	13.0	1.27	466.9
C74	16.0	13.0	0.84	308.8
C75	10.0	9.0	0.18	66.2
C76	21.0	9.0	1.08	397.1
C77	20.0	15.0	2.07	761.0
C78	15.0	8.0	0.69	253.7
C79	12.0	10.0	0.99	364.0
C80	14.0	12.0	0.81	297.8
C81	19.0	11.0	0.78	286.8
<i>Totals</i>			<i>188.97</i>	<i>69474.3</i>

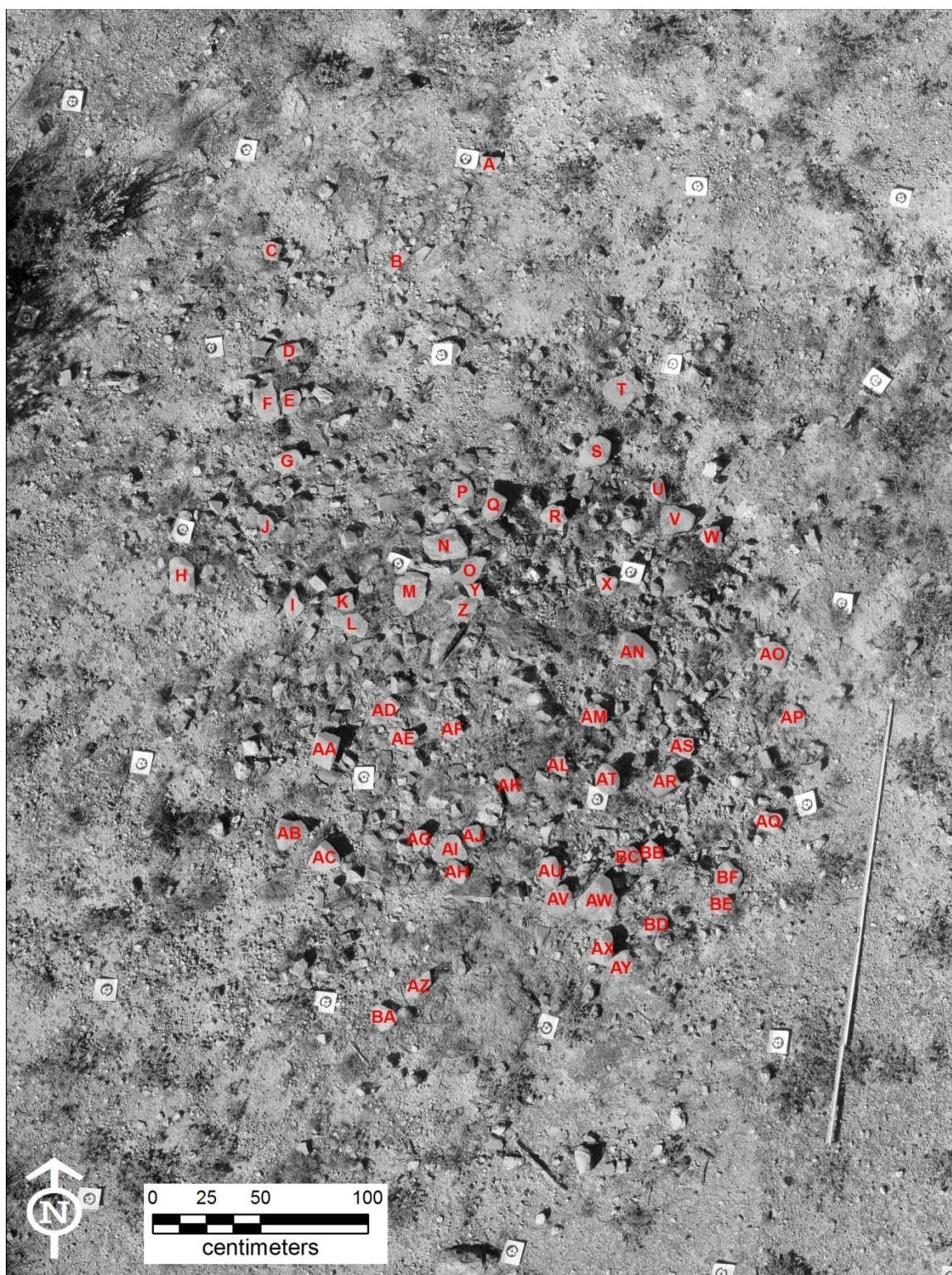


Figure A-4. Feature C004 plan map with measured burned rocks labeled.

Table A-4. Feature C004 burned rock data.

<i>Rock ID</i>	<i>Length (cm)</i>	<i>Width (cm)</i>	<i>Weight (kg)</i>	<i>Volume (cm³)</i>
A	10.0	8.0	0.42	154.4
B	13.0	6.0	0.52	191.2
C	10.0	10.0	0.57	209.6
D	12.0	7.0	0.55	202.2
E	12.0	11.0	0.62	227.9
F	21.0	12.0	1.86	683.8
G	15.0	11.0	0.95	349.3
H	18.0	12.0	2.12	779.4
I	15.0	10.0	0.53	194.9
J	10.0	8.0	0.62	227.9
K	10.0	10.0	0.65	239.0
L	16.0	9.0	1.05	386.0
M	20.0	14.0	1.82	669.1
N	18.0	12.0	3.19	1172.8
O	18.0	11.0	1.02	375.0
P	13.0	10.0	1.61	591.9
Q	15.0	13.0	1.54	566.2
R	12.0	11.0	1.11	408.1
S	17.0	12.0	1.82	669.1
T	17.0	14.0	1.26	463.2
U	11.0	7.0	0.60	220.6
V	18.0	15.0	2.75	1011.0
W	10.0	10.0	0.83	305.1
X	12.0	11.0	0.46	169.1
Y	7.0	8.0	0.51	187.5
Z	15.0	8.0	0.94	345.6
AA	11.0	14.0	3.13	1150.7
AB	16.0	14.0	1.81	665.4
AC	14.0	12.0	1.78	654.4
AD	10.0	7.0	0.65	239.0
AE	21.0	11.0	2.41	886.0
AF	8.0	7.0	0.43	158.1
AG	9.0	8.0	0.60	220.6
AH	11.0	8.0	0.85	312.5
AI	13.0	9.0	0.66	242.6
AJ	10.0	6.0	0.63	231.6
AK	15.0	7.0	0.46	169.1
AL	13.0	9.0	0.57	209.6

Table A-4 continued.

<i>Rock ID</i>	<i>Length (cm)</i>	<i>Width (cm)</i>	<i>Weight (kg)</i>	<i>Volume (cm³)</i>
AM	10.0	11.0	0.80	294.1
AN	19.0	14.0	4.01	1474.3
AO	17.0	14.0	0.82	301.5
AP	12.0	11.0	0.50	183.8
AQ	14.0	8.0	0.64	235.3
AR	13.0	9.0	1.53	562.5
AS	8.0	13.0	0.44	161.8
AT	15.0	12.0	1.85	680.1
AU	16.0	9.0	1.40	514.7
AV	9.0	10.0	0.68	250.0
AW	17.0	14.0	3.20	1176.5
AX	17.0	11.0	1.19	437.5
AY	13.0	11.0	1.62	595.6
AZ	15.0	8.0	1.11	408.1
BA	12.0	10.0	0.77	283.1
BB	13.0	8.0	0.90	330.9
BC	11.0	7.0	0.56	205.9
BD	11.0	11.0	0.58	213.2
BE	9.0	9.0	0.54	198.5
BF	12.0	10.0	1.27	466.9
<i>Totals</i>			<i>68.31</i>	<i>25114.0</i>

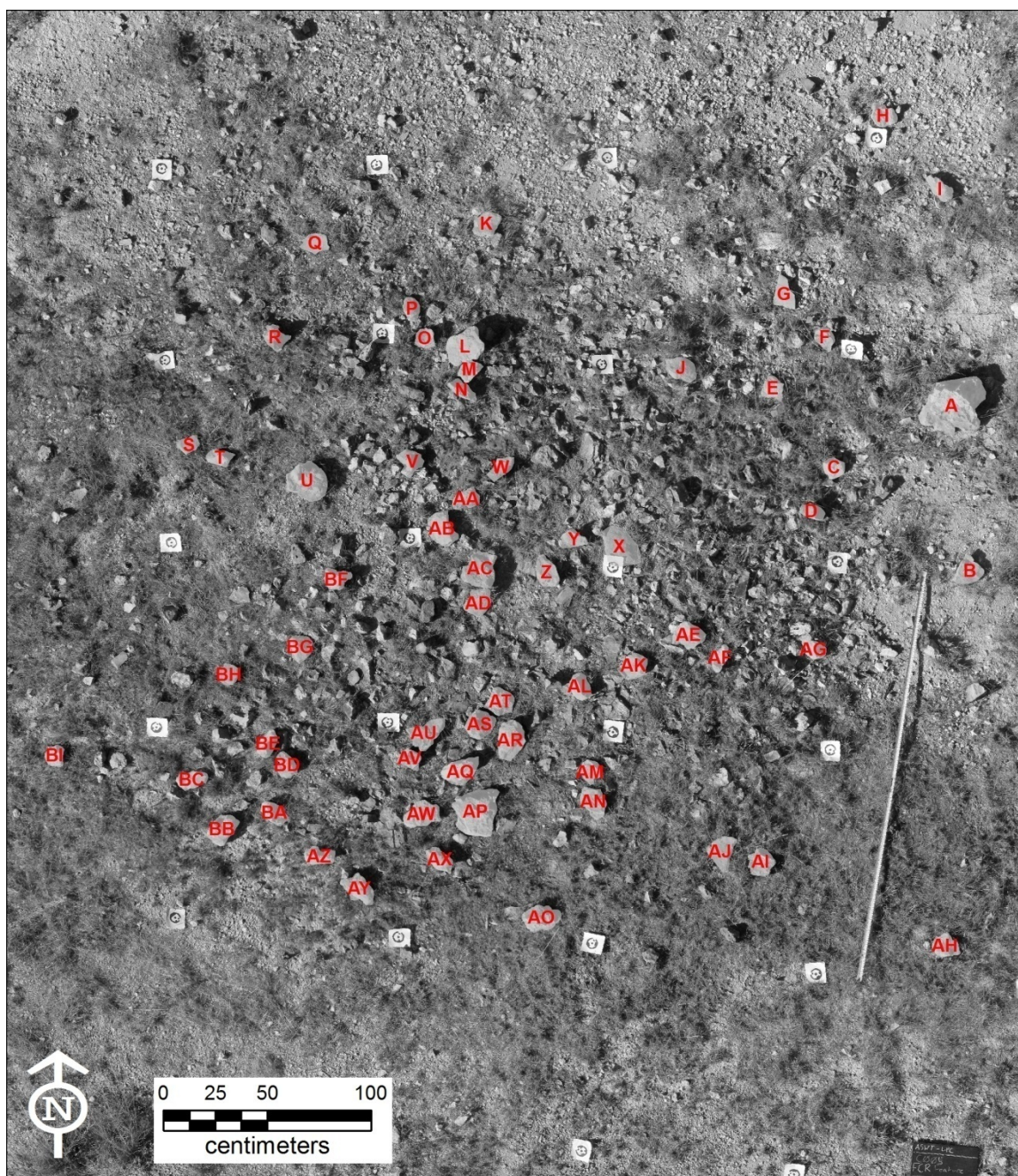


Figure A-5. Feature C005 plan map with measured burned rocks labeled.

Table A-5. Feature C005 burned rock data.

<i>Rock ID</i>	<i>Length (cm)</i>	<i>Width (cm)</i>	<i>Weight (kg)</i>	<i>Volume (cm³)</i>
A	34.0	31.0	12.99	4775.7
B	15.0	16.0	1.08	397.1
C	11.0	10.0	0.60	220.6
D	10.0	8.0	0.68	250.0
E	9.0	9.0	0.43	158.1
F	11.0	8.0	0.42	154.4
G	15.0	10.0	0.44	161.8
H	12.0	13.0	0.62	227.9
I	16.0	6.0	0.52	191.2
J	16.0	13.0	1.30	477.9
K	16.0	11.0	1.03	378.7
L	18.0	18.0	3.47	1275.7
M	12.0	7.0	0.88	323.5
N	15.0	6.0	0.80	294.1
O	11.0	9.0	0.57	209.6
P	12.0	9.0	0.49	180.1
Q	14.0	10.0	0.34	125.0
R	8.0	10.0	0.73	268.4
S	9.0	8.0	0.98	360.3
T	13.0	8.0	0.88	323.5
U	20.0	17.0	4.44	1632.4
V	12.0	9.0	0.94	345.6
W	15.0	11.0	0.73	268.4
X	21.0	15.0	3.43	1261.0
Y	11.0	9.0	0.76	279.4
Z	15.0	9.0	1.01	371.3
AA	15.0	9.0	0.72	264.7
AB	24.0	16.0	3.14	1154.4
AC	20.0	15.0	3.29	1209.6
AD	14.0	14.0	1.19	437.5
AE	13.0	11.0	1.36	500.0
AF	14.0	6.0	0.65	239.0
AG	15.0	12.0	2.17	797.8
AH	11.0	10.0	1.20	441.2
AI	13.0	12.0	1.08	397.1
AJ	15.0	13.0	0.92	338.2
AK	12.0	11.0	0.85	312.5
AL	12.0	10.0	1.21	444.9

Table A-5 continued.

<i>Rock ID</i>	<i>Length (cm)</i>	<i>Width (cm)</i>	<i>Weight (kg)</i>	<i>Volume (cm³)</i>
AM	10.0	10.0	0.86	316.2
AN	15.0	10.0	1.38	507.4
AO	18.0	13.0	2.15	790.4
AP	20.0	20.0	6.11	2246.3
AQ	19.0	14.0	2.54	933.8
AR	21.0	14.0	3.48	1279.4
AS	13.0	11.0	1.61	591.9
AT	12.0	11.0	1.33	489.0
AU	19.0	13.0	2.28	838.2
AV	10.0	7.0	1.02	375.0
AW	17.0	11.0	1.40	514.7
AX	10.0	10.0	0.66	242.6
AY	19.0	11.0	1.25	459.6
AZ	14.0	10.0	1.24	455.9
BA	13.0	8.0	0.79	290.4
BB	16.0	10.0	1.85	680.1
BC	15.0	8.0	0.88	323.5
BD	12.0	8.0	0.90	330.9
BE	14.0	8.0	0.84	308.8
BF	13.0	10.0	1.57	577.2
BG	15.0	11.0	0.82	301.5
BH	10.0	8.0	0.91	334.6
BI	10.0	10.0	0.67	246.3
<i>Totals</i>			<i>94.88</i>	<i>34882.4</i>

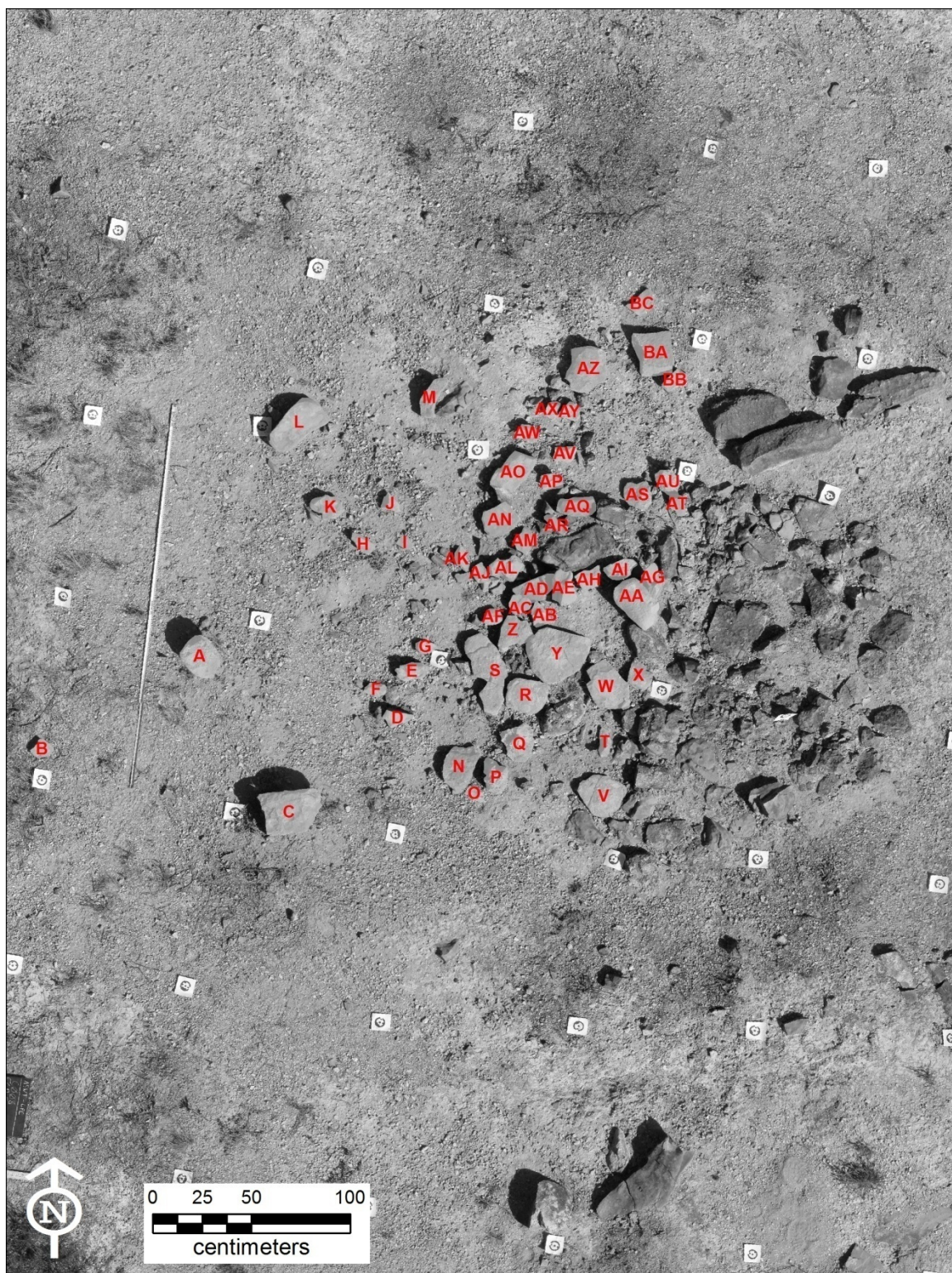


Figure A-6. Feature C006 plan map with measured burned rocks labeled.

Table A-6. Feature C006 burned rock data.

<i>Rock ID</i>	<i>Length (cm)</i>	<i>Width (cm)</i>	<i>Weight (kg)</i>	<i>Volume (cm³)</i>
A	22.0	18.0	7.91	2908.1
B	12.0	10.0	0.77	283.1
C	34.0	22.0	20.40	7500.0
D	16.0	10.0	1.43	525.7
E	18.0	10.0	2.22	816.2
F	12.0	8.0	0.43	158.1
G	11.0	7.0	0.54	198.5
H	13.0	7.0	0.62	227.9
I	12.0	7.0	0.28	102.9
J	11.0	9.0	0.44	161.8
K	17.0	12.0	1.62	595.6
L	31.0	14.0	7.65	2812.5
M	20.0	7.0	1.86	683.8
N	26.0	16.0	4.24	1558.8
O	10.0	6.0	0.44	161.8
P	18.0	11.0	2.96	1088.2
Q	16.0	21.0	3.56	1308.8
R	21.0	17.0	5.53	2033.1
S	45.0	18.0	8.50	3125.0
T	18.0	7.0	0.43	158.1
U	25.0	16.0	NULL	NULL
V	25.0	22.0	7.20	2647.1
W	27.0	18.0	8.40	3088.2
X	12.0	14.0	2.22	816.2
Y	33.0	29.0	14.09	5180.1
Z	18.0	17.0	4.46	1639.7
AA	27.0	11.0	7.27	2672.8
AB	11.0	9.0	1.07	393.4
AC	12.0	10.0	0.46	169.1
AD	26.0	15.0	4.18	1536.8
AE	15.0	13.0	2.49	915.4
AF	8.0	11.0	0.81	297.8
AG	17.0	10.0	3.89	1430.1
AH	14.0	10.0	0.72	264.7
AI	16.0	7.0	1.40	514.7
AJ	10.0	7.0	0.35	128.7
AK	13.0	9.0	0.47	172.8
AL	18.0	14.0	1.87	687.5

Table A-6 continued.

<i>Rock ID</i>	<i>Length (cm)</i>	<i>Width (cm)</i>	<i>Weight (kg)</i>	<i>Volume (cm³)</i>
AM	15.0	12.0	0.80	294.1
AN	17.0	15.0	2.69	989.0
AO	19.0	14.0	4.59	1687.5
AP	12.0	10.0	0.93	341.9
AQ	12.0	18.0	2.15	790.4
AR	14.0	5.0	0.61	224.3
AS	17.0	17.0	1.92	705.9
AT	14.0	9.0	0.59	216.9
AU	21.0	12.0	2.55	937.5
AV	11.0	7.0	0.51	187.5
AW	13.0	9.0	0.72	264.7
AX	8.0	6.0	0.71	261.0
AY	11.0	10.0	0.71	261.0
AZ	28.0	23.0	9.19	3378.7
BA	19.0	23.0	10.45	3841.9
BB	13.0	6.0	1.30	477.9
BC	14.0	7.0	0.67	246.3
<i>Totals</i>			<i>174.27</i>	<i>64069.9</i>

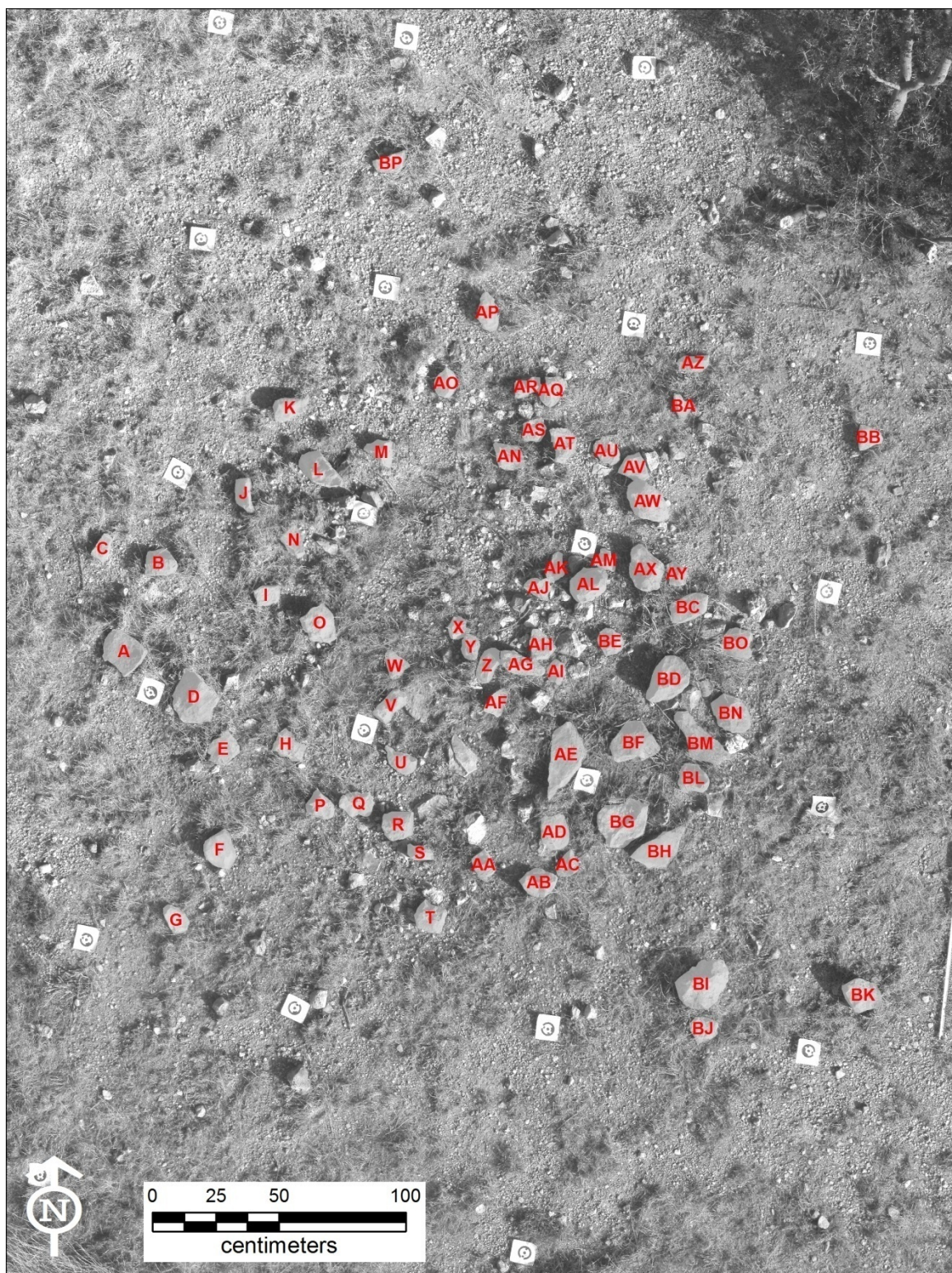


Figure A-7. Feature C007 plan map with measured burned rocks labeled.

Table A-7. Feature C007 burned rock data.

<i>Rock ID</i>	<i>Length (cm)</i>	<i>Width (cm)</i>	<i>Weight (kg)</i>	<i>Volume (cm³)</i>
A	18.0	13.0	2.02	742.6
B	12.0	11.0	1.57	577.2
C	11.0	6.0	0.41	150.7
D	17.0	19.0	3.73	1371.3
E	10.0	13.0	0.91	334.6
F	14.0	13.0	1.98	727.9
G	13.0	8.0	0.98	360.3
H	13.0	10.0	1.16	426.5
I	11.0	7.0	0.60	220.6
J	13.0	6.0	0.69	253.7
K	15.0	8.0	0.95	349.3
L	19.0	14.0	1.45	533.1
M	12.0	9.0	0.74	272.1
N	15.0	10.0	0.65	239.0
O	16.0	13.0	1.86	683.8
P	12.0	10.0	1.03	378.7
Q	15.0	10.0	1.11	408.1
R	12.0	10.0	1.83	672.8
S	11.0	6.0	0.66	242.6
T	11.0	12.0	1.18	433.8
U	15.0	9.0	0.72	264.7
V	15.0	9.0	0.98	360.3
W	12.0	9.0	0.57	209.6
X	8.0	9.0	0.65	239.0
Y	11.0	8.0	0.85	312.5
Z	14.0	9.0	1.35	496.3
AA	11.0	9.0	0.61	224.3
AB	13.0	13.0	1.82	669.1
AC	11.0	9.0	0.49	180.1
AD	15.0	12.0	1.77	650.7
AE	32.0	13.0	4.21	1547.8
AF	12.0	9.0	0.66	242.6
AG	20.0	9.0	1.56	573.5
AH	13.0	10.0	0.67	246.3
AI	11.0	8.0	0.63	231.6
AJ	13.0	9.0	0.80	294.1
AK	13.0	9.0	1.08	397.1
AL	16.0	12.0	2.68	985.3

Table A-7 continued.

<i>Rock ID</i>	<i>Length (cm)</i>	<i>Width (cm)</i>	<i>Weight (kg)</i>	<i>Volume (cm³)</i>
AM	8.0	8.0	0.74	272.1
AN	12.0	12.0	1.33	489.0
AO	12.0	8.0	0.89	327.2
AP	16.0	8.0	1.05	386.0
AQ	13.0	9.0	1.14	419.1
AR	12.0	6.0	0.78	286.8
AS	12.0	8.0	0.71	261.0
AT	14.0	10.0	1.13	415.4
AU	8.0	12.0	0.57	209.6
AV	12.0	12.0	1.08	397.1
AW	20.0	14.0	3.66	1345.6
AX	19.0	14.0	2.95	1084.6
AY	11.0	8.0	0.62	227.9
AZ	13.0	7.0	0.57	209.6
BA	8.0	9.0	0.47	172.8
BB	11.0	9.0	0.59	216.9
BC	17.0	11.0	1.18	433.8
BD	19.0	15.0	3.37	1239.0
BE	12.0	9.0	0.84	308.8
BF	18.0	17.0	2.94	1080.9
BG	20.0	15.0	1.56	573.5
BH	25.0	13.0	2.55	937.5
BI	22.0	15.0	5.34	1963.2
BJ	11.0	10.0	0.69	253.7
BK	14.0	13.0	2.78	1022.1
BL	13.0	10.0	2.30	845.6
BM	26.0	9.0	1.81	665.4
BN	18.0	14.0	3.28	1205.9
BO	13.0	13.0	2.07	761.0
BP	14.0	7.0	0.74	272.1
<i>Totals</i>			<i>97.34</i>	<i>35786.8</i>

REFERENCES CITED

Acuña, Laura I.

- 2006 *The Economic Contribution of Root Foods and Other Geophytes in Prehistoric Texas*. Unpublished Master's thesis, Department of Anthropology, Texas State University, San Marcos.

Alexander, Robert K.

- 1974 *The Archaeology of Conejo Shelter: A Study of Cultural Stability at an Archaic Rockshelter Site in Southwestern Texas*. Unpublished Ph.D. dissertation, Department of Anthropology, University of Texas at Austin.

Antevs, Ernst

- 1955 Geologic-Climatic Dating in the West. *American Antiquity*, 20(4):317-335.

Arlinghaus, Sandra L., Robert F. Austin, and Jim Bethel

- 2004 Photogrammetry and Topographic Mapping. In *The Engineering Handbook*, edited by Richard C. Dorf, pp. 165.1-165.15. CRC Press, Boca Raton, Florida.

Bement, Leland C.

- 1986 *Excavation of the Late Pleistocene Deposits of Bonfire Shelter, 41VV218, Val Verde County, Texas: 1983-1984*. Texas Archeological Survey, Archeology Series 1. University of Texas at Austin.

- 1989 Lower Pecos Canyonlands. In *From the Gulf to the Rio Grande: Human Adaptation in Central, South, and Lower Pecos, Texas*, by T.R. Hester, S.L. Black, D.G. Steele, B.W. Olive, A.A. Fox, K.J. Reinhard, and L.C. Bement, Research Series No. 33. Arkansas Archeological Survey, Fayetteville.

- 2007 Bonfire Shelter: A Jumping off Point for Comments for Byerly et al. *American Antiquity* 72(2):366-372.

Binford, Lewis R.

- 2001 *Constructing Frames of Reference: An Analytical Method for Archaeological Theory Building Using Ethnographic and Environmental Data Sets*. University of California Press, Berkeley.

Black, Stephen L.

1985 Site 41BX228 as a Burned Rock Midden Site. In *The Panther Springs Creek Site: Cultural Change and Continuity within the Upper Salado Creek Watershed, South-Central Texas*, by Stephen L. Black and A. Joachim McGraw, pp. 290-301, Archaeological Survey Report No. 100. Center for Archaeological Research, University of Texas at San Antonio.

1997a Oven Cookery at the Honey Creek Site. In *Hot Rock Cooking on the Greater Edwards Plateau: Four Burned Rock Midden Sites in West Central Texas*, by Stephen L. Black, Linda W. Ellis, Darrell G. Creel, and Glenn T. Goode, pp. 255-268. Studies in Archeology 22. Texas Archeological Research Laboratory, University of Texas, Austin.

1997b Scenarios of Midden Accumulation. In *Hot Rock Cooking on the Greater Edwards Plateau: Four Burned Rock Midden Sites in West Central Texas*, by Stephen L. Black, Linda W. Ellis, Darrell G. Creel, and Glenn T. Goode, pp. 83-87. Studies in Archeology 22. Texas Archeological Research Laboratory, University of Texas, Austin.

Black, Stephen L., and Darrell G. Creel

1997 The Central Texas Burned Rock Midden Reconsidered. In *Hot Rock Cooking on the Greater Edwards Plateau: Four Burned Rock Midden Sites in West Central Texas*, by Stephen L. Black, Linda W. Ellis, Darrell G. Creel, and Glenn T. Goode, pp. 269-305. Studies in Archeology 22. Texas Archeological Research Laboratory, University of Texas, Austin.

Black, Stephen L., and Phil Dering

2008 *Lower Pecos Canyonlands: Before Amistad*. Electronic Document, <http://www.texasbeyondhistory.net/pecos/before.html>, Accessed July 3, 2012.

Black, Stephen L., and Jason R. Lucas

1998 Exploring the Meanings of Burned Rock Data. In *Archeology along the Wurzbach Parkway: Module 3 Investigation and Experimentation at the Higgins Site (41BX184), Volume I*, by Stephen L. Black, Kevin Jolly, Charles D. Frederick, Jason R. Lucas, James W. Karbula, Paul R. Takac, and Daniel R. Potter, Studies in Archeology 27. Texas Archeological Research Laboratory, University of Texas, Austin.

Black, Stephen L., Linda W. Ellis, Darrell G. Creel, and Glenn T. Goode

1997 *Hot Rock Cooking on the Greater Edwards Plateau: Four Burned Rock Midden Sites in West Central Texas*. Studies in Archeology 22. Texas Archeological Research Laboratory, University of Texas, Austin.

Boyd, Carolyn E.

2003 *Rock Art of the Lower Pecos*. Texas A&M University Press, College Station.

Boyd, Douglas K., Gemma Mehalchick, and Karl W. Kibler

- 2004 Rethinking Paluxy Site Archaeology. In *Shifting Sands and Geopyhtes: Geoarchaeological Investigations at Paluxy Sites on Fort Hood*, edited by Gemma Mehalchick, Douglas K. Boyd, Karl W. Kibler, and Christopher W. Ringstaff, pp. 199–224, Archeological Resource Management Series, Research Report 48. United States Army, Fort Hood, Texas.

Brady, Nyle C., and Ray R. Weil

- 2002 *The Nature and Property of Soils*. 13th ed. Pearson Education, Inc., Upper Saddle River, New Jersey.

Brown, Kenneth M.

- 1991 Prehistoric economics at Baker Cave: A plan for research. In *Papers on Lower Pecos Prehistory*, edited by Solveig A. Turpin, pp. 87-140. Studies in Archeology 8. Texas Archeological Research Laboratory, University of Texas, Austin.

Bryant, Vaughn M.

- 1967 Appendix I: Preliminary Pollen Analysis of Arenosa Shelter. In *Excavations at Arenosa Shelter, 1965-66*, by David S. Dibble, pp.77-85. Texas Archeological Salvage Project, University of Texas at Austin.

Bryant, Vaughn M., and Richard G. Holloway

- 1985 A Late-Quaternary Paleoenvironmental Record of Texas: An Overview of the Pollen Evidence. In *Pollen Records of Late-Quaternary North American Sediments*, edited by Vaughan M. Bryant and Richard G. Holloway, pp. 39-70. American Association of Stratigraphic Palynologists Foundation, Dallas, Texas.

Bryant, Vaughn M., Jr., and Harry J. Shafer

- 1977 The Late Quaternary Paleoenvironment of Texas: A Model for the Archeologist. *Bulletin of the Texas Archeological Society*, 48:1-25.

Byerly, Ryan M., David J. Meltzer, Judith R. Cooper, and Jim Theler

- 2007 Exploring Paleoindian Site-Use at Bonfire Shelter (41VV218). *Bulletin of the Texas Archeological Society* 78:125-147.

Byerly, Ryan M., Judith R. Cooper, David J. Meltzer, Matthew E. Hill, and Jason M. LaBelle

- 2005 On Bonfire Shelter (Texas) as a Paleoindian Bison Jump: An Assessment Using GIS and Zooarchaeology. *American Antiquity* 70(4):595-629.

Carr, John T.

- 1967 *The Climate and Physiography of Texas*. Report 53, Texas Water Development Board, Austin, Texas.

- Cooke, M. Jennifer, Libby A. Stem, Jay L. Banner, and Lawrence E. Mack
 2007 Evidence for the Silicate Source of Relict Soils on the Edwards Plateau, central Texas. *Quaternary Research* 67:275-285.
- Creel, Darrell
 1991 Bison Hides in Late Prehistoric Exchange in the Southern Plains. *American Antiquity* 56(1):40-49.
- Davenport, J. Walker
 1938 *Archaeological Exploration of Eagle Cave, Langtry, Texas*. Big Bend Basket Maker Papers No. 4. Witte Memorial Museum, San Antonio.
- Dering, James P.
 1979 *Pollen and Plant Macrofossil Vegetation Record Recovered from Hinds Cave, Val Verde County, Texas*. Unpublished Master's thesis, Department of Botany, Texas A&M University, College Station.
- 1999 Earth-oven plant processing in Archaic Period economies: An example from the semi-arid savannah in south-central North America. *American Antiquity* 64(4):659-674.
- 2002 *Amistad National Recreation Area: Archeological Survey and Cultural Resource Inventory*. Center for Ecological Archaeology. Texas A&M University, College Station.
- 2005 *Hinds Cave: Paleoclimate*. Electronic Document, <http://www.texasbeyondhistory.net/hinds/climate.html>, Accessed July 12, 2012.
- 2008 Late Prehistoric Subsistence Economy on the Edwards Plateau. *Plains Anthropologist* 53:59-77.
- Dibble, David S.
 1967 *Excavations at Arenosa Shelter, 1965-1966*. Report submitted to the National Park Service by the Texas Archeological Salvage Program, University of Texas, Austin.
- Dibble, David S, and Dessamae Lorrain
 1968 *Bonfire Shelter: A Stratified Bison Kill Site, Val Verde County, Texas*. Miscellaneous Papers No. 1, Texas Memorial Museum, Austin, Texas.
- Dibble, David S., and Elton R. Prewitt
 1967 *Survey and Test Excavations at Amistad Reservoir, 1964-1965*. Texas Archeological Salvage Project Survey Reports No. 3, University of Texas, Austin.

Edwards, Sherrian K.

- 1990 *Investigations of Late Archaic Coprolites: Pollen and Macrofossil Remains from Hinds Cave (41VV456), Val Verde County, Texas*. Unpublished Master's thesis, Department of Anthropology, Texas A&M University, College Station.

Ellis, Linda W.

- 1997 Hot Rock Technology. In *Hot Rock Cooking on the Greater Edwards Plateau: Four Burned Rock Midden Sites in West Central Texas*, edited by Stephen L. Black, Linda W. Ellis, Darrell G. Creel, and Glenn T. Goode, pp. 43-82. Studies in Archeology 22. Texas Archeological Research Laboratory, University of Texas, Austin.

Epstein, Jeremiah F

- 1962 Centipede and Damp Caves: Excavations in Val Verde County, Texas, 1958. *Bulletin of the Texas Archeological Society* 33:1-129.

Freeman, Jacob C.

- 2007 *Energy, Intensification, and Subsistence Change: Hunter Gatherer Earth Ovens and Alternatives to Plant Domestication in Central Texas*. Unpublished Master's thesis, Department of Anthropology, University of Texas at San Antonio.

Geologic Atlas of Texas (GAT)

- 1977 *Del Rio Sheet 1:250,000 scale*. The University of Texas Bureau of Economic Geology, Austin, Texas.

- 1981 *Sonora Sheet 1:250,000 scale*. The University of Texas Bureau of Economic Geology, Austin, Texas.

Golden, Michael L., Wayne J. Gabriel, and Jack W. Stevens

- 1982 *Soil Survey of Val Verde County, Texas*. U.S. Department of Agriculture, Soil Conservation Service in cooperation with the Texas Agricultural Experiment Station and Val Verde County Commissioners Court, Washington, D.C.

Gonzalez Rul, Francisco

- 1990 *Reconocimiento Arqueologico en la parte Mexicana de la Presa de la Amistad*. Instituto Nacional de Antropologia e Historia, Roma, Mexico.

Graham, John A., and William A. Davis

- 1958 *Appraisal of the Archeological Resources of Diablo Reservoir, Val Verde County, Texas*. Report submitted to the National Park Service by the Texas Archeological Salvage Program, University of Texas, Austin.

Grussenmeyer, Pierre, Klaus Hanke, and Andre Streilein

- 2002 Architectural Photogrammetry. In *Digital Photogrammetry*, edited by Yves Egels and Michel Kasser, pp. 300-339, Taylor & Francis Inc., New York.

Hall, Stephen A., and Salvatore Valastro, Jr.

- 1995 Grassland Vegetation in the Southern Great Plains during the Last Glacial Maximum. *Quaternary Research* 44:237-245.

Hester, Thomas R.

- 1983 Late Paleo-Indian Occupations at Baker Cave, Southwestern Texas. *Bulletin of the Texas Archeological Society* 53:101-119.

Holliday, Vance T.

- 1997 *Paleoindian Geoarchaeology of the Southern High Plains*. University of Texas Press, Austin.

Jackson, A.T.

- 1938 *Picture Writing of Texas Indians*. University of Texas Publications 3809, Austin.

Johnson, Amber L., and Robert J. Hard

- 2008 Exploring Texas Archaeology with a Model of Intensification. *Plains Anthropologist* 53(205):137-153.

Johnson, Leroy, Jr.

- 1959 The Devils Mouth Site: A River Terrace Midden, Diablo Reservoir, Texas. *Bulletin of the Texas Archeological Society* 30:253-285.

- 1964 *The Devils Mouth Site: A Stratified Campsite at Amistad Reservoir, Val Verde County, Texas*. Archeology Series No. 6. Department of Anthropology, University of Texas at Austin.

Karara, H.M.

- 1980 Non-Topographic Photogrammetry. In *Manual of Photogrammetry*, 4th ed., edited by Chester C. Slama, pp. 785-882, American Society of Photogrammetry, Falls Church, Virginia.

Kirkland, Forrest

- 1938 A Description of Texas Pictographs. *Bulletin of the Texas Archeological and Paleontological Society* 10:11-40, Abilene, Texas.

Krieger, Alex D.

- 2002 *We Came Naked and Barefoot: The Journey of Cabeza De Vaca Across North America*. University of Texas Press, Austin.

Landers, Roger Q., Jr.

- 1987 Native Vegetation of Texas. *Rangelands* 9(5):203-207.

Leach, Jeff D., David L. Nickels, Bruce K. Moses, and Richard Jones

- 1998 A Brief Comment on Estimating Rates of Burned Rock Discard: Results from an Experimental Earth Oven. *La Tierra* 25(3):42-50.

Light, Donald L.

- 1980 Satellite Photogrammetry. In *Manual of Photogrammetry*, 4th ed., edited by Chester C. Slama, pp. 883-978, American Society of Photogrammetry, Falls Church, Virginia.

Linder, Wilfried

- 2006 *Digital Photogrammetry: A Practical Course*, 2nd ed. Springer, Netherlands.

Martin, George C.

- 1933 *Archeological Exploration of the Shumla Caves*. Big Bend Basket Maker Papers No. 3. Witte Memorial Museum, San Antonio.

McKinney, Wilson W.

- 1981 Early Holocene Adaptations in Central and Southwestern Texas: The Problem of the Paleoindian-Archaic Transition. *Bulletin of the Texas Archeological Society* 52:91-120.

McNab, W. Henry, and Peter E. Avers

- 1994 *Ecological Subregions of the United States*. U.S. Department of Agriculture, U.S. Forest Service Electronic Document WO-WSA-5, <http://www.fs.fed.us/land/pubs/ecoregions>, Accessed February 5, 2012.

Mehalchick, Gemma, and Douglas K. Boyd

- 1999 Water in the Desert: Prehistoric Occupations at San Felipe Springs. In *Val Verde on the Sunny Rio Grande: Geoarcheological and Historical Investigations at San Felipe Springs, Val Verde County, Texas*, by Gemma Mehalchick, Terri Myers, Karl W. Kibler, and Douglas K. Boyd, pp.149-160, Reports of Investigations Number 122. Prewitt and Associates, Austin, Texas.

Meltzer, David J.

- 1999 Human Responses to Middle Holocene (Altithermal) Climates on the North American Great Plains. *Quaternary Research* 52:404-416.

Meltzer, David J., Ryan M. Byerly, and Judith R. Cooper

- 2007 On an Alternative Interpretation of the Paleoindian Site Use at Bonfire Shelter. *Bulletin of the Texas Archeological Society* 78:159-160.

National Climatic Data Center (NCDC)

- 2010 Daily Surface Data for Val Verde County, Texas. National Oceanic and Atmospheric Administration. Electronic Document. <http://www.ncdc.noaa.gov/oa/ncdc.html>, Accessed July 20, 2010.

Nunley, John P., Lathel F. Duffield, and Edward B. Jelks

- 1965 *Excavations at Amistad Reservoir, 1962 Season*. Miscellaneous Papers, No. 3, Texas Archeological Salvage Project. Austin, Texas.

Patton, Peter C., and David S. Dibble

- 1982 Archeologic and Geomorphic Evidence for the Paleohydrologic Record of the Pecos River in West Texas. *American Journal of Science* 282:97-121.

Pearce, J.E., and A.T. Jackson

- 1933 *A Prehistoric Rock Shelter in Val Verde County, Texas*. University of Texas Bulletin 3327. Austin.

Prewitt, Elton R.

- 2007 To Jump or To Drag: Reflections on Bonfire Shelter. *Bulletin of the Texas Archeological Society* 78:149-158.

Quigg, J. Michael

- 1997 *The Sanders Site (41HF128): A Late Archaic Camp/Bison Processing Site, Hansford County, Texas*. Technical Report No. 19751, TRC Mariah Associates Inc., Austin, Texas.

Quigg, J. Michael, and Jay Peck

- 1995 *The Rush Site (41TG346): A Stratified Late Prehistoric Locale in Tom Green County, Texas*. TRC Mariah Associates, Inc., Austin.

Reinhard, Karl J.

- 1988 *Diet, Parasitism, and Anemia in the Prehistoric Southwest*. Unpublished Ph.D. dissertation, Department of Anthropology, Texas A&M University, College Station.

- 1992 Patterns of diet, parasitism, and anemia in prehistoric west North America. In *Diet, Demography, and Disease: Changing Perspectives on Anemia*, edited by P. Stuart-Macadam and S. Kent, pp. 219-258. Aldine de Gruyter, New York.

Ross, Richard E.

- 1965 *The Archeology of Eagle Cave*. Papers of the Texas Archeological Salvage Project, No. 7, University of Texas, Austin.

Saunders, Joe W.

- 1992 Plant and Animal Procurement Sites in the Lower Pecos Region, Texas. *Journal of Field Archaeology* 19(3):335-349.

Setzler, Frank M.

- 1934 Cave Burials in Southwestern Texas. In *Explorations and Field-Work of the Smithsonian Institution in 1933*, Publication 3235, pp. 35-37. Smithsonian Institution, Washington, D.C.

Shafer, Harry J.

1975 Clay Figurines from the Lower Pecos Region, Texas. *American Antiquity* 40(2):148-158.

1988 The Prehistoric Legacy of the Lower Pecos Region of Texas. *Bulletin of the Texas Archeological Society* 59:23-52.

Shafer, Harry J., and Vaughn M. Bryant

1977 *Archeological and Botanical Studies at Hinds Cave, Val Verde County, Texas*. Annual Report to the National Science Foundation, Department of Anthropology, Texas A&M University, College Station.

Sobolik, Kristin D.

1991 *Paleonutrition of the Lower Pecos Region of the Chihuahuan Desert*. Unpublished Ph.D. dissertation, Department of Anthropology, Texas A&M University, College Station.

Sorrow, William M.

1968 *The Devil's Mouth Site: The Third Season-1967*. Papers of the Texas Archeological Salvage Project No. 14. University of Texas at Austin.

Steele D. Gentry, and Ben W. Olive

1989 Bioarcheology of Region 3 study area. In *From the Gulf to the Rio Grande: Human Adaptation in Central, South, and Lower Pecos Texas*, edited by Thomas R. Hester, Stephen L. Black, D. Gentry Steele, Ben W. Olive, Anne A. Fox, Karl J. Reinhard, and Leland C. Bement, Arkansas Archeological Survey Research Series 33, pp. 93-114. Fayetteville.

Steele, D. Gentry, Ben W. Olive, Karl J. Reinhard

1999 Central, South and Lower Pecos Texas. In *Bioarcheology of the South Central United States*, edited by Jerome C. Rose, Arkansas Archeological Research Report 55, pp. 133-152. Fayetteville.

Stock, Janet A.

1983 *The Diet of Hinds Cave (41VV456), Val Verde County, Texas: The Coprolite Evidence*. Unpublished Master's thesis, Department of Anthropology, Texas A&M University, College Station.

Taylor, Walter W.

1964 Tethered Nomadism and Water Territoriality: An Hypothesis. *35th International Congress of Americanists 1962*, 2:197-203. Mexico City.

Taylor, Walter W., and Francisco Gonzalez-Rul

1961 An Archeological Reconnaissance Behind the Diablo Dam, Coahuila, Mexico. *Bulletin of the Texas Archeological Society* 31:153-165.

Thoms, Alston V.

1989 *The Northern Roots of Hunter-Gatherer Intensification: Camas and the Pacific Northwest*. Unpublished Ph.D. dissertation, Department of Anthropology, Washington State University, Pullman.

2008 Ancient Savannah Roots of the Carbohydrate Revolution in South-Central North America. *Plains Anthropologist* 53(205):121-136.

2009 Rocks of Ages: propagation of hot-rock cookery in western North America. *Journal of Archaeological Science* 36:573-591.

Tunnell, Curtis, and Enrique Madrid

1988 Making and Taking Sotol in Chihuahua and Texas. In *Papers from the Third Symposium of Resources from the Chihuahuan Desert Region, United States and Mexico, November 10-12, 1988*, edited by A. Michael Powell, Robert R. Hollander, Jon C. Barlow, W. Bruce McGillivray, and David J. Schmidly. Chihuahuan Desert Research Institute Press, Alpine, Texas.

Turpin, Solveig A.

1982 *The Archeology and Rock Art of Seminole Canyon: A Study in the Lower Pecos River Region of Southwest Texas*. Unpublished Ph.D. dissertation, University of Texas, Austin.

1984 *Prehistory in the Lower Pecos: An Overview*. Texas Archeological Survey Research Report 90, University of Texas, Austin.

1991 Time out of mind: The radiocarbon chronology of the Lower Pecos River Region. In *Papers on Lower Pecos Prehistory*, edited by Solveig A. Turpin, pp. 1-49. Studies in Archeology 8. Texas Archeological Research Laboratory, University of Texas, Austin.

1994 Lower Pecos Prehistory: The View from the Caves. In *The Caves and Karst of Texas*, edited by W.R. Elliot and G. Veni, pp. 69-84. National Speleological Society, Huntsville, Alabama.

1997 *The Lewis Canyon Petroglyphs*. Special Report 2, Rock Art Foundation, San Antonio, Texas.

2004 The Lower Pecos River Region of Texas and Northern Mexico. In *The Prehistory of Texas*, edited by Timothy K. Pertulla. Texas A&M University Press, College Station.

Turpin, Solveig A., editor

1985 *Seminole Sink: Excavation of a Vertical Shaft Tomb*. Texas Archeological Survey Research Report 93, Austin, Texas.

Turpin, Solveig A., and Michael W. Davis

- 1990 The 1989 TAS Field School: Devils River State Natural Area. *Bulletin of the Texas Archeological Society* 61:1-58.

U.S. Department of Agriculture (USDA)

- 1999 *Soil Taxonomy: A Basic System of Soil Classification for Making and Interpreting Soil Surveys*. 2nd ed., Agriculture Handbook Number 436, USDA Natural Resources Conservation Service, U.S. Government Printing Office, Washington, D.C.

Walker Phillip L., Rhonda R. Bathurst, Rebecca Richman, Thor Gjerdrum, and Valerie A. Andrushko

- 2009 The Causes of Porotic Hyperostosis and Cribra Orbitalia: A Reappraisal of the Iron-Deficiency-Anemia Hypotheses. *American Journal of Physical Anthropology* 139:109-125.

Wandsnider, LuAnn

- 1997 The roasted and the boiled: Food composition and heat treatment with special emphasis on pit-hearth cooking. *Journal of Anthropological Archaeology* 16:1-48.

Williams-Dean, Glenna J.

- 1978 *Ethnobotany and Cultural Ecology of Prehistoric Man in Southwest Texas*. Unpublished Ph.D. dissertation, Department of Botany, Texas A&M University, College Station.

Wilson, Ernest W.

- 1930 Burned Rock Mounds of South-West Texas. *Bulletin of the Texas Archaeological and Paleontological Society* 2:59-63.

Woltz, Ben V., Jr.

- 1998 *The Use of Agave, Sotol and Yucca at Hinds Cave, Val Verde County, Texas: Reconstructing Methods of Processing through the Formation of Behavioral Chains*. Unpublished Master's thesis, Department of Anthropology, Texas A&M University, College Station.

Wong, K.W.

- 1980 Basic Mathematics in Photogrammetry. In *Manual of Photogrammetry*, 4th ed., edited by Chester C. Slama, pp. 37-101, American Society of Photogrammetry, Falls Church, Virginia.

Woolsey, A.M.

- 1936 *Excavation of a Rock Shelter on the Martin Kelly Ranch Six Miles Southeast of Comstock in Val Verde County, Texas*. Department of Anthropology, University of Texas, Austin.

Yesner, David R.

- 2004 Optimal Foraging Theory and Technoeconomic Evolution Among Northern Maritime Hunter-gatherers. In *Hunters and Gatherers in Theory and Archaeology*, edited by George M. Crothers, pp. 258-275. Occasional Paper No. 31, Center for Archaeological Investigations, Southern Illinois University, Carbondale.

Yu, Pei-Lin

- 2006 *Pit Cooking and Intensification of Subsistence in the American Southwest and Pacific Northwest*. Unpublished Ph.D. dissertation, Department of Anthropology, Southern Methodist University, Dallas.

VITA

John Andrew Campbell was born in Omaha, Nebraska on April 12, 1973 the son of Richard Wayne Campbell and Judith Ann Campbell. He grew up as U.S. Marine Corps dependent on the east and west coasts of the U.S. until his family settled in Hewitt, Texas where he finished secondary schooling at Midway High School. In 1991, he entered Texas A&M University and received a Bachelor of Arts in Anthropology in May of 1996. Following his undergraduate, he worked in cultural resource management in both university and private settings. In August of 2009, he entered the Graduate College of Texas State. He is married to Adrienne Campbell and has two daughters, Lydia and Daisy.

Permanent Address:

1221 Heatherwood

Hewitt, Texas 76643

This thesis was typed by John A. Campbell